

EXTENSION OF THE GAMBLER'S RUIN
PROBLEM PLAYED OVER NETWORKS

THE THESIS IS SUBMITTED IN PARTIAL FULFILMENT OF
THE REQUIREMENTS
FOR THE AWARD OF THE DEGREE DOCTOR OF
PHILOSOPHY
OF THE UNIVERSITY OF PORTSMOUTH.

December 30, 2013

By
Nira Chamberlain

Department of Mathematics

Contents

1	Introduction	1
1.1	Background	2
1.1.1	Random Networks	5
1.1.2	Small World Networks	7
1.1.3	Scale Free Networks	13
1.2	Contribution to Knowledge	18
1.3	Thesis Outline	19
2	Models of Complex Systems played over Networks	21
2.1	Models of Complex Systems	21
2.2	How Networks Influence the Behaviour of Complex Systems and Evolutionary Games	25
2.2.1	Schelling's Model with Underlying Network Topology	27
2.2.2	Evolutionary Games	30
3	Extending the Gambler's Ruin Problem	35
3.1	Classical Gambler's Ruin Problem	35
3.1.1	Properties of the Two Player Gambler's Ruin Problem	36
3.1.2	The N -Player Gambler's Ruin Problem	38
3.2	Gambler's Ruin Problem Played Over Networks	42
3.2.1	The Contracting Model	46
3.2.2	The Evolving Network Model: The Pure Ring Case	48
3.2.3	The Effect of the Watts-Strogatz Model's Rewiring Probability	54
3.2.4	The Fixed Model	59
4	The Evolving Network Model	65
4.1	Offspring and the Fish-Plankton Model	65

4.2	Offspring within the Gambler's Ruin Problem	66
5	Bespoke Preferential Attachment Rules	78
5.1	Examples of Bespoke Preferential Attachment Rules	78
5.1.1	Preferential Attachment Based on Attractiveness	79
5.2	Preferential Attachment Rule for the Extended Gambler's Ruin Problem	84
5.3	The Kudos Preferential Attachment Rule	84
5.3.1	Comparison with the Other Preferential Attachment Rules	89
5.3.2	Varying the Target with a Fixed Initial Resource	94
5.3.3	Critical Targets and the Scaling Laws	115
5.3.4	Incorporating Regulation	122
6	Conclusion and Future Work	127
6.1	Synopsis	127
6.2	Future Work	132
A	The Robustness of the Numerical Simulations	136
B	References	141

List of Tables

1	Number of nodes, average degree and clustering coefficient for different real world networks, along with the expected value of the clustering coefficient on a corresponding random graph with the same number of nodes and same average degree [Newman et al (2006)].	9
2	The effect of using a biased or unbiased coin on the probability of achieving the target (200 units) as well as the expected duration of the game. $a=b=100$ units.	37
3	Comparison between analytical and numerical simulations for the expected duration of a game. Results are accurate to two decimal places. The number of histories for the numerical simulation is 10,000. The initial resource for the two players is 100 with a target of 200.	39
4	The initial network topologies and players' configurations to be considered in order to determine their influences on the results produced by the extended version of the GR problem. Cases chosen to be consistent with Figure 23.	49
5	The list of network topologies to be investigated in order to determine their influence on the fixed model. All networks are fixed to 100 players, initial resource of 110 and a target of 200.	61
6	Details of the cases investigated by varying the attachment rules and neighbours k	67
7	Details of cases investigated by varying the initial size of network N and neighbours k	72
8	Comparing the contracting and evolving model key statistics. Initial network topology lattice with 10,000 rounds. Results averaged over 50 histories.	76

9	Details of cases to be investigated by varying the attachment rules and neighbours k . Similar to Table 6 but with the kudos preferential attachment rule added.	89
10	Estimating the critical target from the simulated results selected data points (Figure 60) where $ratio = \frac{MTTA}{MTTB}$. Here $T_{supercritical}$ is the target whose respected ratio $ratio_{supercritical}$ is greater than one. Also, $T_{subcritical}$ is the target whose respected ratio $ratio_{subcritical}$ is less than one.	113
11	Investigation of the scaling properties of the evolving model. The normalised inputs are the number of the initial network size =100, initial resource = 100, target = 200. The initial network topology was a pure ring lattice; 10,000 rounds were played. Results averaged over 50 histories.	116
12	Details of the cases investigated and parameter settings as well as critical target and scaling factors for the analytical and numerical estimating techniques.	117
13	Variation of the MTTA, MTTB and Nf over 50 and 100 histories. Initial resource is fixed at 100 units, initial network size is 100 players and there are 10,000 rounds. Results averaged over 50 or 100 histories. Results rounded to 2 decimal places.	138

List of Figures

1	The town of Königsberg in the eighteenth century. The seven bridges are highlighted in red [Newman et al (2006)].	2
2	Simple properties of a Network (a) The Shortest Path (represented by the blue edges). There are a number of routes from v_4 to v_7 , however the route v_4 to v_3 to v_7 is the shortest. Also v_4 to v_6 to v_7 is another possibility. The diameter of the two networks is easily seen to be 3 [Albert and Barabási (2002)]. (b) The Diameter. In the left-hand figure in which nodes are connected only to their nearest neighbour the diameter is 8, whilst in the right-hand figure next-nearest neighbours are included and the diameter is 4 [Watts (2003)].	4
3	Erdős-Rényi model of a random network: network size of 10 and probability of connection between two nodes equal to (upper diagram) 0.025, (middle diagram) 0.050 and (lower diagram) 0.100. . .	8
4	A pure ring 14 nodes network. Each vertex is connected to its nearest two neighbours on either side of it.	10
5	The Watts-Strogatz model shows how the topology has changed from Figure 4 when the rewiring probability p is set to 0.1 (left diagram) and 1.0 (right diagram).	11
6	The influence of the Watts-Strogatz model's rewiring probability, p , on the normalized clustering coefficient $C(p)/C(0)$ and the average shortest path length $L(p)/L(0)$. In this example, all the networks consist of 1000 nodes and an average degree (defined as $\langle k \rangle$) of 10 edges [Watts and Strogatz (1998)].	12

- 7 The approach of [Yan et al (2004)] to the preferential attachment rule in order to develop a scale free network with a high clustering coefficient. A new node is introduced at each time step and will connect randomly to an existing node but with a probability q to that node's neighbours at the next time step. The left, middle and right networks represent three consecutive time steps. Here node 7 is introduced at the first time step. The successive time steps show the growth in the number of node 7's neighbours. Nodes 8 and 9 are shown to have arrived but the process of connecting to the network is omitted from this figure. In the second time step, the dash lines extending from node 7 show which nodes it might attach to with a probability of q . It is seen later that node 4 was the only one selected for connection. In the final step, node 4's neighbours are now to be considered for connection to node 7. This again is also shown by the dash lines. 17
- 8 Comparison of the Barabási-Albert (BA) and Yan's model clustering coefficient for varying network sizes N . In this case $m = 2$, $q = 0.06$ and $J = 1$ [Yan et al (2004)]. 18
- 9 Schelling's one-dimensional segregation model [Schelling (1971)]. The "circles" and "crosses" represent two different racial groups. Here the individual prefers to live in a neighbourhood where the majority are of the same racial type. The red circle is an individual wishing to move while the green circle is content with its location. 23

- 10 Cellular automata version of Benito's variation of Schelling's one-dimensional segregation model. The top example has 23 black individuals and 27 white individuals. The lower example has 32 black individuals and 29 white individuals. In both cases an individual is happy if one of its neighbours either side is of the same type [Benito et al (2009)]. 24
- 11 Schelling's two-dimensional segregation model; here 5 percent of space is free, which an unhappy individual can move into. The difference between case (a) and (b) is that the thresholds Ψ are 20 percent and 80 percent respectively. In case (a) the residential pattern cannot be distinguished from a random one, while in case (b) the residential pattern is a segregated one [Benenson et al (2009)]. 26
- 12 Initial state of a social group; 50 individuals support the red party and 50 support the blue party. The empty cells indicate an empty vacancy or position within the social network. Every individual would prefer to have at least 75 percent of its neighbours supporting the same party as itself. Here 86 out of the 100 individuals are unhappy with their current social group as the previously stated criterion is not being met. 29
- 13 The state of a social group after 1000 individual movements to the nearest empty vacancy; 50 individuals support the red party and 50 support the blue party. Every individual would prefer to have at least 75 percent of neighbours who support the same party as itself. Here 3 out of the 100 individuals are unhappy with their current social group as the previously stated criterion is not being met. . . 30

14	The influence of a Watts-Strogatz model's rewiring probability p on the number of unhappy individuals within a social group network throughout the simulation duration of 1000 rounds. An unhappy individual is someone who does not have at least 75 percent of neighbours who support the same party as itself. The lower the number of unhappy individuals the more segregated the social network is.	31
15	Schematic diagram representing how connected structures produce one another in Southwell's model for the first six time steps starting with an isolated node where $Q = 4$ [Southwell and Cannings (2010)].	33
16	Frequency distribution of the expected duration of a game with the given scenario of flipping a biased coin with probability 0.42 of landing on one side (Table 2). 10,000 histories were undertaken. $a=b=100$ units.	38
17	A numerical simulation of how a player's resources vary with each round in four different histories (cases 1 to 4) with the given scenario of flipping a biased coin with probability 0.42 of landing on one side (Table 2). $a=b=100$ units.	39
18	Frequency distribution of the expected duration of a game with the given scenario of flipping an unbiased coin with probability 0.5 of landing on one side (Table 2). 10,000 histories were undertaken. $a=b=100$ units.	40
19	A numerical simulation of how a player's resources vary with each round in four different histories (cases 1 to 4) with the given scenario of flipping an unbiased coin with probability 0.5 of landing on one side (Table 2). $a=b=100$ units.	41
20	Example of the payment mechanism rule for three players on a fully connected network.	44

21	Example of the payment mechanism rule for four players on a non fully connected network.	45
22	The influence of the contracting model on network topology. Network topology is a pure ring, 100 players with 10 neighbours (opponents) each, initial resource of 100 and a target of 200. (a) This is the first round. (b) After 1000 rounds: network topology is no longer a pure ring, the size of the network has reduced from 100 to 53 players. If players 8 or 13 achieve or become bankrupt, there is the possibility that the network will become disconnected. (c) After 4751 rounds: network topology has evolved to the two player GR problem.	47
23	The influence of initial network size N and degree of each player k on the first time to bankruptcy. Comparison of a fully connected network $k = N - 1$ [Rocha and Stern (2004)] with two pure ring networks: $k = 2$ pure ring network with two neighbours; $k = 10$ pure ring network with 10 neighbours. Initial resource I is the numerical value 10 more than the initial network size N . For the contracting model case, results are averaged over 50 histories. For each game, the target is set at a large enough value to ensure that there are no achievements. This is because the [Rocha and Stern (2004)] results do not incorporate players who achieve.	48
24	The normalised network size Nr throughout the game for the cases in Table 4. Results averaged over 50 histories. The normalised player per resource is calculated from its respected value for a round, divided by the initial figure for round 1.	50

25	Influence of initial network size N and neighbours k on the mean time to bankruptcy $MTTB$ (left diagram) and mean time to achievement $MTTA$ (right diagram). Initial network topology: pure ring network. Initial resource: 10 more than the numerical size of the network. Target: double the numerical size of the network. Results averaged over 50 histories.	51
26	Influence of initial network size N and entrance degree on the exit k (exit degree) of players who became bankrupt (left diagram) and who achieved (right diagram). Initial network topology: pure ring network. Initial resource: 10 more than the numerical size of the network. Target: double the numerical size of the network. Results averaged over 50 histories.	52
27	The influence of initial network size, degree, initial resources and target (Table 4) on the average player's strength (average strength) in the network throughout the game. Results averaged over 50 histories.	53
28	The influence of initial network size, degree, initial resources and target (Table 4) on the gain loss parameter ($GainLoss$) of the network throughout the game. Results averaged over 50 histories. . . .	54
29	The influence of initial network size, degree, initial resources and target (Table 4) on the normalised resource per player parameter of the network throughout the game. Results averaged over 50 histories.	55

30	The influence of initial network size, degree, initial resources and target (Table 4) on the normalised network size Nr throughout the game for the network generated by the Watts-Strogatz model $p = 0.1$ (left diagram) and $p = 1.0$ (right diagram). Results averaged over 50 histories.	56
31	The influence of initial network size, degree, initial resources and target (Table 4) on the average strength throughout the game for the network generated by the Watts-Strogatz model $p = 0.1$ (left diagram) and $p = 1.0$ (right diagram). Results averaged over 50 histories.	57
32	The influence of initial network size, degree, initial resources and target (Table 4) on the gain loss parameter (<i>GainLoss</i>) throughout the game for the network generated by the Watts-Strogatz model $p = 0.1$ (left diagram) and $p = 1.0$ (right diagram). Results averaged over 50 histories.	58
33	The influence of initial network size, degree, initial resources and target (Table 4) on the normalised parameter resource per player throughout the game for the network generated by the Watts-Strogatz model $p = 0.1$ (left diagram) and $p = 1.0$ (right diagram). Results averaged over 50 histories.	58
34	The influence of the fixed model on the normalised Resource/Player parameter throughout the game. Network topology is a pure ring, 100 players with 10 neighbours (opponents) each, initial resource of 110 and a target of 200. Results averaged over 50 histories.	60

35	The influence of the network topology generated by the Watts-Strogatz model with $p = 0.0, 0.1$ and 1.0 on the gain loss parameter (<i>GainLoss</i>) throughout the game for the fixed model. Initial network size 100, initial resources of 110 and a target of 200. Results averaged over 50 histories.	63
36	The influence of different network topologies (Table 5) on the gain loss (<i>GainLoss</i>) parameter after 10000 round for the fixed model. Initial network size 100, initial resources of 110, a target of 200. Results were averaged over 50 histories.	64
37	The influence of different network topologies (Table 5) on the achieving player's exit degree k for the fixed model. Initial network size 100, initial resources of 110, a target of 200. Results were averaged over 50 histories.	64
38	The influence of the attachment rule, number of neighbours and initial size of network N on the final population Nf . For cases see Table 6. The initial resource is the initial network size plus 10. The target is double the initial size. Results averaged over 50 histories.	68
39	The initial evolving model's network topology at the first round. This is a 10 by 10 lattice network.	69
40	The evolving model's network topology after 500 rounds. The player's attributes are an initial resource of 110 and a target of 200.	70
41	The evolving model's network topology after 9500 rounds. The player's attributes are an initial resource of 110 and a target of 200.	71

- 42 The influence of the random attachment rule (left diagram) and degree dependent attachment rule (right diagram), number of neighbours and initial network size N on the normalised population (size of network) Nr through time. The Nr value of 1.0 equates to the initial population size. A full description of the cases is shown in Table 7. The initial resource is the numerical initial network size plus 10. The target is double the numerical initial network size. Results averaged over 50 histories. 72
- 43 The influence of attachment rule, number of neighbours and initial size of network N on the MTTB (left diagram) and MTTA (right diagram). For cases see Table 6. The initial resource is the initial network size plus 10. The target is double the initial size. Results averaged over 50 histories. 73
- 44 The influence of attachment rule, number of neighbours and initial size of network N on the achiever's (left diagram) and bankrupt player's (right diagram) exit degree $Exit\ k$. For cases see Table 6. The initial resource is the initial network size plus 10. The target is double the initial size. Results averaged over 50 histories. 73
- 45 The influence of the random attachment rule (left diagram) and degree dependent attachment rule (right diagram), number of neighbours and initial network size on the average strength. A full description of the cases is shown in Table 7. The initial resource is the numerical initial network size plus 10. The target is double the numerical initial network size. Results averaged over 50 histories. . . 74

- 46 The influence of the random attachment rule (left diagram) and degree dependent attachment rule (right diagram), number of neighbours and initial network size on the gain loss parameter *GainLoss*. A full description of the cases is shown in Table 7. The initial resource is the numerical initial network size plus 10. The target is double the numerical initial network size. Results averaged over 50 histories. 75
- 47 The influence of the random attachment rule (left diagram) and degree dependent attachment rule (right diagram) on the normalised resource per player parameter throughout the game. The normalised resource per player is calculated from its respected value for a round, divided by the initial figure for round 1. A full description of the cases is shown in Table 7. The initial resource is the numerical initial network size plus 10. The target is double the numerical initial network size. Results averaged over 50 histories. . . 76
- 48 Evolving network topology in Poncela et al's model with (a) $\varepsilon = 0$ (b) $\varepsilon = 0.1$ (c) $\varepsilon = 1.0$; figures on the left show the degree distribution for a network of size 1000; figures on the right show a snapshot of a network of size 100 [Poncela and Vespignani (2009)]. 83
- 49 The kudos value (upper diagram), degree (middle diagram) and resource (lower diagram) of individual players throughout the duration of the game. Snapshots result from the evolving model. Initial resource: 100, target: 200, initial network size: 100, initial network topology: lattice with periodic boundary conditions. 87

50	Comparison of preferential attachment rule's influence on achiever's exiting degree k (upper diagram), MTTA and MTTB (lower diagram). Initial periodic boundary condition lattice network, 10 by 10, 10,000 rounds, initial resource of 100 and a target of 200. Results averaged over 50 histories.	88
51	The final population size Nf in each of the cases of Table 9 after 10,000 rounds. Results averaged over 50 histories.	90
52	The influence of the kudos preferential attachment rule, number of neighbours and initial network size N on the normalised population (size of network) Nr through time. The Nr value of 1.0 equates to the initial population size. A full description of cases is shown in Table 7. The initial resource is the numerical initial network size plus 10. The target is double the numerical initial network size. Results averaged over 50 histories.	90
53	The influence of the preferential attachment rule, number of neighbours and initial network size N on MTTA (left diagram) and MTTB (right diagram). The initial resource is 10 more than the numerical initial network size and the target is double the numerical initial network size. A full case description is shown in Table 9. Results averaged over 50 histories.	91
54	The influence of the preferential attachment rules, number of neighbours and initial network size N on the achiever's (left diagram) and bankrupt's (right diagram) exit degree $Exit\ k$. The initial resource is 10 more than the numerical initial network size and the target is double the numerical initial network size. A full case description is shown in Table 9. Results averaged over 50 histories.	92

55	The influence of the kudos preferential attachment rule, number of neighbours and initial network size on the average strength. A full description of cases is shown in Table 7. The initial resource is the numerical initial network size plus 10. The target is double the numerical initial network size. Results averaged over 50 histories.	93
56	The influence of the kudos preferential attachment rule, number of neighbours and initial network size on the gain loss performance indicator <i>GainLoss</i> . A full description of cases is shown in Table 7. The initial resource is the numerical initial network size plus 10. The target is double the numerical initial network size. Results averaged over 50 histories.	93
57	The influence of the kudos preferential attachment rule, number of neighbours and initial network size on the normalised resource per player parameter of the network throughout the duration of the game. A full description of cases is shown in Table 7. The initial resource is the numerical initial network size plus 10. The target is double the numerical initial network size. Results averaged over 50 histories. The normalised player per resource is calculated from its respective value for a round, divided by the initial figure for round 1.	94
58	The influence of the target and attachment rule on final population N_f (upper diagram), MTTA (middle diagram) and MTTB (lower diagram). The initial resource is fixed at 100 units; the initial network size is 100 players; 10,000 rounds. Results averaged over 50 histories.	95

59	The influence of the target and attachment rule on the ratio $\frac{MTTA}{MTTB}$ (upper diagram) and exit degree k (lower diagram). The initial resource is fixed at 100 units; the initial network size is 100 players; 10,000 rounds. Results averaged over 50 histories.	97
60	Varying the target and initial network size N : effect on ratio $\frac{MTTA}{MTTB}$ (upper diagram) and exit degree k (lower diagram). The initial resource is fixed to 100 units; the initial network size is 100 players; 10,000 rounds. Results averaged over 50 histories.	98
61	Varying the target and offspring: effect on final population N_f (lower diagram) and $MTTA$ (upper diagram). The initial resource is fixed to 100 units; the initial network size is 100 players; 10,000 rounds. Results averaged over 50 histories.	99
62	Probability distribution of the exiting degree k in the subcritical region (target of 150 - left diagram) and supercritical region (target of 550 - right diagram). The initial resource is fixed at 100 units; the initial network size is 100 players; 10,000 rounds. Results averaged over 50 histories.	100
63	Frequency of achievement in the subcritical region (target of 150 - left diagram) and supercritical region (target of 550 - right diagram). This is shown as a probability distribution. The initial resource is fixed at 100 units; the initial network size is 100 players; 10,000 rounds. Results averaged over 50 histories.	101
64	Probability distribution of the kudos population when a player achieves in the subcritical region (target of 150 - left diagram) and supercritical region (target of 550 - right diagram). The initial resource is fixed at 100 units; the initial network size is 100 players; 10,000 rounds. Results averaged over 50 histories.	102

65	Probability distribution of the number of rounds it takes a player to achieve in the subcritical region (target of 150 - left diagram) and supercritical region (target of 550 - right diagram) when they have kudos. The initial resource is fixed at 100 units; the initial network size is 100 players; 10,000 rounds. Results averaged over 50 histories.	102
66	First of four successive illustrative rounds (round 9981) of the evolving model. Game played in the subcritical region (target of 150). Orange nodes are players with kudos. Player 16214 is about to achieve.	103
67	Second of four successive illustrative rounds (round 9982) of the evolving model. Game played in the subcritical region (target of 150). Orange nodes are players with kudos. When Player 16214 achieves it causes mass isolation.	104
68	Third of four successive illustrative rounds (round 9983) of the evolving model. Game played in the subcritical region (target of 150). Orange nodes are players with kudos. Player 16351 is about to achieve.	105
69	Fourth of four successive illustrative rounds (round 9984) of the evolving model. Game played in the subcritical region (target of 150). Orange nodes are players with kudos. When Player 16351 achieves it causes mass isolation.	106
70	First of three illustrative rounds of the evolving model: round 7000. Game played in the supercritical region (target of 550). Orange nodes are players with kudos.	107
71	Second of three illustrative rounds of the evolving model: round 8000. Game played in the supercritical region (target of 550). Orange nodes are players with kudos.	108

- 72 Third of three illustrative rounds of the evolving model: round 9000. Game played in the supercritical region (target of 550). Orange nodes are players with kudos. 109
- 73 The influence of varying the target upon the number of neighbours of an achiever and average number of isolated players per achievement event (upper diagram). The influence upon units gained beyond the target - Excess Resources (lower diagram). The initial resource is fixed at 100 units; the initial network size is 100 players; 10,000 rounds. Results averaged over 50 histories. 110
- 74 How the target influences the kudos population size as a proportion of the total network through time (Round). The initial resource is fixed at 100 units; the initial network size is 100 players; 10,000 rounds. Results averaged over 50 histories. 111
- 75 Critical target estimate comparison between the numerical simulation model and the analytical approximation. The initial resource is fixed at 100 units; offspring entrance degree = 2; 10,000 rounds. Result averaged over 50 histories for the numerical simulation. . . . 114
- 76 How the player's target influences the proportion of the network connected to the node with the largest degree (upper diagram) and network's clustering coefficient C (lower diagram). The initial resource is fixed at 100 units; the initial network size is 100 players; 10,000 rounds. Results averaged over 50 histories. 115

- 77 Normalising the MTTA (Top row), MTTB (Middle row) and final population Nf (Bottom row) to the reference case when the degree of the player's offspring k is equal to one. Left column - the analytical results, Right column - the numerical results. For the non reference scenarios, the MTTA, MTTB, final population Nf and Targets are scaled by the corresponding factor shown in Table 12 Case 2. The initial resource is fixed at 100 units; the initial network size is 100 players; 10,000 rounds. Results averaged over 50 histories. 118
- 78 Normalising the MTTA (Top row), MTTB (Middle row) and final population Nf (Bottom row) to the reference case when the number of offspring is four or five. Left column - the analytical results, Right column - the numerical results. For the non reference scenarios, the MTTA, MTTB, final population Nf and Targets are scaled by the corresponding factor shown in Table 12 Cases 3 and 4. The initial resource is fixed at 100 units; the initial network size is 100 players; 10,000 rounds. Results averaged over 50 histories. 119
- 79 Normalising the MTTA (Top row), MTTB (Middle row) and final population Nf (Bottom row) to the reference case when the initial resource is 50 or 150 units. Left column - the analytical results, Right column - the numerical results. For the non reference scenarios, the MTTA, MTTB, final population Nf and Targets are scaled by the corresponding factor shown in Table 12 Cases 5 and 6. The initial resource is fixed at 100 units; the initial network size is 100 players; 10,000 rounds. Results averaged over 50 histories. 120

- 80 Normalising the MTTA (Top row), MTTB (Middle row) and final
population Nf (Bottom row) to the reference case when the initial
network size N is equal to 225. Left column - the analytical results,
Right column - the numerical results. For the non reference scenar-
ios, the MTTA, MTTB, final population Nf and Targets are scaled
by the corresponding factor shown in Table 12 Case 7. The initial
resource is fixed at 100 units; the reference initial network size is
100 players; 10,000 rounds. Results averaged over 50 histories. . . . 121
- 81 How the target and the degree of the player's offspring k influences
the kudos population size as a proportion of the total network after
10,000 rounds. The initial resource is fixed at 100 units; the initial
network size is 100 players. Results averaged over 50 histories. . . . 123
- 82 Upper diagram is the non regulating and regulating attachment
rules' influence on the population size Nr throughout the game. The
 β value is initially set at 10,000 while the reduction is 10 percent.
The target is 200. Lower diagram is the kudos population as a
proportion of the network size with regulation for different targets;
regulation activated when the exiting degree exceeds 25, β value is
initially set at 10,000 and the influence factor β is reduced by 10
percent. The initial resource is fixed at 100 units; the initial network
size is 100 players; 10,000 rounds. Results averaged over 50 histories. 125
- 83 Influence of kudos and regulating attachment rule on the final pop-
ulation Nf (upper diagram) and the achiever's exiting degree k
(lower diagram). Regulation activated when exiting degree exceeds
25 and the influence factor β is reduced by 10 percent. The initial
resource is fixed at 100 units; the initial network size is 100 players;
10,000 rounds. Results averaged over 50 histories. 126

- 84 Variation of the MTTA - Left column and MTTB - Right column over the number of histories simulated. Contracting model - Top row, Fixed model - Middle row and Evolving model (kudos attachment rule) - Bottom row. Network topology is a pure ring with 100 players, initial resources of 100 and a target of 200. 137
- 85 The influence of target on the MTTA. The error bars represent plus and minus one standard deviation from the mean. Initial resource is fixed at 100 units, initial network size is 100 players, 10,000 rounds. Results averaged over 50 histories. 139
- 86 The influence of target and of the probability of the strongest player beating the weakest opponent on the MTTA. Initial resource are fixed at 100 units, initial network size is 100 players, 10,000 rounds. Results averaged over 50 histories. 139

Abstract

In this thesis we consider the problem of extending and adapting the classical Gambler's Ruin (GR) problem so that it can be played over networks in a manner consistent with both the classical two-player and the fully connected N -player GR problem.

We introduce an extended GR problem, in which players in a network compete against the opponents to whom they are connected, and in which players exit the network either when they achieve a specified target or when they become bankrupt. In both cases, the game continues with the remaining players. While a bankrupted player simply leaves the network, successful players (achievers) may produce one or more offspring who connect to the network and continue playing the game with a share of the achiever's resources. We simulate the extended GR problem in the case of contracting, fixed and evolving networks.

A key motivation is to understand the interplay between the game and the network, i.e., how the topology of the network influences the progression of the GR problem game, and, conversely, how the game influences the evolution of the network topology. Therefore we consider several attachment rules, including random and preferential attachment. We also introduce a bespoke preferential attachment rule called *kudos*. Unlike the established preferential attachment rules, we find that *kudos* induces a phase transition in the network, as the size of target is varied.

Whilst registered as a candidate for the above degree, I have not been registered for any other research award.

The results and conclusions embodied in this thesis are the work of the named candidate and have not been submitted for any other academic award.

This thesis is dedicated to my family but especially to my sons Phillip and Nathan Chamberlain who always believed in me.

I like to thank my Director of Studies Professor Andrew Osbaldestin and my second supervisor Dr Andrew Burbanks for their invaluable guidance, advice and support.

I would like to thank my proof readers: Gerry Blunt, Jacqueline Rhules-Martin, Beverley and David Maynard and Dr Martin Hughes.

I would also like to thank those who gave me constant encouragement: Simon Lock, Amanda Padbury, Caroline Sergrave Kovacs, Dr Ryan Chan, Dr Melrose Stewart and Dr Martine Barons.

I would like to thank those who inspire me throughout my mathematical career: Professor Clive Fraiser (my cousin), Professor Keith Still, Dr Snezana Lawrence, Dr Janylle Carter and Dr Faith Carter.

Finally, I would like to thank the man who first introduced me to the Gambler's Ruin problem in 2007, Dr James Nyambayo.

I can do all things through Him who strengthens me.

The King James Bible: Philippians 4:13

Do not judge me by my successes, judge me by how many times I fell
down and got back up again.

Nelson Mandela

1 Introduction

In the Gambler's Ruin (GR) problem we are concerned with the likelihood of a player becoming bankrupt given an initial resource and a chance of winning a single "bet" [Shoesmith (1986)]. Typically, a player competes against an entity that is theoretically represented by an opponent or opponents with an infinite resource, for instance, a player playing the stock market [Hadjiliadis and Vecer (2006)] or even a lottery game [Hunter et al (2008)]. Here the "bet" is represented by some form of competitive engagement with the entity. On the other hand, the Classical GR problem considers two players with finite resources engaging with each other [Sandell (1989)]. In these circumstances, the player's objective(s) is to make the other bankrupt or to cease when they have reached a certain target [Hadjiliadis (2004)].

The motivation of this thesis is not to model the behaviour of a gambler *per se*, but the generic competitive behaviour of players in the business and social environment. This leads us to consider networks of players. For example, in the business world, a multinational company may have a single objective but engage a multiple number of opponents who do not necessarily compete with each other. To demonstrate, Richard Branson's Virgin Group's objective is to maximize its profits. Although it competes against British Airways and British Telecom, British Airways does not compete against British Telecom as they are from separate industrial sectors. Similarly, the UK food chain Sainsbury's competes against the local corner shop and also the UK car insurance firm Swinton. Conversely, Swinton does not compete against a local corner shop. Another aspect of competitive behaviour in the business and social environment is the emergence of new opponents and the removal of existing ones. Consequently, in this type of environment a player may engage a multiple number of opponents which can change through time.

This thesis is concerned with extending the GR problem to account for such

competitive behaviour. In order to do this, it is necessary to adapt the GR problem so it can be played over networks.

The rest of this chapter has been organized as follows: section 1.1 considers the background and the mathematical properties of networks, section 1.2 summarizes the contribution of knowledge that has emerged from this thesis, while section 1.3 provides an outline of the content for the rest of this thesis.

1.1 Background

In 1736, Leonhard Euler became interested in the Königsberg Bridge problem [Biggs et al (1976)]. The residents of Königsberg, a town consisting of seven bridges and two islands, considered the problem whether it was possible to cross all seven bridges in sequence without traversing any bridge more than once (Figure 1). Euler showed the existence of a path that traversed each bridge once and only once was impossible. Many consider Euler's proof to be the first theorem in the field of graph theory, the mathematical language for describing the properties of networks.

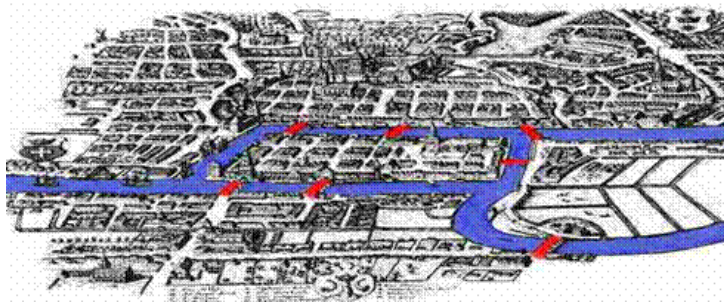


Figure 1: The town of Königsberg in the eighteenth century. The seven bridges are highlighted in red [Newman et al (2006)].

In its simplest form, a network can be described as a set of discrete elements (called **vertices/nodes**) and a set of connections (defined as **links/edges**) that

connect the elements. A node is usually identified with a number $i = 1, \dots, N$ where N is the **size of the network** (total number of nodes). We will only consider networks that contain at most one edge joining two nodes. No node is joined to itself. Where two nodes are connected by an edge they are called **neighbouring** nodes. A **walk** from node i to node j describes the sequence starting from node i through edges and nodes until node j has been reached. The number of edges contained in this sequence is defined as the **length** of the walk. A **path** is a walk in which no node is visited more than once. A **shortest path** is a walk of minimal length between two nodes. Defining d_{ij} as the length of a shortest path between nodes i and j then the **average shortest path length** is:

$$L = \frac{1}{N(N-1)} \sum_{i,j, i \neq j} d_{ij}. \quad (1.1.1)$$

Furthermore, the length of the longest shortest path between any pair of nodes in the network is called the network's **diameter**. We illustrate this in Figure 2.

Other simple properties of a network include the degree of the nodes, the degree distribution, and the clustering coefficient. The **degree of a node** in a network is defined as the number of edges the node has to other nodes. The **degree distribution** is defined as follows: For $k = 1, 2, 3, \dots$ let $P(k)$ be the probability that a randomly chosen node of the network has degree k , in other words, the fraction of nodes in the graph having degree k . Thus if there are N nodes in total in a network and N_k of them have degree k , then:

$$P(k) = \frac{N_k}{N}. \quad (1.1.2)$$

The **average degree**, denoted $\langle k \rangle$, is then $\langle k \rangle = \sum_{k=1}^{\infty} kP(k)$. The **clustering coefficient** indicates the level of clique formation in the neighbourhood of any given node. Firstly, the clustering coefficient c_i of a node i with the degree k_i is

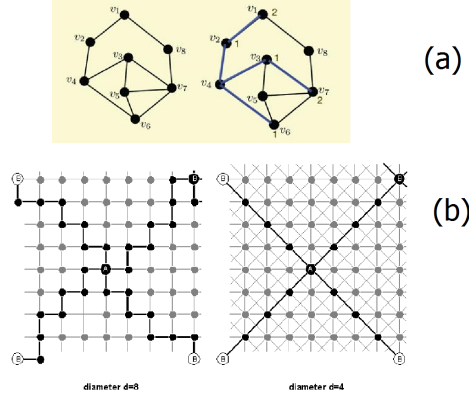


Figure 2: Simple properties of a Network (a) The Shortest Path (represented by the blue edges). There are a number of routes from v_4 to v_7 , however the route v_4 to v_3 to v_7 is the shortest. Also v_4 to v_6 to v_7 is another possibility. The diameter of the two networks is easily seen to be 3 [Albert and Barabási (2002)]. (b) The Diameter. In the left-hand figure in which nodes are connected only to their nearest neighbour the diameter is 8, whilst in the right-hand figure next-nearest neighbours are included and the diameter is 4 [Watts (2003)].

defined as follows: Let g_{edge} be the number of edges connecting nodes that are connected to the node i . The edges connecting these nodes to node i are not counted. Then:

$$c_i = \frac{2g_{edge}}{k_i(k_i - 1)}. \quad (1.1.3)$$

The clustering coefficient C of the network is then defined to be the average of all individual clustering coefficients:

$$C = \frac{1}{N} \sum_{i=1}^N c_i. \quad (1.1.4)$$

Defining **triples** as sub-networks which contain exactly three nodes, [Newman et al (2001)] expressed the clustering coefficient as:

$$C = \frac{3 \times g_{\Delta}}{g_{total}}. \quad (1.1.5)$$

where g_{Δ} is the number of fully connected triples and g_{total} is the total number of triples in the network. The factor of 3 is present due to the fact that each triple contains three nodes. Clustering coefficients are further discussed in sections 1.1.1, 1.1.2 and 1.1.3.

The **network's topology** is defined as the structure of the network, which considers properties such as degree distribution, clustering coefficient and average shortest path length. Different classifications of network topologies include, but are not limited to, lattice, random, small world and scale free networks. In sections 1.1.1, 1.1.2 and 1.1.3 the different type of network topologies are discussed further.

1.1.1 Random Networks

One important class of network topology is a random network. A **random network** with N nodes and E edges can be generated by randomly selecting, from a uniform distribution, a pair of unconnected nodes and placing an edge between them. This is done E times. Alternatively a random network is obtained by connecting a pair of unconnected nodes with a given connection probability p . We will consider the Erdős–Rényi model of a random network [Erdős and Rényi (1959)]. For the Erdős–Rényi model, the derived probability for generating a particular network $G_{N,E}$ with N nodes and exactly E edges is

$$p(G_{N,E}) = p^E (1-p)^{\frac{1}{2}N(N-1)-E}. \quad (1.1.6)$$

In order to compute the average degree, it can be observed that the average number of edges generated in the construction of the network is

$$\langle E \rangle = \frac{1}{2} N (N - 1) p. \quad (1.1.7)$$

Since each edge contributes to the degree of two nodes, then the average degree is

$$\langle k \rangle = \frac{2 \langle E \rangle}{N} = (N - 1) p \approx N p. \quad (1.1.8)$$

which is valid for large N . In order to obtain the degree distribution $P(k)$, the probability of creating a node of degree k is equal to the probability that it is connected only to k nodes. Moreover, if generating an edge is an independent event then the probability is simply given by the binomial distribution

$$P(k) = \binom{N-1}{k} p^k (1-p)^{N-1-k}. \quad (1.1.9)$$

As N becomes larger, the binomial distribution can be approximated by the Poisson distribution and using $Np \approx \langle k \rangle$

$$P(k) \approx e^{-\langle k \rangle} \frac{\langle k \rangle^k}{k!}. \quad (1.1.10)$$

The average clustering coefficient is calculated from this argument. For any node, the probability that any two of its neighbours are also connected to each other is given by the connection probability p . Therefore, the average clustering coefficient is equal to

$$C = p = \frac{\langle k \rangle}{N}. \quad (1.1.11)$$

Hence, in the Erdős-Rényi model for fixed $\langle k \rangle$ the clustering coefficient decreases with graph size and approaches zero in the limit of an infinitely large network. As well as this, random graphs exhibit a small average shortest path length L which has been shown to vary logarithmically with the network's size N according to:

$$L \propto \frac{\ln(N)}{\ln(\langle k \rangle)}. \quad (1.1.12)$$

An interesting property that can be found in the Erdős–Rényi model of a random network is the existence of a giant component [Newman et al (2006)]. A **giant component** is a connected set of nodes that contains a large proportion of the network. Giant components were first discussed by [Solomonoff and Rapoport (1951)]. It was found that when the average degree of all the nodes is less than one, the network is broken into many small islands. Moreover, when the average degree exceeds one, a giant component is formed that contains a large proportion of all the nodes in the network.

Figure 3 illustrates this giant component property by fixing the size of the network and varying the probability of connection between two nodes. In Figure 3 right hand side diagram, it can be seen that one of the nodes is connected to more than half of the network and these nodes constitute a giant component. Giant components will be discussed further in Chapter 5.

1.1.2 Small World Networks

The clustering coefficient of the Erdős–Rényi model of a random network does not correlate well with those of real world networks. Most notably, this parameter vanishes in the limit of very large network sizes. Table 1 illustrates this point by considering the clustering coefficient for a number of different real world networks, along with the expected value of the clustering coefficient for corresponding random networks with the same number of nodes and same average degree. We see that the measured clustering coefficient is much higher than that of the corresponding random network.

[Watts and Strogatz (1998)] proposed a model which would tune the clustering coefficient by interpolating between ordered pure ring networks (which have a large clustering coefficient) and a purely random network (possessing a small average shortest path length). Hence, Watts and Strogatz initially commenced with a

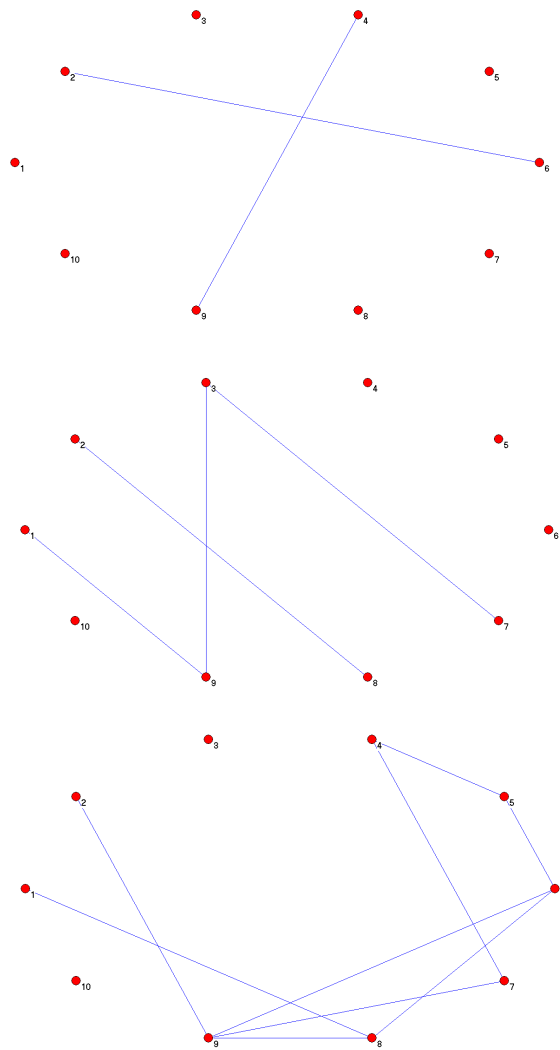


Figure 3: Erdős–Rényi model of a random network: network size of 10 and probability of connection between two nodes equal to (upper diagram) 0.025, (middle diagram) 0.050 and (lower diagram) 0.100.

pure ring network of N nodes in which each node is symmetrically connected to its m nearest neighbours on either side, so that the average degree $\langle k \rangle = 2m$. An example of a pure ring 14 noded network with $m = 2$ is illustrated in Figure 4.

Starting from a pure ring network, Watts and Strogatz obtained a new network

Network	Number of nodes	Average Degree	Measured Clustering Coefficient	Random Networks Clustering Coefficient
Internet (December 1999)	6374	3.8	0.24	0.00060
World Wide Web	153127	35.2	0.11	0.00023
Power grid	4941	2.7	0.080	0.00054
Biology collaboration	1520251	15.5	0.081	0.000010
Film actor collaboration	449913	113.4	0.20	0.00025
Company directors	7673	14.4	0.59	0.0019
Word co- occurrence	460902	70.1	0.44	0.00015
Neural network	282	14.0	0.28	0.049
Metabolic network	315	28.3	0.59	0.090
Food web	134	8.7	0.22	0.065

Table 1: Number of nodes, average degree and clustering coefficient for different real world networks, along with the expected value of the clustering coefficient on a corresponding random graph with the same number of nodes and same average degree [Newman et al (2006)].

using the following rewiring algorithm. Let us label the nodes v_1, \dots, v_N . For convenience we continue the labelling so that $v_{N+1} = v_1, v_{N+2} = v_2, \dots$ etc. For each node we consider the m edges connecting v_i to v_{i+1}, \dots, v_{i+m} . For each edge we rewire with probability p as follows: We select at random node v_j from one of the nodes $v_{i+m+1}, v_{i+m+2}, \dots, v_{i+N-m-1}$ that has not already been selected.

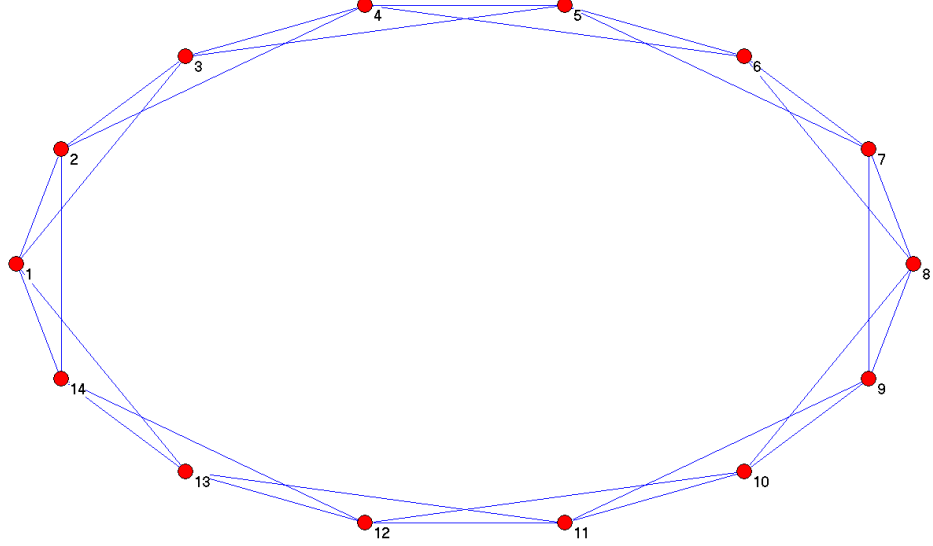


Figure 4: A pure ring 14 nodes network. Each vertex is connected to its nearest two neighbours on either side of it.

We connect v_i to v_j and continue to the next edge. Once all the edges have been considered we continue to the next node v_{i+1} and repeat. As a result, the rewiring probability p tunes the level of randomness in the network while keeping the number of edges constant.

Figure 5 illustrates the influence of rewiring probabilities of 0.1 and 1.0 respectively. For $p = 1$, all edges are rewired resulting in a random network (right diagram of Figure 5). However, for $10^{-3} \leq p \leq 10^{-1}$ (i.e. left diagram of Figure 5), Watts and Strogatz showed that the average shortest path length suddenly drops while the clustering coefficient remains approximately constant. By the addition of shortcuts during the rewiring process a small world network is generated.

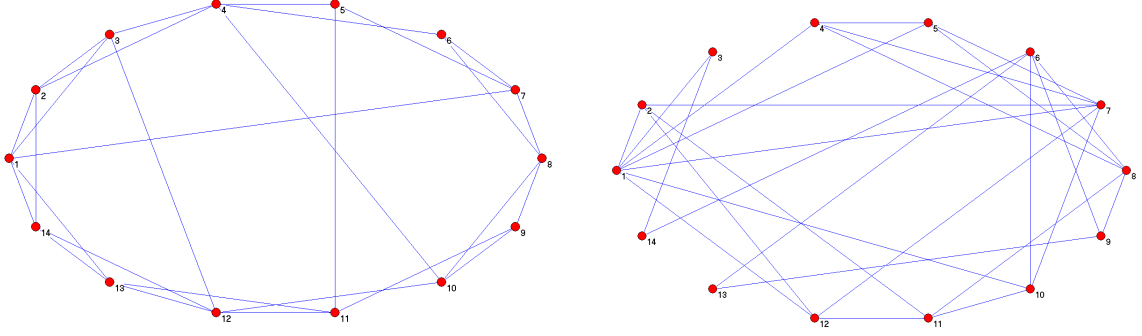


Figure 5: The Watts-Strogatz model shows how the topology has changed from Figure 4 when the rewiring probability p is set to 0.1 (left diagram) and 1.0 (right diagram).

Small world networks are characterised both by the high clustering coefficient observed in pure ring networks and the small average shortest path length observed in random networks. This is illustrated in Figure 6.

The results shown in Figure 6 were obtained by means of numerical simulation. However, authors such as [Barrat and Weigt (2000)] and [Barth  l  my and Amaral (1999)] investigated the analytical properties of the Watts-Strogatz model. For instance, [Barrat and Weigt (2000)] showed that the degree distribution of the Watts-Strogatz model can be expressed as follows:

$$P(k) = \sum_{n=0}^{\min(k-\langle k \rangle, \langle k \rangle)} \binom{\langle k \rangle}{n} p^{\langle k \rangle - n} (1-p)^n \frac{(p \langle k \rangle)^{k - \langle k \rangle - n}}{(k - \langle k \rangle - n)!} e^{-p \langle k \rangle}. \quad (1.1.13)$$

In the limit $p \rightarrow 1$ the above expression reduces to

$$\frac{(\langle k \rangle)^{k - \langle k \rangle}}{(k - \langle k \rangle)!} e^{-\langle k \rangle}. \quad (1.1.14)$$

This is the Poisson distribution for the variable $k' = k - \langle k \rangle$ with average value $\langle k' \rangle = \langle k \rangle$.

The rewiring probability, p , also influences the clustering coefficient and the

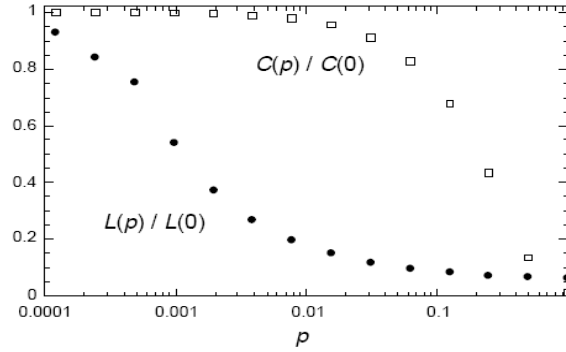


Figure 6: The influence of the Watts-Strogatz model's rewiring probability, p , on the normalized clustering coefficient $C(p)/C(0)$ and the average shortest path length $L(p)/L(0)$. In this example, all the networks consist of 1000 nodes and an average degree (defined as $\langle k \rangle$) of 10 edges [Watts and Strogatz (1998)].

average shortest path length. When $p = 0$ the average clustering coefficient C is

$$C = \frac{3(\langle k \rangle - 1)}{2(2\langle k \rangle - 1)}. \quad (1.1.15)$$

and the shortest average length $\langle l \rangle \sim N$. For $p \neq 0$, Barrat derived the average clustering coefficient as

$$C(p) \cong \frac{3(\langle k \rangle - 1)}{2(2\langle k \rangle - 1)}(1 - p)^3. \quad (1.1.16)$$

In investigating the analytical properties of the Watts-Strogatz model, [Barth  l  my and Amaral (1999)] considered varying the network size N as well as the rewiring probability p . It was noted that the average shortest length for an one dimensional lattice network is $\frac{N}{2\langle k \rangle}$ while for a random network it is $\frac{\log(N)}{\log(\langle k \rangle)}$. For example in a network containing 1000 nodes and an average degree of 10 edges, the average shortest length for a one dimensional lattice and

a random network are 50 and 3 respectively. By varying N and fixing $p \ll 1$, [Barthélemy and Amaral (1999)] defined a critical network size N^* for which a network topology changes from lattice to a small world network. Moreover, the shortest average length behaves as

$$L(p) \sim N^* F\left(\frac{N}{N^*}\right). \quad (1.1.17)$$

where $L(p)$ is proportional to the scaling function F whose independent variable is the ratio $(\frac{N}{N^*})$. Here the scaling factor's limiting behaviour is such that $F(x \ll 1) \sim x$ and $F(x \gg 1) \sim \log x$. In other words for the Watts-Strogatz model, unlike the clustering coefficient, the average shortest length is influenced by both the rewiring probability p and the network size N .

1.1.3 Scale Free Networks

We now turn to an evolving network model that can capture yet more features of real-world networks. [Barabási and Albert (1999)] argued that the Watts-Strogatz small world model's degree distribution follows a Poisson distribution, while for a number of real life networks, such as the worldwide web, the degree distribution follows a power law. Barabási and Albert's motivation for going beyond the Watts-Strogatz model was the fact that, in most real networks, new edges are not located at random but tend to connect to nodes which already have a large number of connections (a large degree). In other words, Barabási and Albert's model objectives is to reproduce how a network grow, instead of modelling a network in its final, equilibrium state. Thus, Barabási and Albert considered combining such preferential attachment conditions with the growing nature of many networks, defining a simple model based on the following evolutionary rules:

- **Growth:** The network initially contains a small core of m_0 connected nodes. At every time step a new node, with m edges ($m < m_0$), is added to the

network.

- **Preferential Attachment:** Each new edge is connected to an existing node (node s) with a probability Π_s proportional to the degree of that node. This can be expressed as

$$\Pi_s = \frac{k_s}{\sum_j k_j}. \quad (1.1.18)$$

where k_j is the degree of node j and $\sum_j k_j$ is the total number of degrees over the entire network. This model is referred to as the scale free model.

However, according to [Bianconi and Barabási (2001)], in order to derive the degree distribution for the Barabási and Albert model of a scale free network, the rate at which a node degree will grow through time needs to be considered. A node s will increase its degree k_s at a rate that is proportional to the probability that a new node will attach to it. Furthermore, at time t , each new edge contributes to the total degree with a factor 2. Therefore $2mt$ edges have been added to the total of the degrees. Hence we have $\sum_j k_j = 2mt + m_0 \langle k \rangle_0$, where $\langle k \rangle_0$ is the average connectivity of the initial core of nodes. Recognising the limitation of using a continuous equation to model a discrete problem, a differential equation that approximates the rate at which a node degree grows can be expressed as follows:

$$\frac{\partial k_s(t)}{\partial t} \approx \frac{m k_s(t)}{2mt + m_0 \langle k \rangle_0}. \quad (1.1.19)$$

Recall that the factor m accounts for the event when each new node adds m edges to the network. Moreover, considering the boundary condition $k_s(s) = m$ in the limit of a large network, then

$$k_s(t) \cong m \left(\frac{t}{s} \right)^{\frac{1}{2}}. \quad (1.1.20)$$

[Newman et al (2006)] showed the degree distribution at time t is:

$$P(k, t) = 2m^2 \frac{t + (m_0/2m)\langle k \rangle_0}{t + m_0} k^{-3}. \quad (1.1.21)$$

and in the limit of large sizes $t \rightarrow \infty$. The solution is therefore

$$P(k) \simeq 2m^2 k^{-3}. \quad (1.1.22)$$

Thus preferential linking of this form provides a power law degree distribution with the exponent equal to 3 as the number of nodes added to the network tends to infinity.

In general, a power law distribution of node degrees suggests a heterogeneous nature of the network's connectivity, in contrast to bell-shaped (i.e. Poisson) distributions where the connectivity is homogeneous and the concept of a typical node can be defined with respect to the average degree $\langle k \rangle$. The heterogeneity of the network's connectivity implies the existence of a large number of nodes that have few edges and a small number of highly-connected nodes, commonly defined as **hubs**. Networks with power law degree distribution are often referred to as **scale free networks** to reflect the scale invariance of the degree distribution.

According to [Barabási et al (2000)], the average shortest distance for a network generated by the Barabási-Albert model is approximately $\log(N)$ for large N . However, [Bollobás and Riordan (2004)] state that this result is only true when m (the number of edges of the new node) is equal to one. Conversely, [Bollobás and Riordan (2004)] showed that when $m \geq 2$ then the average shortest path is approximately

$$L \approx \frac{\log(N)}{\log \log(N)}. \quad (1.1.23)$$

Consequently for networks with the same size N and average degree $\langle k \rangle$, the average shortest distance for those which were generated by the Barabási-Albert model is smaller than those created by Erdős-Rényi model [Boccaletti et al (2006)].

Nevertheless unlike the Watts-Strogatz model, the clustering coefficient is not independent of the network size N and according to [Boccaletti et al (2006)] is approximately $N^{-\frac{3}{4}}$. In other words, as the network size N increases, the clustering coefficient C will tend to 0. In addition to this, the clustering coefficient is lower in comparison with many real life networks. To address this, [Yan et al (2004)] argue for a self-organized model of a scale free network. Similarly to the Barabási-Albert model, Yan et al's approach considered a network that consist of a small number of nodes that are connected with each other. The attachment rules are as follows:

1. At each time step a new node s is added to the network. However, it only connects to m randomly selected nodes.
2. The node s connects to the neighbours of the nodes that it connected to in the previous step, with probability q . For the next $J - 1$ steps (J is a fixed integer), node s executes a similar operation.

This approach leads to the generation of a scale free network whose clustering coefficient is more representative of a real world network. Figure 7 illustrates the schematics of the attachment rule. Figure 8 shows that, for a given size of network N and tuning the probability q and the fixed integer J , a scale free network can be generated with a higher clustering coefficient. In this case $m = 2$, $q = 0.06$ and $J = 1$, and the clustering coefficient of the Yan's model is at least four times as much as the Barabási-Albert model. In comparison [Holme and Kim (2002)] discusses a model that generates a scale free network with a high clustering coefficient of up to 0.5 with $m = 3$. However in this case, the Holme-Kim method generates the scale free network through preferential attachment and then by triad formation. Triad formation is when new node connects randomly (with a probability q) to one of its new neighbour's neighbours. Nevertheless, the new node and its new neighbour's neighbour must not be already connected otherwise another node is

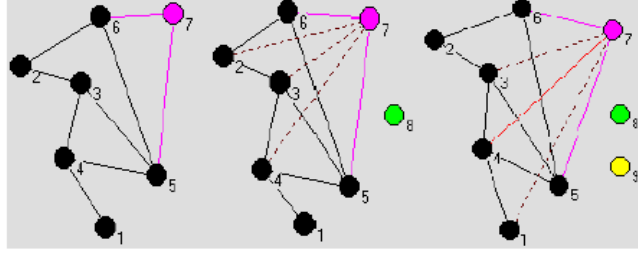


Figure 7: The approach of [Yan et al (2004)] to the preferential attachment rule in order to develop a scale free network with a high clustering coefficient. A new node is introduced at each time step and will connect randomly to an existing node but with a probability q to that node's neighbours at the next time step. The left, middle and right networks represent three consecutive time steps. Here node 7 is introduced at the first time step. The successive time steps show the growth in the number of node 7's neighbours. Nodes 8 and 9 are shown to have arrived but the process of connecting to the network is omitted from this figure. In the second time step, the dash lines extending from node 7 show which nodes it might attach to with a probability of q . It is seen later that node 4 was the only one selected for connection. In the final step, node 4's neighbours are now to be considered for connection to node 7. This again is also shown by the dash lines.

chosen preferentially in the network. The modelling of real life networks and especially the dynamical processes that take place on them [Barrat et al (2008)] will be discussed further in Chapter 2.

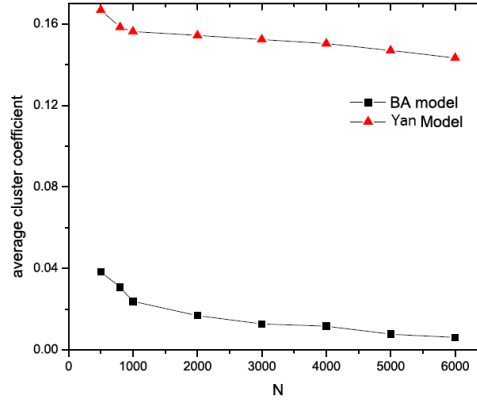


Figure 8: Comparison of the Barabási-Albert (BA) and Yan’s model clustering coefficient for varying network sizes N . In this case $m = 2$, $q = 0.06$ and $J = 1$ [Yan et al (2004)].

1.2 Contribution to Knowledge

By extending the GR problem, in order for it to be played over networks, there have been a number of contributions to current knowledge. A summary of the contributions is given below:

1. To demonstrate the value of modelling a complex system with an underlying network topology, a numerical simulation model was developed. Based on the works of social segregation [Schelling (1971)], this model considered the process of the separation of two political groups over a social network where the maximum number of acquaintances was limited. The results are presented in section 2.2.1.
2. A novel payment mechanism for the GR problem is proposed in order for this game to be played over networks. However, this payment mechanism is still

consistent with the classical and N -player GR problem [Rocha and Stern (2004)]. The methodology is presented in section 3.2 and it is possibly the first time the GR problem has been adapted to be played over networks.

3. In order to model how businesses preferentially connect to each other, a bespoke attachment rule called “kudos” was developed. The methodology is illustrated in section 5.3. Furthermore, for the kudos preferential attachment rule, the network topology undergoes a distinctive phase transition when the player’s target is increased. This does not occur for the degree dependent or randomly selected preferential attachment rules. The results are presented in section 5.3.2.
4. A scaling law for the Extended GR problem was developed and the relationship between it and the critical targets was investigated. The effect of varying a number of parameters to the scaling law was also explored. The results are presented in section 5.3.3

1.3 Thesis Outline

The remainder of the thesis is organized as follows. Chapter 2 introduces the concept of an evolutionary rule which examines the current state of a complex system/game and then indicates what will happen next. Several examples are presented where the evolutionary rules have been adapted so the game can be played over networks.

Chapter 3 reviews a variety of GR problems, including the classical and the N -player. Following on from this, two extended network versions of the GR problem are presented: the “contracting” and “fixed” models.

Chapter 4 addresses the limitations of the contracting and fixed models by introducing a third variation: the “evolving” model. Here, the concept of offspring

is discussed and all three models are compared.

Chapter 5 considers a bespoke preferential attachment rule based on competitive behaviour called “kudos”. An evaluation of how the kudos preferential attachment rule influences the GR problem as well as the evolving network topology will be discussed.

The thesis concludes in Chapter 6, with a summary of the findings and suggestions for future work.

2 Models of Complex Systems played over Networks

According to [Weaver (1948)] the term **complex system** refers to problems that involve dealing simultaneously with a sizeable number of factors which are inter-related into an organic whole. In addition to this, [Barabási (2009)] argues the importance of networks to complex systems by stating that:

The underlying connectivity has such a strong impact on a system's behaviour that no approach to complex systems can succeed unless it exploits the underlying system's connectivity.

For instance, in the field of mathematical epidemiology [Bailey (1975)] it was believed that a virus would eventually die out if its transition rate was below a certain epidemic threshold. However, [Pastor-Satorras et al (2001)] demonstrated, taking the example of a computer viruses, that network topology influences the epidemic threshold. Their results implied that the higher the nodes' connectivity the smaller the epidemic threshold. Furthermore [Pastor-Satorras et al (2001)] showed that, in the case of a scale free network, there is an absence of an epidemic threshold meaning that in this case a virus may never completely die out.

In this thesis, we are concerned with a model of a complex system and associated network topology that influence each other simultaneously. Firstly, in this chapter we consider an example of a complex system and the type of models used to model it. Secondly, a complex system which incorporates the underlying network topology will be considered.

2.1 Models of Complex Systems

The notion of a complex system is not necessarily limited to physical applications but can also help us understand the dynamics of social behaviours too. Models

of the dynamics of social behaviour can be represented by evolutionary rules. To clarify, an **evolutionary rule** examines the current state of the complex system and then indicates what will happen next. Therefore, we use evolutionary rules but specifically those that have a mixture of deterministic and stochastic elements. To illustrate this, [Schelling (1971)] used evolutionary rules to model social segregation. In this context, **segregation** is defined as the process of separating two or more groups from each other. Schelling’s model represented this social behaviour by having two coloured types of individuals living on a chessboard city with the capacity to change their place of living if they did not like the colour of their neighbours. Schelling demonstrated that if individuals have a mild preference for neighbours of the same colour then complete segregation may occur at the city scale.

Schelling produced two models of this complex system: a one- and a two-dimensional segregation version. In the first model, an individual is randomly positioned along a straight line. There are not any blank spaces on this straight line, so every individual will have a neighbour. An individual is happy if a certain proportion of its neighbours located within a specified radius from its location are the same colour as itself. For instance, consider the case where there are two racial groups represented by “circles” and “crosses”, as shown in Figure 9. In this example, the individual assesses the neighbours that are within two places of its location. The individual’s preference is to have more than 50 percent of its neighbours within that defined radius from the same racial group as itself. As can be seen in Figure 9, the red circle indicates that this individual is unhappy because only one of its four neighbours is a circle. In contrast, the green circle indicates that this individual is happy because the majority of its neighbours are circles. Furthermore, each unhappy individual moves by simply inserting itself between two other individuals in a place in which it would be happy. However, as a consequence

of this action other individuals' states may change from happy to unhappy resulting in them moving. As a result, this procedure may go on indefinitely or reach an equilibrium. In a variation of Schelling's work, [Benito et al (2009)] allowed

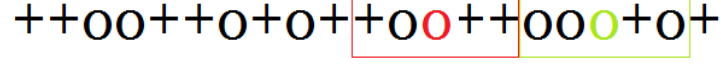


Figure 9: Schelling's one-dimensional segregation model [Schelling (1971)]. The "circles" and "crosses" represent two different racial groups. Here the individual prefers to live in a neighbourhood where the majority are of the same racial type. The red circle is an individual wishing to move while the green circle is content with its location.

an individual who is unhappy to only move one site to the right (in doing so they might remain unhappy). In Benito's model periodic boundary conditions are imposed. To illustrate, Figure 10 demonstrates two results of Benito's approach. A cell is occupied by an individual who is either of type black or type white. The rows moving downwards indicate how the location of each individual has changed through time. An individual is only happy if one of its neighbours either side of it is of the same colour. From Figure 10, it can be seen that segregation emerges from this simple evolutionary rule where the individual has a mild preference to relocate to be close to individuals of the same colour. In addition to this, note that some individuals become happy without moving. This is because the movement of others influences them directly, transforming their neighbourhoods in ways that satisfy their demands in terms of their neighbours' colour/type. We recognise this model as an example of a cellular automaton [Wolfram (2002)], a much-studied class of discrete time, discrete space systems.

Schelling also proposed a two-dimensional version of the same model. For Schelling's original two-dimensional model, the evolutionary rules are as follows:

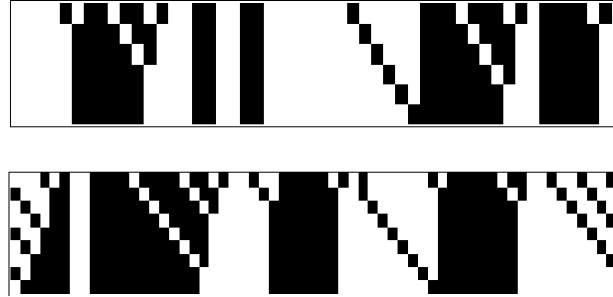


Figure 10: Cellular automata version of Benito's variation of Schelling's one-dimensional segregation model. The top example has 23 black individuals and 27 white individuals. The lower example has 32 black individuals and 29 white individuals. In both cases an individual is happy if one of its neighbours either side is of the same type [Benito et al (2009)].

1. The city is a grid of cells and each cell's neighbourhood has a 3 by 3 square around it, truncated by the city boundaries if close to them.
2. The city is populated by individuals, each belonging to one of two types of groups of equal size. Here they are called Blue and Green.
3. The initial distribution of the individuals across the grid is random, but there is a fraction of vacant cells not occupied by either Blue or Green individuals. This is a departure from the one-dimensional version.
4. At every iteration, every individual calculates the fraction f of its neighbours that are of its own type (friends) within its neighbourhood (empty places are ignored).

5. A threshold value, Ψ , is defined of the fraction of friends within the neighbourhood. This is common to all individuals. Any individual located at the centre of the neighbourhood where $f < \Psi$ decides to leave the cell and relocate to the closest empty cell satisfying the condition $f > \Psi$.
6. Information about any cell changes by an individual immediately becomes available to all other individuals.

[Laurie and Jaggi (2003)] and [Benenson et al (2009)] developed a variation of this model with the inclusion of an additional rule such that if none of the vacant cells satisfy the condition $f > \Psi$, then an individual may move to the closest empty cell. [Benenson et al (2009)] concluded that there is little difference between a randomly generated residential pattern and one which was created through time by the model when there is a weak tendency to reside in a friendly neighbourhood (low Ψ). However, a segregated residential pattern did emerge when there is a strong tendency to reside in a friendly neighbourhood (high Ψ). Figure 11 shows one case where the residential pattern appears random while the other case contains one or more homogeneous patches of Blue and Green individuals separated by unpopulated boundaries. Unpopulated cells are shown in black.

2.2 How Networks Influence the Behaviour of Complex Systems and Evolutionary Games

There are a number of examples of models of complex systems that incorporate an underlying network topology. For instance, [Barrat et al (2008)] discuss models of rumour and information spreading as well as opinion formation. In these examples, the network topology influences the behaviour of the complex system. On the other hand, [Fan and Chen (2004)] and [Gong and van Leeuwen (2003)] considered models where the complex system also influenced the network topology.

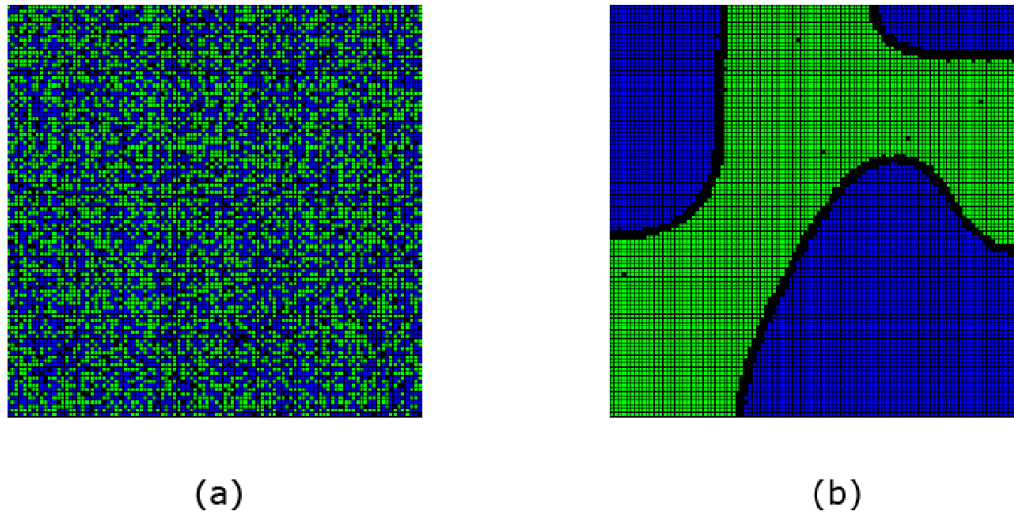


Figure 11: Schelling's two-dimensional segregation model; here 5 percent of space is free, which an unhappy individual can move into. The difference between case (a) and (b) is that the thresholds Ψ are 20 percent and 80 percent respectively. In case (a) the residential pattern cannot be distinguished from a random one, while in case (b) the residential pattern is a segregated one [Benenson et al (2009)].

In both papers, each node's property included an output value calculation from its own logistic map equation plus a weighted average value of the other nodes connected to it. Moreover, new nodes would attach preferentially to the existing nodes. Hence, the complex model influences the network topology but the network topology also influences the complex model.

2.2.1 Schelling's Model with Underlying Network Topology

Section 2.1 discussed the complex system that is Schelling's model of social segregation; as well as this, it also defined segregation as the process of separating two or more groups. An important element of this is an individual is defined as **happy** if a certain percentage of its surrounding neighbours are of the same type, such as nationality, class, religion or racial grouping; otherwise the individual is defined as **unhappy** and tries to move to another location. For example, an individual may wish to live in an area with individuals of the same racial or religious group as itself and move if these conditions are not met. However, consider the segregation of a social network group such as those that occur in Facebook as opposed to geographical locations; in this circumstance the network topology becomes an important element.

[Fagiolo et al (2009)] developed a version of the Schelling's model to accommodate the underlying network topology. Fagiolo defined two types of moves: global or local. **Global** implies that the individual can move to anywhere in the network where there is an empty node (space). **Local** implies that the individual can only move within a certain distance of its current location if there is an empty node within that region; if not, then it remains at its current location. Fagiolo decided, however, that the individual could move from its current location to an available location without being affected by the topology of the network. Fagiolo stated that:

This implies that average path length has no [effect] whatsoever on the dynamic process leading to segregation. A way we can vary a network's average path length in a Watts-Strogatz model is to vary the rewiring probability [Fagiolo et al (2009)]

Nevertheless, to investigate this further, we adapted the rules for Schelling's model of social segregation to the following:

1. The number of individuals of type 1 and 2, the number of empty spaces, the

network topology and the threshold tolerance are chosen.

2. The individuals and empty spaces are randomly assigned to a node within the network.
3. At each time step, an unhappy individual is chosen at random and is moved to the nearest empty node.

The greatest difference between Fagiolo's Global model and the above approach is rule 3. In the earlier approach, the randomly selected unhappy individual is only allowed to move within a certain distance from its location, while in Fagiolo's Global model, an individual can move to any randomly selected empty node within the network. Figure 12 gives an example that illustrates the initial state of a social group of friends where the network topology is a pure ring. The blue nodes are those that support the blue party and the red nodes are those that support the red party. However in this example, an individual desires to have at least 75 percent of its neighbours (social group) support the same party as itself. In this example there are 50 supporters of each party and 15 empty positions. Under the circumstances described, 86 out of the 100 individuals are unhappy with their current social group. In Figure 13, the above rule is repeated 1000 times and it can be seen that the two groups become more segregated. Furthermore, the number of individuals that are unhappy with their social group is now 3 out of 100. Figure 14 illustrates this exercise repeated over a Watts-Strogatz network but with different rewiring probabilities. From Figure 14 it is observed that the pure ring network (rewiring probability of zero) after 1000 rounds has the least number of unhappy individuals and hence the greatest segregation of the two groups. As the rewiring probability increases the rate of segregation becomes slower and the level of segregation decreases as there are more unhappy individuals within their current social group. Hence, by adapting Fagiolo's rules it is observed that there

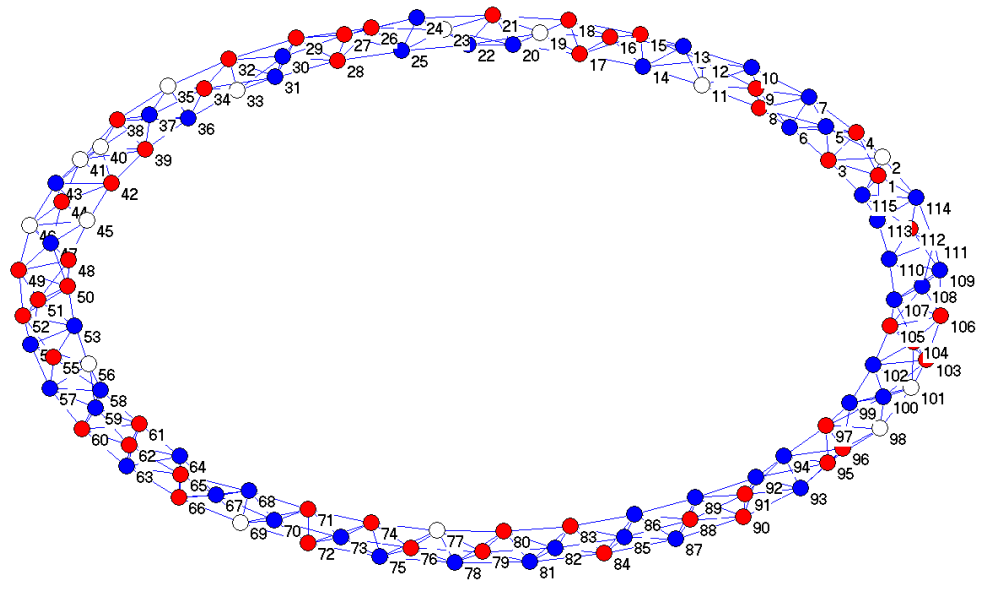


Figure 12: Initial state of a social group; 50 individuals support the red party and 50 support the blue party. The empty cells indicate an empty vacancy or position within the social network. Every individual would prefer to have at least 75 percent of its neighbours supporting the same party as itself. Here 86 out of the 100 individuals are unhappy with their current social group as the previously stated criterion is not being met.

is an influence on network topology that affects the behaviour of the complex system. The potential problem shown by Fagiolo was that the influence of the network topology on the complex system was limited unless the evolutionary rules were varied.

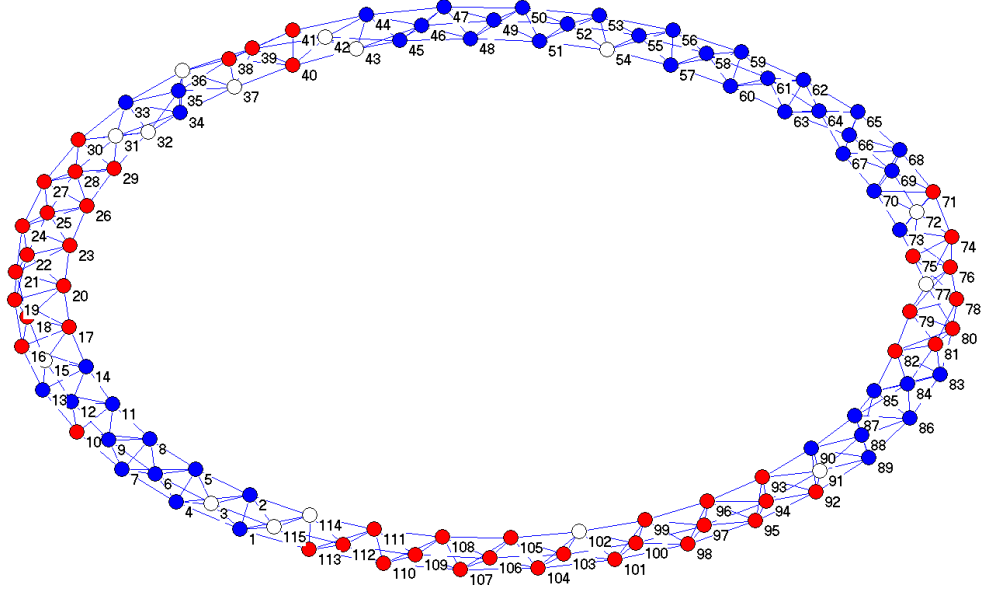


Figure 13: The state of a social group after 1000 individual movements to the nearest empty vacancy; 50 individuals support the red party and 50 support the blue party. Every individual would prefer to have at least 75 percent of neighbours who support the same party as itself. Here 3 out of the 100 individuals are unhappy with their current social group as the previously stated criterion is not being met.

2.2.2 Evolutionary Games

The field of evolutionary game theory [Szabo and Fath (2007)] explores how players choose to cooperate or compete against each other. Through time, a player may change their strategy in order to achieve a certain objective. Models of this behaviour can incorporate the underlying network topology; for example, [Eguiluz and Zimmerman (2005)] and [Nowak and May (1992)] considered itera-

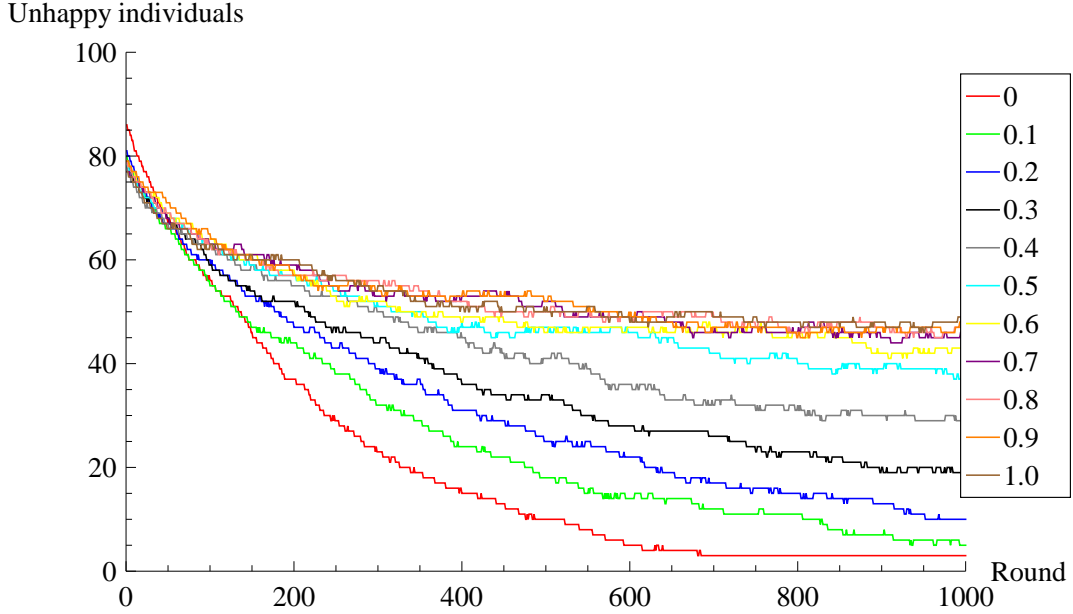


Figure 14: The influence of a Watts-Strogatz model’s rewiring probability p on the number of unhappy individuals within a social group network throughout the simulation duration of 1000 rounds. An unhappy individual is someone who does not have at least 75 percent of neighbours who support the same party as itself. The lower the number of unhappy individuals the more segregated the social network is.

tive prisoner’s dilemma problems played over a Watts-Strogatz network. In these papers, the player adopts a strategy and depending on their neighbours’ strategies receives a certain payoff (score). Furthermore, after a certain number of rounds, the player may wish to review their strategy and adopt a neighbour’s approach if they have a greater payoff. As well as this, [Gómez-Gardeñes et al (2008)] considered how this evolutionary game affected the topology of networks by introducing new players who preferentially attach depending on existing players’ payoffs.

Another evolutionary game theory model developed by

[Southwell and Cannings (2010)] explored a variation of the iterative prisoner's dilemma which is based on an animal social network. In their model, the successful players reproduce in the summer and the weak ones die in the winter. Therefore, they introduce a new concept of successful players having offspring. Successful players having offspring is an important theme and will be discussed in greater depth in Chapters 4 and 5. In addition to this, within their model, the offspring adopt the same strategy as their parent and share their parent's neighbours. In this way the model is mimicking how a newborn inherits their parent's genes and environment.

The evolutionary rules are as follows. Each player employs one of a number of different strategies, which, unlike most other iterative dilemma models, remains fixed throughout the duration of the game. The players' payoff per round is dependent on their neighbours' strategy and the respective payoff related to that strategy. Throughout the duration of the game, the player's payoff from each round is accumulated into a total points score. Irrespective of the strategy, all payoff combinations are set to equal -1 . Therefore, in each round a player's total points score will be reduced by the number of neighbours they are connected to.

The model states that in each round:

- The player is removed from the network if their total points score is less than or equal to $-Q$ (where Q is a positive integer).
- Otherwise, the player has one offspring. The offspring will be connected to the parent as well as the parent's neighbours in the next round.

As a consequence, any player only remains in the network for a finite time (no more than Q rounds).

Unlike previous models of networks, the network in their model will grow and break into sub networks. The theme of networks evolving and fracturing is a

concept that will be explored in Chapter 4. The networks not only break but self-replicate. This means that, after a finite number of steps, the network will not evolve to its original topology but will create multiple separate versions of that topology. Figure 15 illustrates this point. In this example, starting with an isolated node and $Q = 4$, the schematic diagram represents the first six time steps of their model and how the connected structures produce one another. Each row working downwards represents the next time step. Every box in the row represents the network topology produced at that time step. By the fourth time step, the model has self replicated the original topology four times.

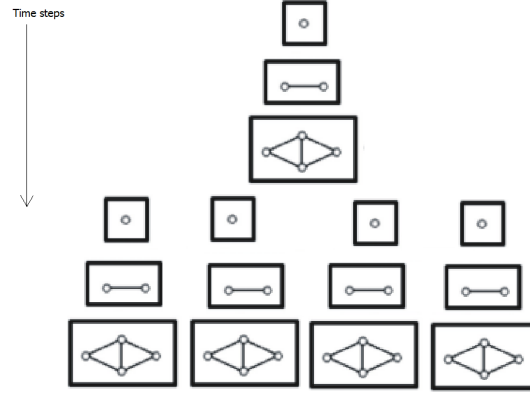


Figure 15: Schematic diagram representing how connected structures produce one another in Southwell’s model for the first six time steps starting with an isolated node where $Q = 4$ [Southwell and Cannings (2010)].

[Southwell and Cannings (2010)] do not discuss scale free networks, small world networks or clustering coefficients. Nor do they try to measure any other properties of their evolving network. This is due to the fact that their main motivation is to model how an animal social network changes over time. When new offspring

are born they will share resources with their parents and their parents' associates. When an individual shares its resources with too many other individuals it starves and dies. In essence, the key question that they are addressing is how the behaviour of the players affects the topology of the network. This is an important theme and will be discussed in greater detail in Chapters 3 and 4.

3 Extending the Gambler's Ruin Problem

The GR problem will be discussed at length in this chapter. In the original GR problem two or more players compete for each other's resources until ultimately a player is ruined (i.e. they lose all of their resources). Subsequently, this probability model has had a number of variants, for example, the classical GR problem which will be considered together with its origins and its properties. We shall note the analytical solution of the N -player GR problem that was derived by [Rocha and Stern (2004)] showing the relationship between the initial resources of the players and the time it takes for an individual player to become ruined.

In Rocha's version of the N -player GR problem all players play each other. In other words, the game is conducted over a fully connected network. However, in this thesis we will describe a version of the GR problem that can be played over any type of network topology and we shall investigate how the game influences the network topology and, conversely, how the network topology influences the game.

3.1 Classical Gambler's Ruin Problem

The origins of the GR problem can be attributed to correspondence in 1656 between Blaise Pascal and Pierre de Fermat. The original problem was posed in this way:

Let two men play with three dice, the first player scoring a point whenever 11 is thrown, and the second whenever 14 is thrown. But instead of the points accumulating in the ordinary way, let a point be added to a player's score if his opponent's score is nil, but otherwise let it instead be subtracted from his opponent's score. It is as if opposing points form 'pairs', and annihilate each other, so that the trailing player always has zero points. The winner is the first to reach twelve points; what are the relative chances of each player winning? [Edwards (1983)]

In 1657, the Dutch mathematician, Christiaan Huygens adapted the problem in his book *De Ratiociniis in Aleae Ludo* (On Reasoning in Games of Chance) [Shoensmith (1986)]. Huygens proposed that each player starts with twelve points. A win for a player would result in a transfer of a resource from their opponent to themselves. The overall winner would be the player who bankrupts the other of all their resources. Eventually, Huygen's adaption became the GR problem.

3.1.1 Properties of the Two Player Gambler's Ruin Problem

In this section we consider the properties of the most well understood GR problem: the two player game. The two player game is defined as follows:

Let two players each have a finite number of resources (say, a for player one and b for player two). Now, flip a coin with each player having 50 percent probability of winning, and transfer a resource from the loser to the winner. Now repeat the process until one player has all the resources. What are the probabilities of each player winning and how long will the game last for? [Ore (1953)]

The two player game can be extended to incorporate a biased as opposed to an unbiased coin. Moreover, the two player game can be extended to encompass a player having a specific upper target to gain. If the player achieves that upper target then the game is halted.

To consider the analytical solution, a player starts with an initial number of resources, a which will increase by one unit with probability p , and decrease by one unit with probability $1-p$. The process stops when the player achieves $a + b$ resources or becomes bankrupt (i.e. loses all of their resources).

Denoting time to achieve (expected duration of the game) by TTA , the probability p_a of a player gaining b resources before losing a resources is [Hadjiliadis (2004)]

$$p_a = \begin{cases} \frac{\left(\frac{1-p}{p}\right)^a - 1}{\left(\frac{1-p}{p}\right)^{a+b} - 1} & p \neq \frac{1}{2} \\ \frac{a}{a+b} & p = \frac{1}{2}. \end{cases} \quad (3.1.1)$$

and the expected duration of the game is

$$TTA = \begin{cases} \frac{a}{1-2p} - \frac{a+b}{1-2p} \times \frac{\left(\frac{1-p}{p}\right)^a - 1}{\left(\frac{1-p}{p}\right)^{a+b} - 1} & p \neq \frac{1}{2} \\ ab & p = \frac{1}{2}. \end{cases} \quad (3.1.2)$$

To illustrate this further, Table 2 considers two numerical examples: flipping an unbiased and a biased coin. As can be seen there is almost zero probability of achieving the target when the probability of winning a round is 0.42. To investigate

	Probability of winning a round	Probability of achieving target	Expected duration of game
Biased coin	0.42	10^{-14}	625
Unbiased coin	0.50	0.50	10,000

Table 2: The effect of using a biased or unbiased coin on the probability of achieving the target (200 units) as well as the expected duration of the game. $a=b=100$ units.

this further, a number of numerical simulations were undertaken using the software tool Mathematica. The simulation was repeated 10,000 times (this is defined as the number of **histories**). Figure 16, for a biased coin, illustrates that a game duration can vary from 250 to 1500 rounds. However, the average duration is close to the expected value of 625. In Figure 17 four out of the total number of histories has been selected to showcase how the resources of the representative player vary over the rounds. Indeed, in these four different cases it is observed that the duration is approximately 600 rounds. Moreover, Figure 16 shows that any duration is possible. Additionally, Table 2 shows the second scenario where the coin is unbiased. From the two player numerical simulation results in Figure 18, it is apparent that in some exceptional cases the game can vary beyond 80,000 rounds even though the expected duration is 10,000. Figure 19 demonstrates that in two out of the four histories showcased, the game finishes beyond 10,000

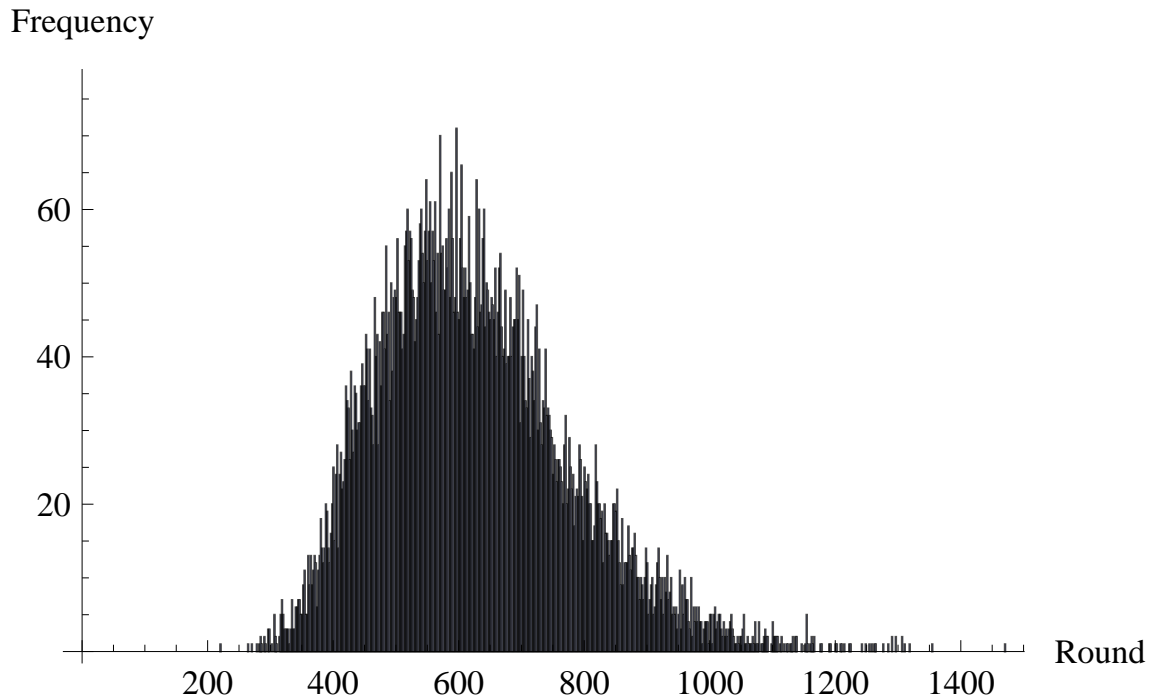


Figure 16: Frequency distribution of the expected duration of a game with the given scenario of flipping a biased coin with probability 0.42 of landing on one side (Table 2). 10,000 histories were undertaken. $a=b=100$ units.

rounds. Nonetheless, Table 3 reveals that the numerical simulation (with 10,000 histories) has an expected duration of 10,115.40 (2 dp) rounds which is just above 1 percent away from the analytical solution. The biased coin scenario in Table 3 demonstrates that the numerical simulation for expected duration is 623.90 (2 dp) in comparison to the actual analytical solution of 625.00 (2dp).

3.1.2 The N -Player Gambler's Ruin Problem

Papers written by [Chang (1995)] and [Sandell (1989)] described analytical solutions for problems that go beyond the two player game. Furthermore, [Rocha and Stern (1999)] discussed an analytical solution for a general N -player

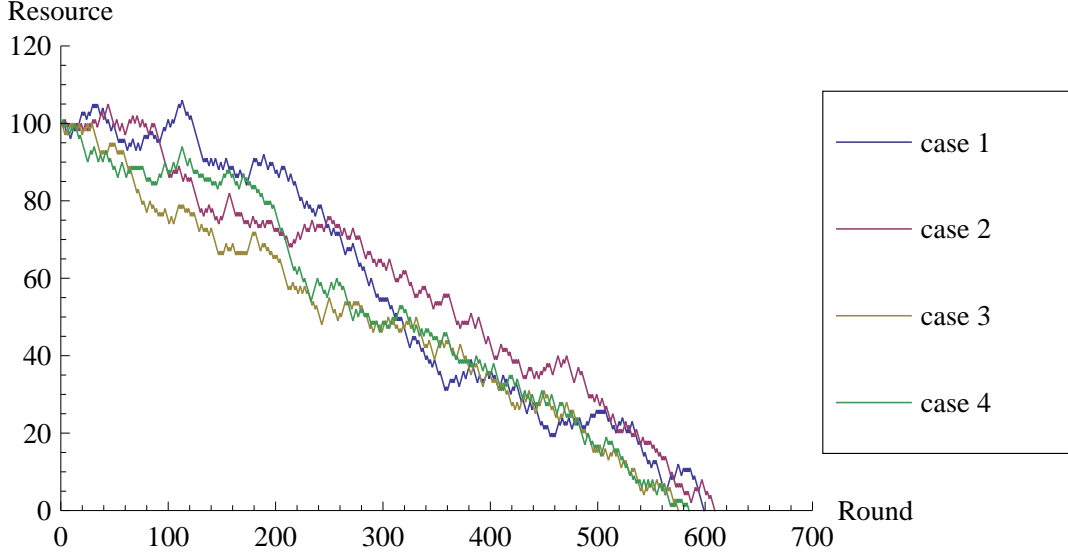


Figure 17: A numerical simulation of how a player's resources vary with each round in four different histories (cases 1 to 4) with the given scenario of flipping a biased coin with probability 0.42 of landing on one side (Table 2). $a=b=100$ units.

	Analytical	Numerical Simulation
	Expected duration of game	Predicted duration of game
Biased coin	625.00	623.90
Unbiased coin	10,000.00	10,115.40

Table 3: Comparison between analytical and numerical simulations for the expected duration of a game. Results are accurate to two decimal places. The number of histories for the numerical simulation is 10,000. The initial resource for the two players is 100 with a target of 200.

game. Rocha and Stern's version of the GR problem encompasses similar objectives to the two player game, namely expected duration to ruin and individual probabilities of ruin. Denoting time to bankruptcy (expected duration to ruin) by **TTB**, their problem can be stated as follows:

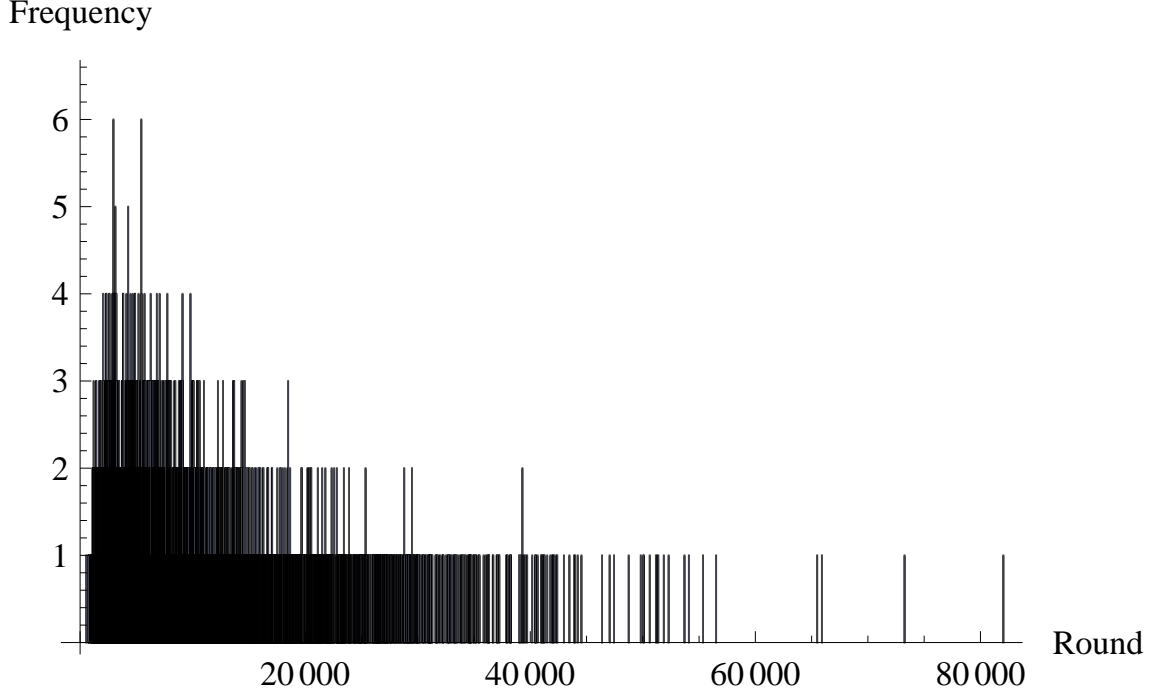


Figure 18: Frequency distribution of the expected duration of a game with the given scenario of flipping an unbiased coin with probability 0.5 of landing on one side (Table 2). 10,000 histories were undertaken. $a=b=100$ units.

Let all N players have an initial and equal resource of I , respectively. In each round, one player, say player i , is randomly chosen to be the “winner” with probability p_i , $i = 1, \dots, N$, where $p_1 + \dots + p_N = 1$. When the probabilities are equal, the game is said to be symmetric; otherwise it is asymmetric. The “winning” player of the round is paid one resource by each of the other “losing” players, for a total gain of $n-1$ resources for the round. The game continues until the first time, TTB , when one or more of the players are ruined. Of interest is the expected time of ruin and the individual probabilities of ruin at time TTB [Rocha and Stern (2004)].

For the symmetrical case Rocha derived the following: if I is the initial resource

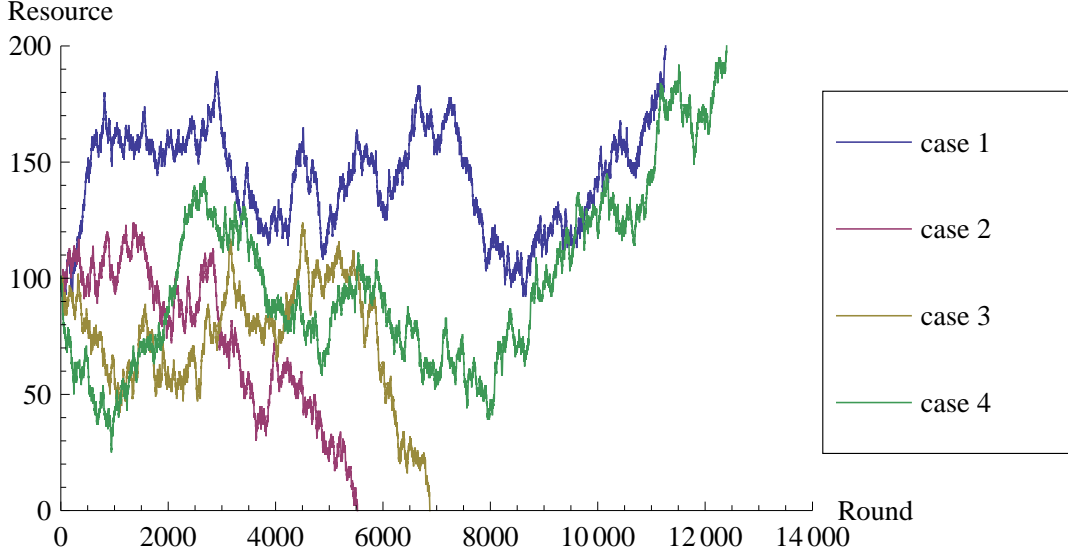


Figure 19: A numerical simulation of how a player's resources vary with each round in four different histories (cases 1 to 4) with the given scenario of flipping an unbiased coin with probability 0.5 of landing on one side (Table 2). $a=b=100$ units.

for all the players, then the expected duration is

$$TTB = \begin{cases} I & 0 \leq I \leq N-1 \\ \frac{N}{1-\alpha} & I = N \\ 1 + \frac{N}{1-\frac{\alpha(N+1)}{2}} & I = N+1. \end{cases} \quad (3.1.3)$$

where $\alpha = N!p_1p_2 \dots p_N$ and $0 \leq I \leq N+1$. The players' individual probabilities of ruin, $P(\text{player}_i)$ in the symmetrical case are:

$$P(\text{player}_i) = \begin{cases} (1-p_i)^I & 0 \leq I \leq N-1 \\ \frac{(1-p_i)^I}{1-\alpha} & I = N \\ \frac{(1-p_i)^I}{1-\frac{\alpha(N+1)}{2}} & I = N+1. \end{cases} \quad (3.1.4)$$

where $p_1 = p_2 = \dots = p_N$. However [Rocha and Stern (2004)] explored when the player's initial resource I is more than the number of players N . A special case for

the expected duration which applied to both the symmetrical and asymmetrical cases was derived. If the initial resource is partitioned into

$$I = N + u. \quad (3.1.5)$$

where u is an arbitrary integer $u = 0, 1, 2, 3, \dots$ and I is the initial resource for all the players then

$$\lim_{N \rightarrow \infty} (TTB - (N + u)) = 0. \quad (3.1.6)$$

This is important as the above expression indicates a relationship between time to bankruptcy, number of players and the initial resource; this argument will be addressed again in sections 3.2.1 and 4.2.

3.2 Gambler's Ruin Problem Played Over Networks

In the previous section we considered the N -player GR problem as described by [Rocha and Stern (2004)]. In their model there were a number of limiting features, in particular players did not have targets, the networks was fully connected and the game ended at the first bankruptcy. In this section, we will explore and remove these limitations. To begin with, we make the following definitions:

A **Round** is one iteration of the GR problem where the players compete/gamble against their opponent or opponents.

A **Game** is a sequence of rounds until a specified conclusion has been reached.

A **specific conclusion**, for example, can be a certain number of rounds being played or only one player being left in the network.

For the network version of the GR problem, it must be determined which player has won a round. Firstly, in order to do this each player will be allocated a score in every round. This is done as follows:

1. At the start of a game each player is given their own normal distribution. For each round, the players' scores are sampled from their normal distributions.

2. The mean of the player's normal distribution is defined as their **strength**.
3. The scores between two competing players are then compared to establish who is the winner of this round.

Each player's strength is sampled from a uniform distribution. In this study the standard deviation remains fixed for each player. Appendix A demonstrates the robustness of the numerical solution to the choice of standard deviation and other statistical parameters. The standard deviation was chosen to calibrate with earlier methodology undertaken in the research.

In order to determine the exchange of resources over this network, the following **payment rule** was adopted:

- In each round, a player gives one unit of resource to its highest scoring neighbour, provided that neighbour scores higher than the player.
- Otherwise the player keeps their resource.

In general, the network version of the GR problem possesses some advantages over previous methodologies and hence makes it suitable to be played over different network topologies. These advantages are:

1. The tossing of a coin is only suited to a two player game.
2. The game does not need to end when the first player becomes bankrupt.
3. The scoring mechanism is linked to the players' strength. The players' strengths do not need updating when the size of the network changes.

When the network is generated, each player is given an unique identification number. In the unlikely event of a tie, the player with the lowest value identification number obtains the resource. Figure 20 demonstrates an example of the payment

mechanism. Here there are three players: A , B and C who score 0.8, 0.3 and 0.5 respectively. Player A has scored higher than its neighbours and will not lose any of its resource. On the other hand, players B and C both lose to A and hence give it one resource. Player B will give only to its highest scoring neighbour. Hence player C , despite scoring higher than player B , receives nothing. Figure 21 demon-

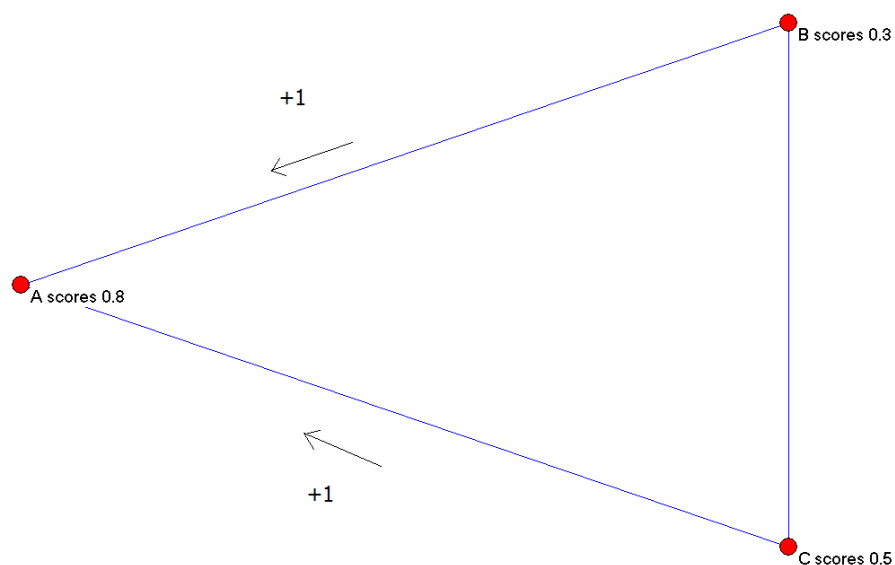


Figure 20: Example of the payment mechanism rule for three players on a fully connected network.

strates another example of the payment mechanism. Players A and D do not play each other but they do have a common neighbour, player C . Both players A and D have scored higher than player C . However, as player D is player C 's highest scoring neighbour, this player will receive one resource from player C .

For each round, a player's score changes and hence the direction and exchange

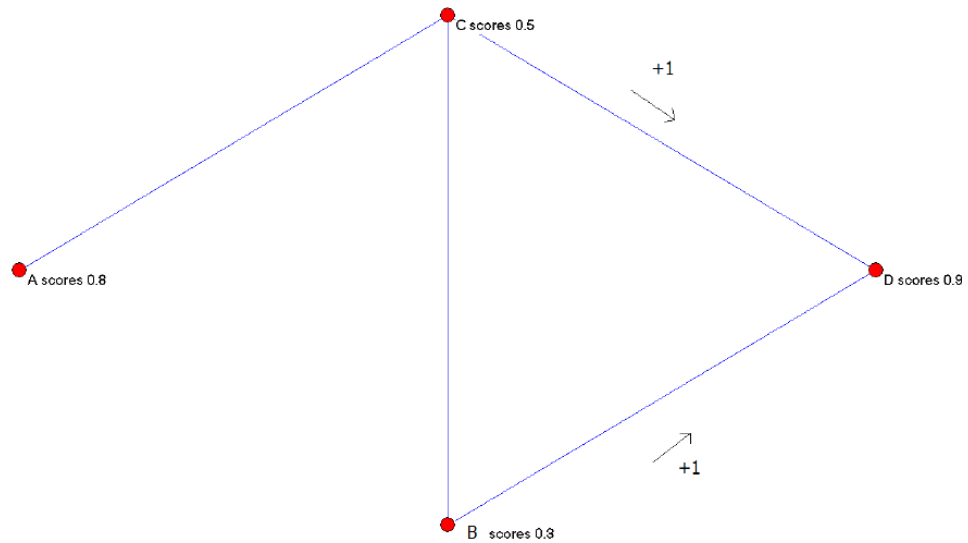


Figure 21: Example of the payment mechanism rule for four players on a non fully connected network.

of resources between the players may change as well.

In our Extended GR problem each player has a target. If the player achieves their target, they leave the network. Those who meet or exceed their target as achievers are defined as **achievers** and those who lose all of their resources as **bankrupt**. Players who do not have any opponents but still have resources are defined as **isolated**.

In the following sections two variations of the Extended GR problem, the contracting and the fixed network models, will be introduced.

3.2.1 The Contracting Model

For the contracting model, a player is removed from the network when they achieve their target or become bankrupt. In addition to this, any isolated players for the current round reconnect to the network in the following round by randomly selecting a prescribed number of existing players. For the numerical simulations, this value was up to three opponents. A higher number of opponents is explored in Chapter 5. Nevertheless, the network topology will always evolve to the two player GR problem. Figure 22 illustrates this point. The left hand diagram shows the first round when the pure ring network consists of 100 players, each having 10 neighbours (opponents). Each player has an initial resource of 100 and a target of 200. After 1000 rounds, the size of the network has reduced from 100 to 53 players. The topology no longer represents a pure ring network. Furthermore, if players 8 or 13 achieve or become bankrupt, there is the possibility that the network will become disconnected. After 4751 rounds, the network topology has evolved into the two player GR problem.

In the previous section we described how [Rocha and Stern (2004)] showed a relationship between the expected duration to ruin and initial network size. However, the contracting model equivalent for the expected duration to ruin is the round in which the first player becomes bankrupt. Nonetheless, the contracting model shares some similar properties to the N -player GR problem. Figure 23 compares Rocha and Stern's fully connected network with the contracting model's results which are played over a pure ring network. For comparison purposes, two pure ring networks, where the player has two and ten neighbours respectively, have been considered. In both cases, in agreement with Rocha and Stern's results, it is observed that the first time to bankruptcy increases with initial network size. Moreover, it is noted that for the two neighbour case, it takes longer for the first player to become bankrupt. As explained in the previous section, in our version of

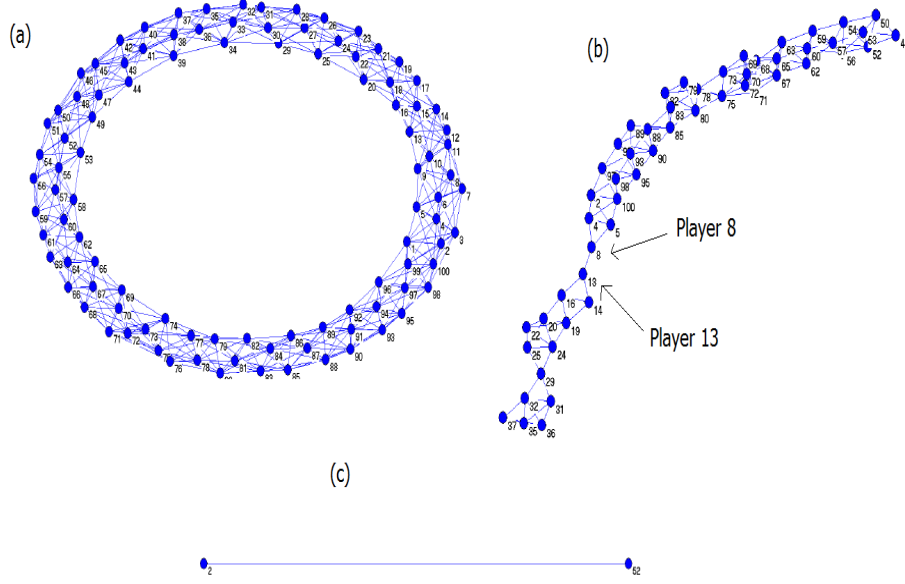


Figure 22: The influence of the contracting model on network topology. Network topology is a pure ring, 100 players with 10 neighbours (opponents) each, initial resource of 100 and a target of 200. (a) This is the first round. (b) After 1000 rounds: network topology is no longer a pure ring, the size of the network has reduced from 100 to 53 players. If players 8 or 13 achieve or become bankrupt, there is the possibility that the network will become disconnected. (c) After 4751 rounds: network topology has evolved to the two player GR problem.

the Extended GR problem, the game does not cease when the first player become bankrupt. Thus, there is a need to explore the properties of the contracting model beyond the first bankruptcy. Furthermore, it will be of interest to see how such parameters are influenced not only by the player's initial resource I and target T but also by the initial configuration of the network topology.

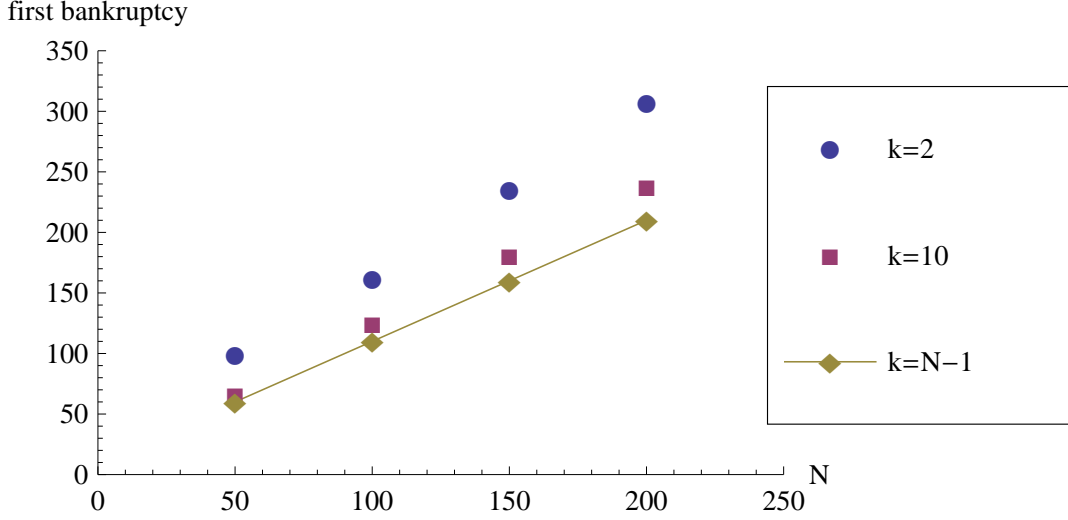


Figure 23: The influence of initial network size N and degree of each player k on the first time to bankruptcy. Comparison of a fully connected network $k = N - 1$ [Rocha and Stern (2004)] with two pure ring networks: $k = 2$ pure ring network with two neighbours; $k = 10$ pure ring network with 10 neighbours. Initial resource I is the numerical value 10 more than the initial network size N . For the contracting model case, results are averaged over 50 histories. For each game, the target is set at a large enough value to ensure that there are no achievements. This is because the [Rocha and Stern (2004)] results do not incorporate players who achieve.

3.2.2 The Evolving Network Model: The Pure Ring Case

In this section we shall investigate further the properties of the contracting model on a pure ring network. This may be considered as the Watts-Strogatz model with rewiring probability $p = 0$. The influence of starting with a network generated by a larger rewiring probability will be discussed in section 3.2.3. Table 4 shows the network topology cases to be investigated. The first property to be considered is the network size. The **Network Size** Nr is defined as the number of players

Cases	Size N	Neighbours k	Initial Resource	Target
Case 1	50	2	60	100
Case 2	50	10	60	100
Case 3	100	2	110	200
Case 4	100	10	110	200
Case 5	150	2	160	300
Case 6	150	10	160	300
Case 7	200	2	210	400
Case 8	200	10	210	400

Table 4: The initial network topologies and players' configurations to be considered in order to determine their influences on the results produced by the extended version of the GR problem. Cases chosen to be consistent with Figure 23.

within the network at a specified round. It is of interest to see how the network size for different topologies and scenarios change through the game. For each case in Table 4, Figure 24 shows the normalised network size, as the game progresses. In each case the game eventually evolves into a two player GR problem. Another two properties to be considered are the mean time to bankruptcy (MTTB) and mean time to achievement (MTTA). **MTTB** and **MTTA** are defined as the average number of rounds for players to become bankrupt or to achieve their targets respectively. The motivation for these parameter is to measure how long the players are expected to remain within the game for differing scenarios. Figure 25 show the MTTB and MTTA. It is worth pointing out that the results shown in Figure 25 results are consistent with those shown in Figure 23 (*TTB* first to bankruptcy) inasmuch as there is a steady linear rise in the result with respect to the initial size of the network. However, the players that have fewer neighbours (opponents) have a longer MTTB and MTTA. For the classical GR problem, a player is expected

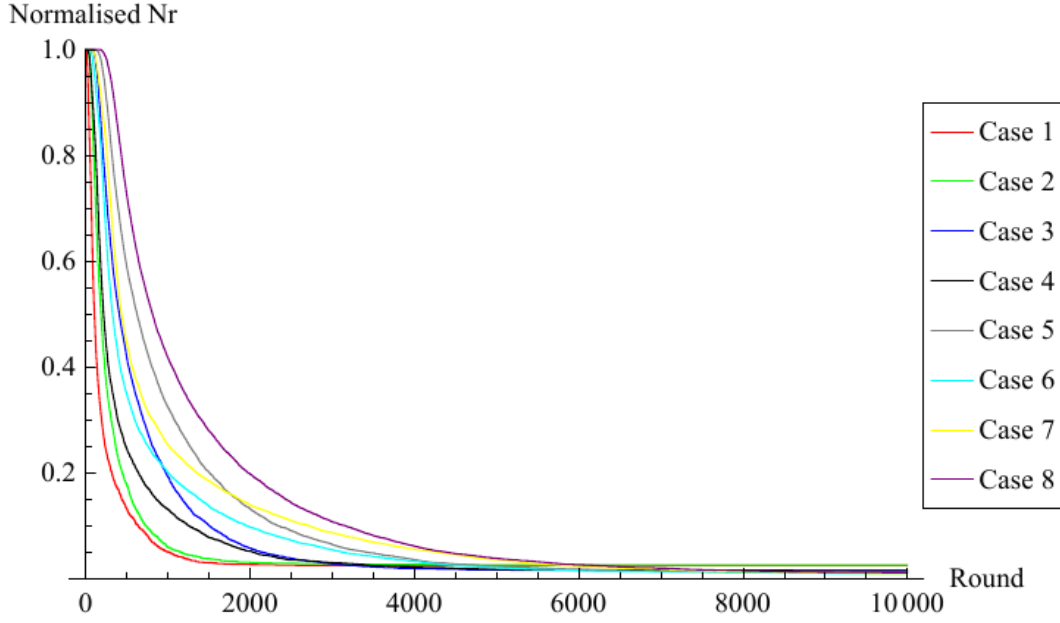


Figure 24: The normalised network size Nr throughout the game for the cases in Table 4. Results averaged over 50 histories. The normalised player per resource is calculated from its respected value for a round, divided by the initial figure for round 1.

to either achieve or become bankrupt; with probability 1 they will not continue playing forever [Stern (1975)].

A key theme for this thesis is how a player's degree changes throughout the game. This is because the player's degree through time gives an indication how the network topology is evolving. Denoting the **Exit Degree** as the number of neighbours the player is connected to when they are about to leave the game through achievement or bankruptcy and **Entrance Degree** as the number of neighbours the player is connected to when they start playing the game, we are able to observe the how the player's degree evolves. Figure 26 show the influence the entrance degree and initial network size N have on the exit degree. This figure

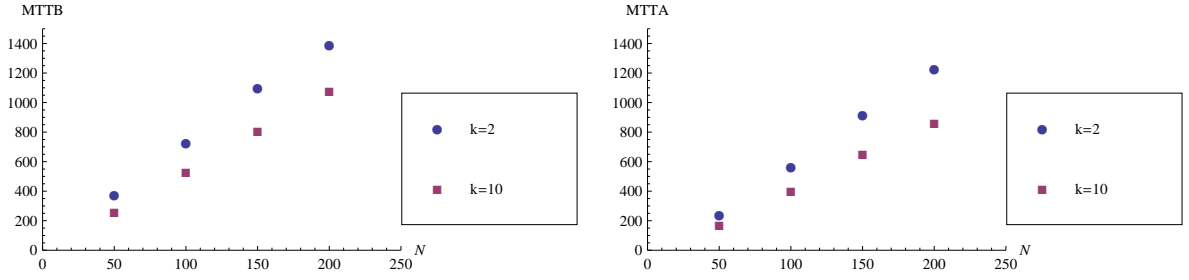


Figure 25: Influence of initial network size N and neighbours k on the mean time to bankruptcy $MTTB$ (left diagram) and mean time to achievement $MTTA$ (right diagram). Initial network topology: pure ring network. Initial resource: 10 more than the numerical size of the network. Target: double the numerical size of the network. Results averaged over 50 histories.

demonstrates that in all cases the exit degree remains steady over the different sizes of networks. However in both figures, the players with an entrance degree of 10 undergo a greater decline to their exit degree than the players with an entrance degree of 2. Furthermore, the exit degree for achievers is higher than those who become bankrupt; this is more apparent when the entrance degree is 10.

As stated in section 3.2 every player is given a mean strength sampled from a uniform distribution. However, as the players start to leave the network, the average strength of the existing players might change. The **Average Strength** is simply the average of all the players' strengths within the network. Figure 27 shows how the initial network size, number of neighbours, initial resources and target influence the average strength of the network, utilizing the cases documented in Table 4. Generally, it is noted that in most cases there is an immediate decrease in average strength after which there is a steady rise to approximately the value of 0.5. However, *case 1* (initial network size of 50 and number of neighbours of 2) presents differently as it steadily converges to a value just over 0.4. This may be due to the relative size of this network and a higher proportion of the strongest players

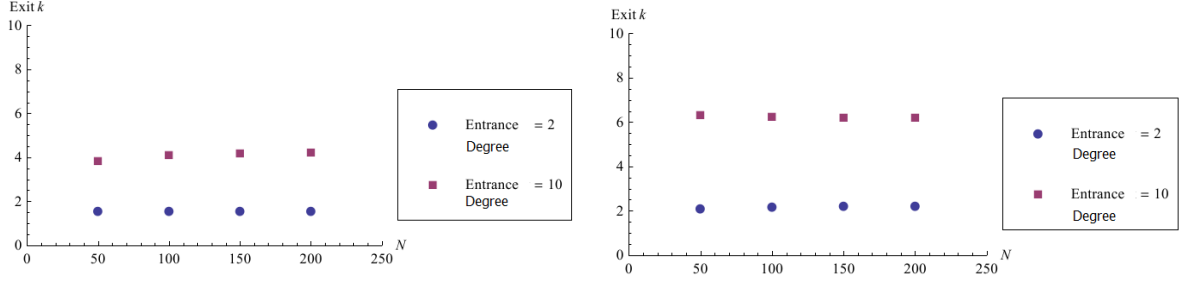


Figure 26: Influence of initial network size N and entrance degree on the exit k (exit degree) of players who became bankrupt (left diagram) and who achieved (right diagram). Initial network topology: pure ring network. Initial resource: 10 more than the numerical size of the network. Target: double the numerical size of the network. Results averaged over 50 histories.

achieving prematurely during the game. The **gain loss** parameter is defined as the difference between the total resources acquired to achieve by the achieving group of players and the total resources lost by the bankrupt group of players respectively. This parameter is updated every time a player leaves the game. The gain loss parameter provides a metric that could indicate which network topology is the more suitable for players to achieve. Figure 28 shows how the initial network size, number of neighbours, initial resources and target influences the gain loss parameter of the network, again utilizing the cases documented in Table 4. Notably in *case 8*, where the size of the network is 200 and the number of neighbours is 10, it is observed that at first there is a rapid rise in the gain of the network, followed by a loss. This is due to a large number of players achieving and leaving the network, followed by those who become bankrupt. Moreover, for the same case another oscillation is observed at approximately the 2,000 round mark. Finally, **resource per player** is defined as the total of the resources in the network divided by the number of players within the network. This parameter measures how competitive

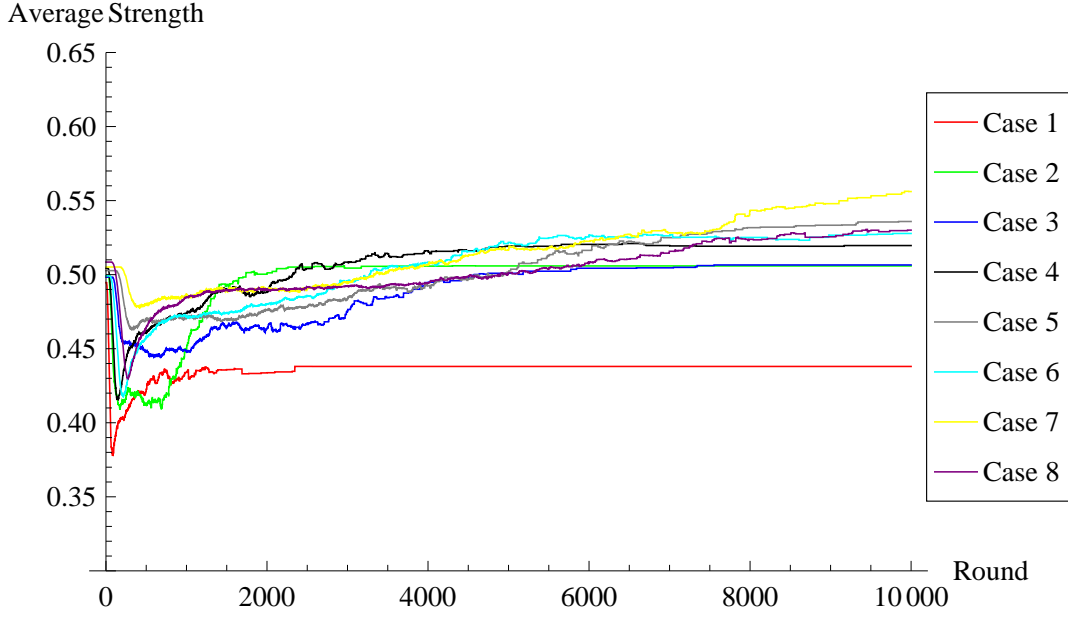


Figure 27: The influence of initial network size, degree, initial resources and target (Table 4) on the average player's strength (average strength) in the network throughout the game. Results averaged over 50 histories.

a game has become due to, for example, a decrease in the total resource in the network because of achievement. Figure 29 illustrates how the initial network size, number of neighbours, initial resources and target influence the resource per player of the network utilizing the cases documented in Table 4. An interesting result is found in the smaller networks $N = 50$ (*case 1 and 2*) where the resource per player parameter reacts more sensitively to the number of neighbours. For *case 1* (*two neighbours*), the normalised resource per player reduces to approximately 0.8 of its initial value while for *case 2* (*10 neighbours*) it increases to 1.4. This suggests that for the contracting model, the player with a higher degree exhibits a shorter *MTTB* which is consistent with the results observed in Figure 25.

To conclude, this section has considered different key parameters to indicate

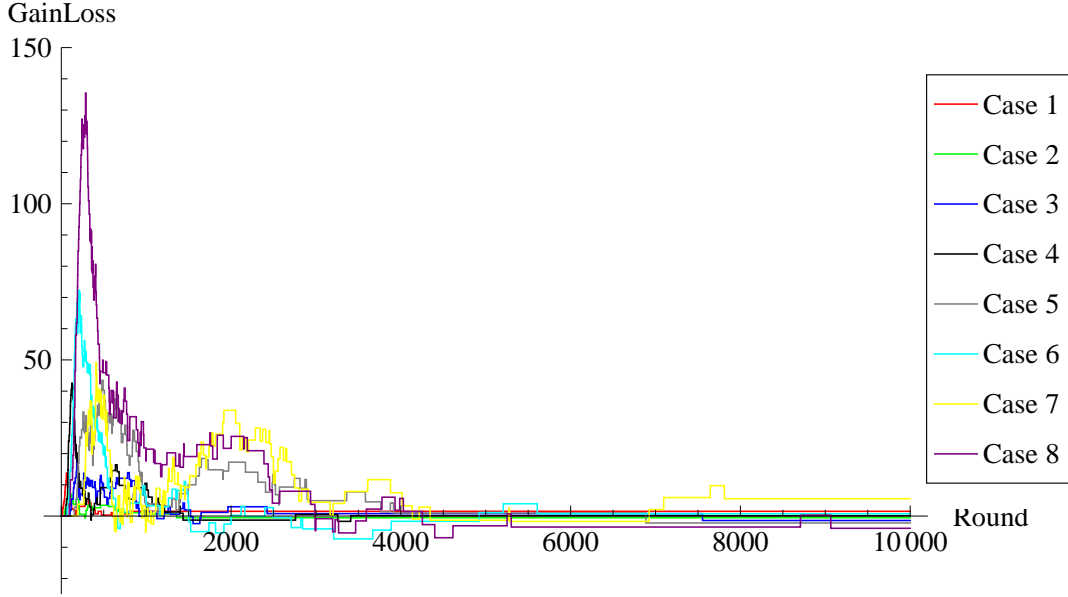


Figure 28: The influence of initial network size, degree, initial resources and target (Table 4) on the gain loss parameter (*GainLoss*) of the network throughout the game. Results averaged over 50 histories.

how the network evolves under the influence in our extended version of the GR problem. As well as this, the question of how the extended version of the GR problem itself has been influenced by generic network properties was also considered.

3.2.3 The Effect of the Watts-Strogatz Model's Rewiring Probability

In section 3.2.1, we showed the influence of the Watts-Strogatz model's rewiring probability p on the number of unhappy individuals within a social group network as an example how a game can be influence by its network topology. In the previous section we discussed the properties of the contracting model played over a pure ring network. In this section, however, we will explore how those properties may alter when we increase the Watts-Strogatz model's rewiring probabilities. According to

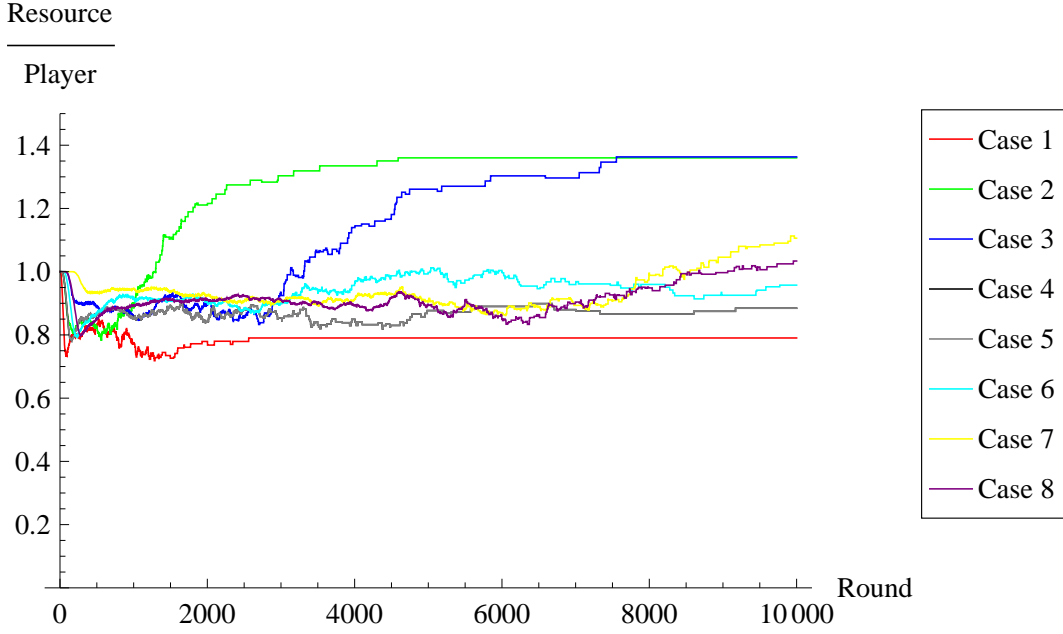


Figure 29: The influence of initial network size, degree, initial resources and target (Table 4) on the normalised resource per player parameter of the network throughout the game. Results averaged over 50 histories.

[Newman and Watts (1999)], the region for which the network crosses over from pure ring to small world is approximately $p = \frac{1}{N \times k}$. For all the cases in Table 4, we have chosen a rewiring probability of $p = 0.1$ to ensure that these networks indeed fall into the small world region. As well as this, we have chosen the rewiring probability of $p = 1.0$ to represent random networks.

Firstly we will investigate the influence the initial network size and player's degree has on the numbers of players throughout the game for varying network topologies. Figure 24 illustrated the pure ring network. However, Figure 30 shows the results from repeating the numerical simulations on small world and random network topologies respectively. Notably, it was observed that all the three initial topologies for the contracting model converges to a two player GR problem. *Cases*

1 and 2: initial network size of 50 players show the most rapid decline for the three different network topologies. Figure 30 shows that case 5: initial network size of 150 players and two neighbours before rewiring and case 7: initial network size of 200 players and two neighbours before rewiring have the slowest decline as opposed to case 8: initial network size of 200 players and 10 neighbours. Indeed it is presumed that this is a result of the rewiring functionality of the Watts-Strogatz model.

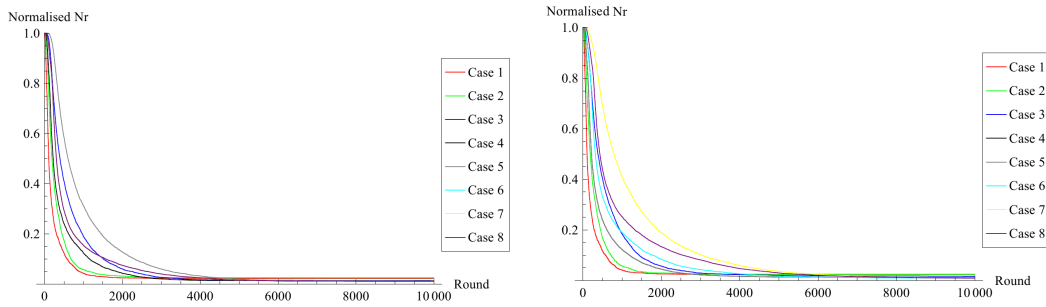


Figure 30: The influence of initial network size, degree, initial resources and target (Table 4) on the normalised network size Nr throughout the game for the network generated by the Watts-Strogatz model $p = 0.1$ (left diagram) and $p = 1.0$ (right diagram). Results averaged over 50 histories.

Now we will investigate the influence the initial network size and player's degree have on the average strength throughout the game for varying network topologies. Figure 27 demonstrated the pure ring network while Figure 31 represents the small world and random network topologies respectively. In comparing the three different topologies, it is observed that there are a number of similarities between the pure ring and small world network topologies. For instance, the average strength for each topology in most cases approaches a steady state. As in the pure ring topology, the case 1 average strength converges to a value of approximately 0.42 for these topologies. In contrast, in the random network topology, the average

strength in some cases converges to a slighter higher value. This suggests that for the random network topology, the stronger players remain longer in this game than weaker opponents. By repeating the gain loss parameter exercise in Figure 28

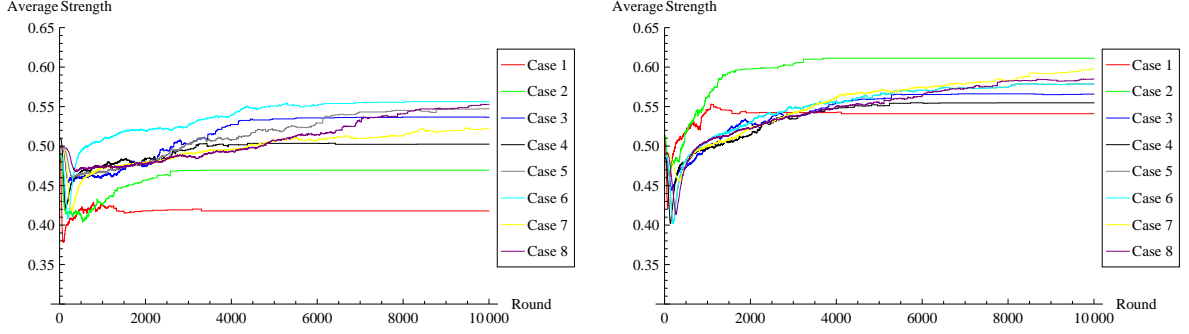


Figure 31: The influence of initial network size, degree, initial resources and target (Table 4) on the average strength throughout the game for the network generated by the Watts-Strogatz model $p = 0.1$ (left diagram) and $p = 1.0$ (right diagram). Results averaged over 50 histories.

for the small world and the random networks, it can be seen that each result is largely the same (Figure 32). *Case 8: initial network size of 200 players and 10 neighbours* oscillates for all network topologies with its second peak occurring at approximately round 2000, but decaying to zero value after about 4000 rounds. However, this is not the case for the small world network, as the average strength becomes approximately zero after about 6000 rounds.

The resource per player parameters have previously been discussed in terms of the influence the pure ring network topology had on this parameter as demonstrated in Figure 29. This will now be compared and contrasted with the small world and the random networks (Figure 33). There is little significant difference between the network topologies.

The main conclusion that can be drawn is that, despite the differing network topologies, the contracting model always evolves to a two player GR problem.

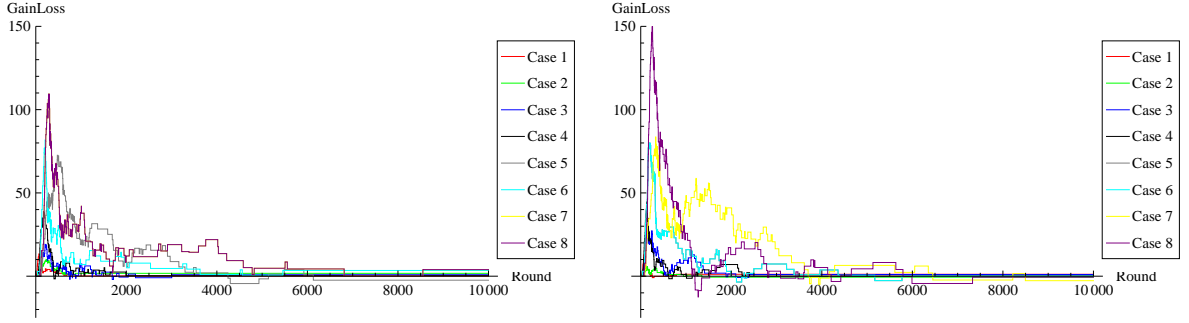


Figure 32: The influence of initial network size, degree, initial resources and target (Table 4) on the gain loss parameter (*GainLoss*) throughout the game for the network generated by the Watts-Strogatz model $p = 0.1$ (left diagram) and $p = 1.0$ (right diagram). Results averaged over 50 histories.

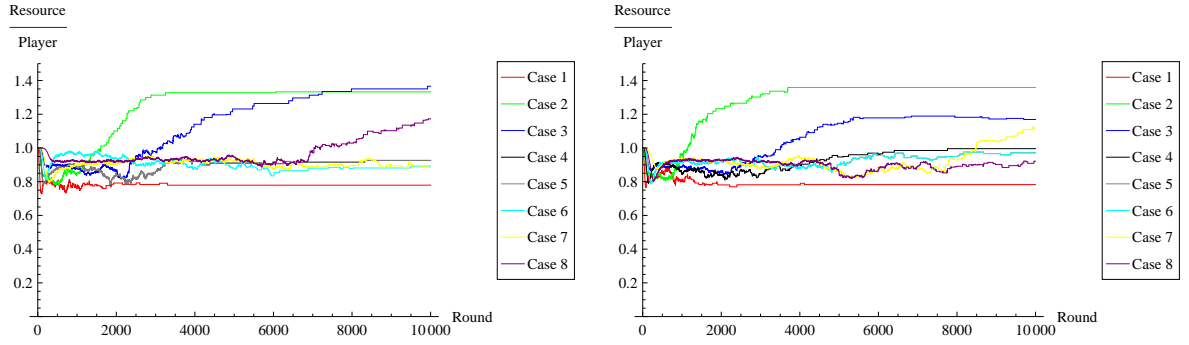


Figure 33: The influence of initial network size, degree, initial resources and target (Table 4) on the normalised parameter resource per player throughout the game for the network generated by the Watts-Strogatz model $p = 0.1$ (left diagram) and $p = 1.0$ (right diagram). Results averaged over 50 histories.

As well as this for the global parameters described in this section, there appears, surprisingly, to be little significance difference between the networks generated by the Watts-Strogatz model when $p = 0.1$ and $p = 1.0$.

3.2.4 The Fixed Model

[Nowak and May (1992)] and [Huang et al (2004)] have undertaken numerical simulations of complex systems which are influenced by the underlying network topology. Nowak studied the iterative prisoner's dilemma problem while Huang simulated the spread of SARS in Singapore. Nowak and Huang both incorporated the Watts-Strogatz model to produce a small world network and chose to keep the network topology fixed for the entire duration of the numerical simulation. Although this is in contrast to the contracting model, this serves to inspire another version of the Extended GR problem, where the network topology remains fixed throughout the numerical simulation. This version will be known as the fixed model. The rules for the fixed model remain similar to those of the contracting model, although one rule is different: when a player achieves or becomes bankrupt they rejoin the network immediately, restarting with their original initial resources. The player also reconnects and plays with its original opponents. Under these circumstances, the network topology remains fixed throughout the game. Consequently, the network size and the average strength of the network remain constant. Although this may be true, the gain loss parameter and resource per player will not remain constant. However, in the resource per player case Figure 34 illustrates that over the simulation duration this parameter exhibits a small variation. This value is not constant because a player can achieve with resources beyond their target and this extra resource is not allocated to them when they rejoin the game. However this imbalance is addressed when the bankrupt player restarts with their original initial resource. This means that the total resources in the network will experience a small fluctuation as different players do not necessarily achieve and become bankrupt at the same time. The resource per player parameter will not be discussed any further in this section.

Figure 35 illustrates the gain loss parameter for the Watts-Strogatz model pure

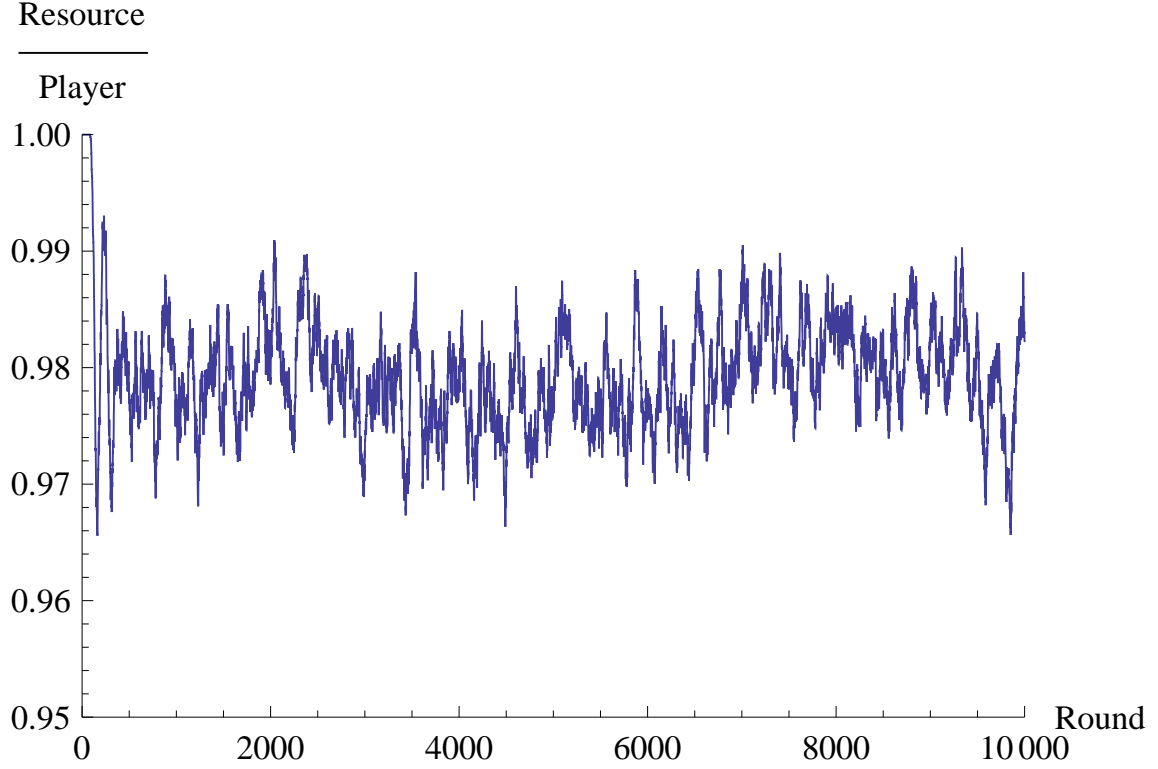


Figure 34: The influence of the fixed model on the normalised Resource/Player parameter throughout the game. Network topology is a pure ring, 100 players with 10 neighbours (opponents) each, initial resource of 110 and a target of 200. Results averaged over 50 histories.

ring ($p = 0.0$), small world ($p = 0.1$) and random ($p = 1.0$) networks respectively. In contrast to the contracting model (Figures 28 and 32), the fixed model gain loss parameter oscillates without the damping effects. Nevertheless for the fixed model, there appears to be little difference between the results for the three different network topologies generated by the Watts-Strogatz model. The Watts-Strogatz network for the fixed model produced similar results. On the other hand other network topologies such as those generated by Erdős-Rényi and Barabási-Albert may generate a different result. Table 5 describes the cases considered where all

network topology sizes are fixed to 100 players. The influence of different network sizes will be discussed in Chapter 5. We wish to consider the value of the gain

Case	Network description
ER 0.25	Erdős-Rényi model of a random network probability of connection = 0.25
ER 0.5	Erdős-Rényi model of a random network probability of connection = 0.5
ER 0.75	Erdős-Rényi model of a random network probability of connection = 0.75
WS 0.0	Watts-Strogatz model probability of rewiring = 0.0
WS 0.1	Watts-Strogatz model probability of rewiring = 0.1
WS 1.0	Watts-Strogatz model probability of rewiring = 1.0
BA	Barabási-Albert model scale free network

Table 5: The list of network topologies to be investigated in order to determine their influence on the fixed model. All networks are fixed to 100 players, initial resource of 110 and a target of 200.

loss parameter after 10,000 rounds. Figure 36 shows for that there is a noticeable difference between results produced by the Erdős-Rényi and Barabási-Albert models and those produced by the Watts-Strogatz model. This is especially true for the network generated by the Erdős-Rényi model with a probability of connection $p = 0.75$. This suggests that the network topology may have an influence on the game. To understand the results shown in Figure 36 further, we explore

the achieving player's exiting degree of each of the network topologies considered in Table 5. This is because, given that each case considered in Table 5 has every player with the same initial resource and target, then there must be another factor that results in more achievements in one type of network topology as opposed to another. Figure 37 illustrates the achieving player's exit degree for each of the network topologies considered in Table 5. In most cases, a network topology that exhibits a gain loss parameter also has a high exit degree for its achieving players. This theme will be investigated further in Chapter 5, with different network sizes also taken into consideration.

In conclusion to this chapter, [Rocha and Stern (2004)] extended the classical GR problem from a two player to a N -player game. They derived a result linking the number of players and initial resource to the first expected time of bankruptcy. However, they assume a fully connected network and their analytical results are only valid under simplifying conditions, i.e. for an initial resource whose value approximates the number of players, an equal initial resource and an infinite target. Unlike previous models, the version of the GR problem presented in this thesis goes beyond the first expected time of bankruptcy. As a result, new parameters such as MTTB (mean time to bankruptcy) and MTTA (mean time to achievement) have been introduced in this thesis. In addition to this, two variations of the Extended GR problem were introduced: the contracting and fixed models. The contracting model had the property of always evolving into a two player GR problem while the fixed model indicated the importance of the achievers player's exiting degree in influencing the game.

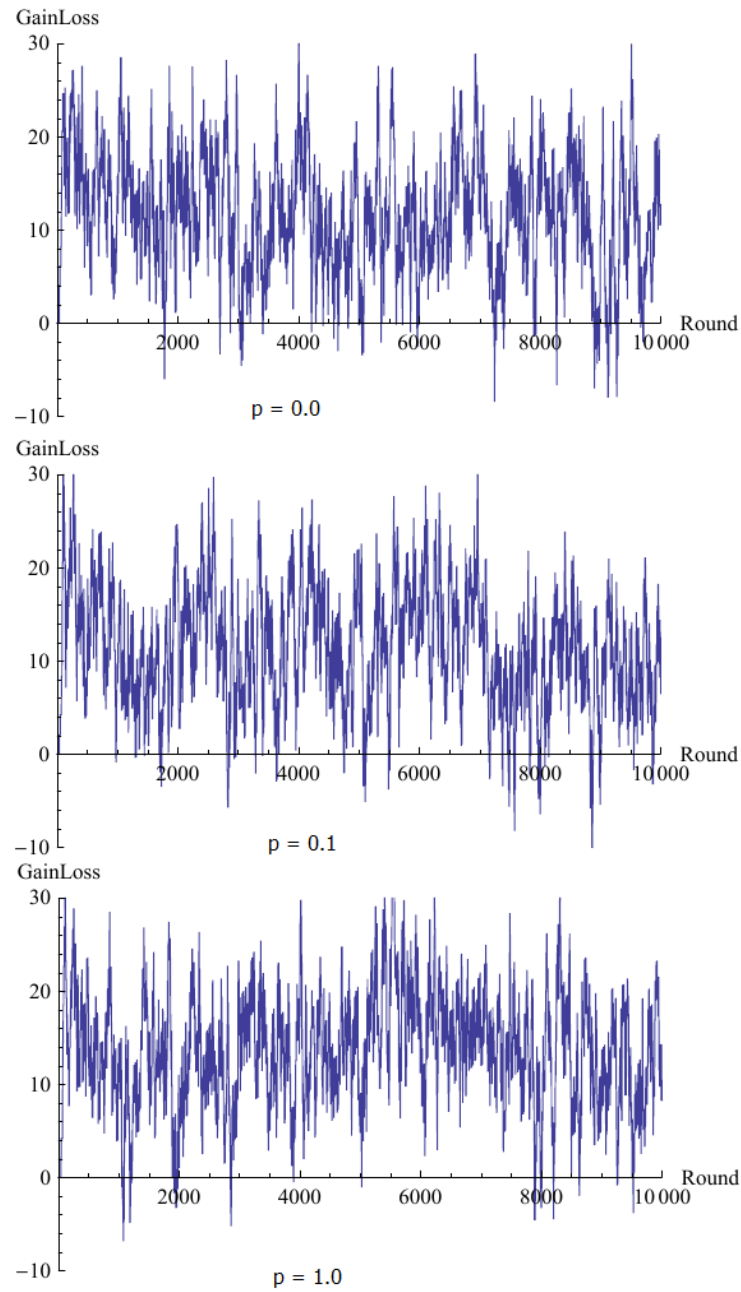


Figure 35: The influence of the network topology generated by the Watts-Strogatz model with $p = 0.0, 0.1$ and 1.0 on the gain loss parameter (*GainLoss*) throughout the game for the fixed model. Initial network size 100, initial resources of 110 and a target of 200. Results averaged over 50 histories.

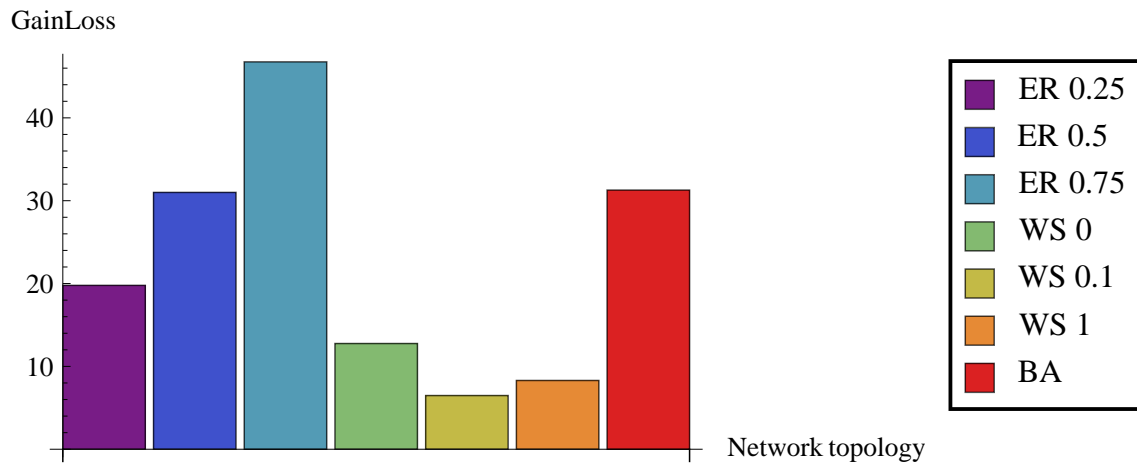


Figure 36: The influence of different network topologies (Table 5) on the gain loss ($GainLoss$) parameter after 10000 round for the fixed model. Initial network size 100, initial resources of 110, a target of 200. Results were averaged over 50 histories.

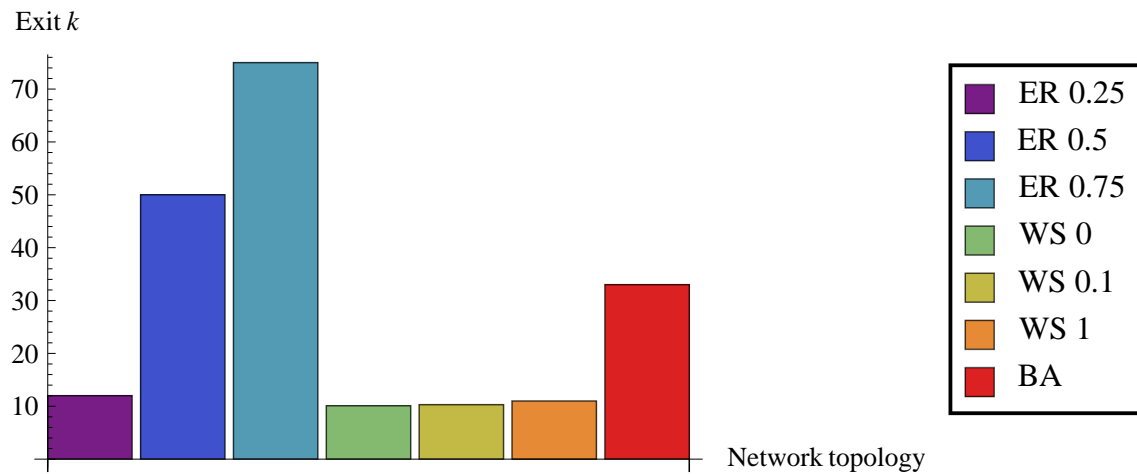


Figure 37: The influence of different network topologies (Table 5) on the achieving player's exit degree k for the fixed model. Initial network size 100, initial resources of 110, a target of 200. Results were averaged over 50 histories.

4 The Evolving Network Model

In this chapter we introduce another variation of the Extended GR problem, in which the network topology evolves more generally as the game is played as opposed to remaining fixed or contracting as in the previous cases.

4.1 Offspring and the Fish-Plankton Model

In the real world of competition, a successful business or social enterprise may deliver what can be thought of as **offspring** (see section 2.2.2). For example, a successful fast food company will create franchises of its brand and locate the new restaurants around the world [Kalnins and Lafontaine (1960)]. Likewise, a successful church with a large congregation may plant new churches in different communities even if a rival church is there already [Hayward (1999)].

In order to investigate competitive behaviour and offspring further, the Fish-Plankton model [Klopfer (2008)] will now be considered.

The Fish-Plankton model is played over a three-dimensional lattice and is a variation of the predator-prey model [Kot (2001)]. Initially each individual entity, whether fish or plankton, is placed randomly within the three-dimensional lattice, and then each fish move, eats plankton, reproduces and dies. On the other hand, the plankton move around more slowly and reproduce. The Fish-Plankton evolutionary rules for the fish are as follows:

- F1. Allocate to each fish an initial and a target energy figure.
- F2. At each time step, the fish moves into an adjacent cell which has been randomly chosen. The fish loses a small amount of energy.
- F3. Plankton that occupy the same cell as a fish will be eaten. Subsequently, the fish will gain a large amount of energy.

F4. A fish that loses all of its energy dies.

F5. A fish that has reached a target energy figure produces an offspring. In the next round, both the parent and the offspring's energy figures are set to the initial value.

The Fish-Plankton evolutionary rules for the plankton are as follows:

P1. At each time step, the plankton moves into an adjacent cell which has been randomly chosen.

P2. The plankton produces offspring after a certain number of time steps.

The Fish-Plankton model shares a similarity with the contracting version of the Extended GR problem. Notably in both models, if a player fails they are eliminated from the simulation, for example, when a fish dies or a player becomes bankrupt. In contrast, however, in the Fish-Plankton model, a fish is rewarded for success (reaching a target energy figure) by having an offspring. In our contracting model a player who achieves their target simply leaves the network. We now enhance our model to incorporate the possibility of successful players producing offspring.

4.2 Offspring within the Gambler's Ruin Problem

As discussed in the previous section, there are examples from the real world of competition as well as theoretical models where successful players are rewarded with offspring. To incorporate offspring, the model rules were adapted in the following manner:

1. When a player achieves or exceeds their target, they leave the network.
2. The total resource (those gained plus the initial resource) is divided equally between the achiever's offspring.

3. Any resources remaining are randomly given to one of the offspring.
4. All offspring connect to the existing players in the network and play with the same target as their achieving parent.
5. The offspring inherit the same strength as their achieving parent.

In order to investigate the properties of the evolving model, a comparison with the contracting version of the Extended GR problem was used. As was previously stated in Chapter 3, the contracting model converges to the classical GR problem. However, the evolving model introduces offspring whenever a player achieves. To understand the influence of offspring, we consider four different cases which are detailed in Table 6. Here the attachment rule and number of neighbours are varied. The number of offspring per achiever and their degree will be explored in Chapter 5.

Case	Attachment	Neighbours k	Offspring per Achiever	Offspring k
case a	random	2	3	3
case b	random	10	3	3
case c	degree dependent	2	3	3
case d	degree dependent	10	3	3

Table 6: Details of the cases investigated by varying the attachment rules and neighbours k .

The **final population** N_f is defined as the size of the network after 10,000 rounds. Figure 38 illustrates the influence on the final population when the numerical simulation receives a variation in the initial size of the network, the attachment rule and the number of neighbours. Overall, the final population increases with the size of the initial network; the attachment rule and number of neighbours do not have a dominant influence on this parameter. Consequently, unlike the

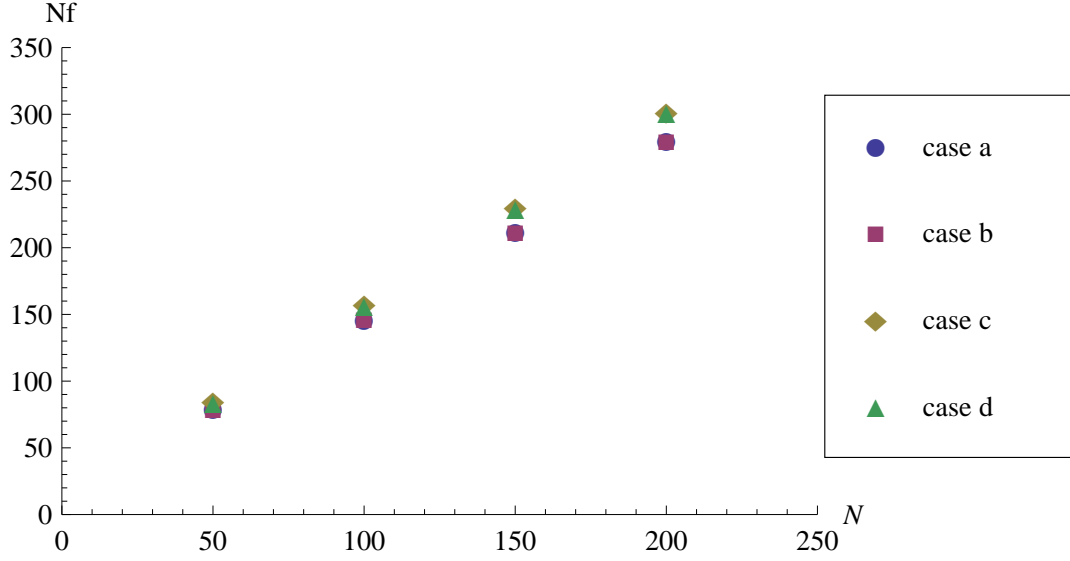


Figure 38: The influence of the attachment rule, number of neighbours and initial size of network N on the final population Nf . For cases see Table 6. The initial resource is the initial network size plus 10. The target is double the initial size. Results averaged over 50 histories.

contracting version, the evolving model does not converge to the classical GR problem in all situations. Moreover, the evolving model's network topology does not necessarily decay into a two player game. To illustrate this, Figures 39 to 41 demonstrate an initial network size of 100 players growing to 130 after 500 rounds and then 146 after 9500 rounds. However, it is possible for the network to become segmented; for example, three players could separate from the remainder of the population. Nonetheless, over time this could be resolved in one of two ways. Firstly, offspring or recently isolated players may connect to both parts of the network, hence forming a bridge. Alternatively, one of the players reconnects to the main body when their opponents achieve or become bankrupt. In contrast, unlike Southwell's model this evolving model exhibits no numerical evidence of self-replication (section 2.2.2).

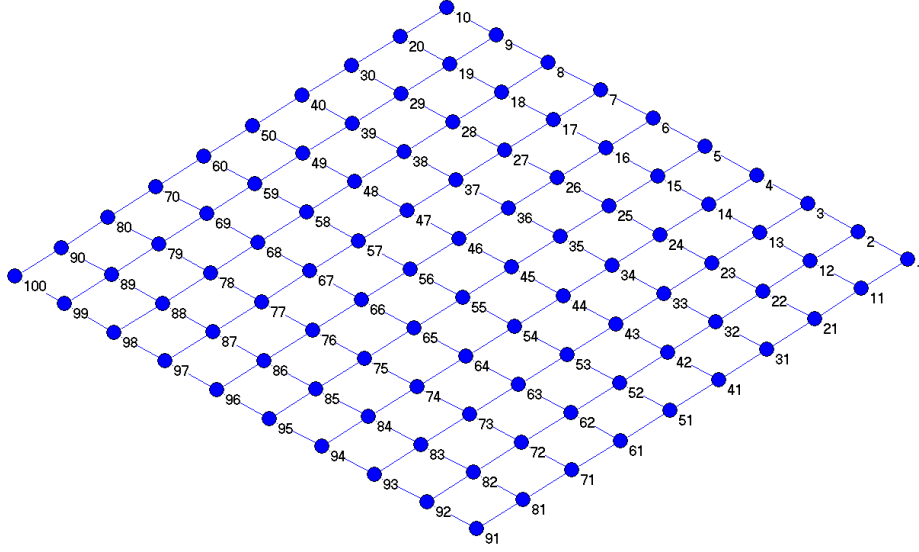


Figure 39: The initial evolving model's network topology at the first round. This is a 10 by 10 lattice network.

As discussed previously, the evolving model's network size may increase from its initial configuration. Figure 42 demonstrates the numerical growth of the network throughout the simulation. In each case, the population is normalised by dividing it by its original value for round 1. Table 7 depicts the various scenarios to be simulated. In all cases, the network size grows to a steady state, where the degree dependent attachment rule leads to a higher value than its random counterpart. A possible explanation is that an achieving player possesses a higher exiting degree when the attachment rule is degree dependent. Furthermore, for this attachment rule, a player achieves more rapidly which in turns causes more offspring to be introduced into the network than in its random counterpart. Also to be noted,

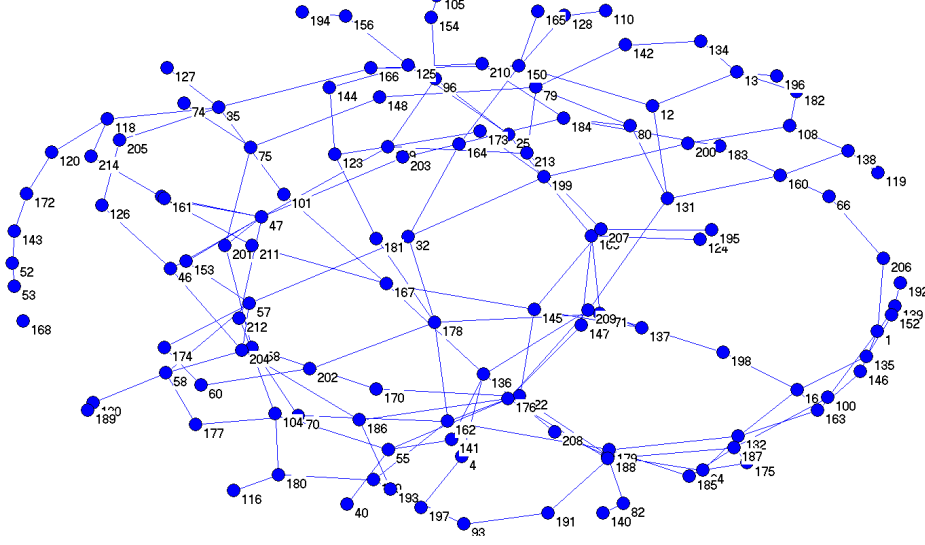


Figure 40: The evolving model's network topology after 500 rounds. The player's attributes are an initial resource of 110 and a target of 200.

the network size reaches a steady state between 2,000 and 4,000 rounds but the results quoted in this thesis are for 10,000 rounds, which suggests the solution is robust (see appendix A).

Figure 43 provides numerical evidence that players do achieve more quickly in networks with degree dependent attachment rules. Indeed the MTTA is lower in the degree dependent attachment cases than in its random counterpart. In addition, Figure 43 shows a similar result for the MTTB. Nevertheless, the evolving model's results compared to the contracting model's (Figure 25) reveal the following facts:

1. The MTTB for players in the evolving model is lower than in the contracting

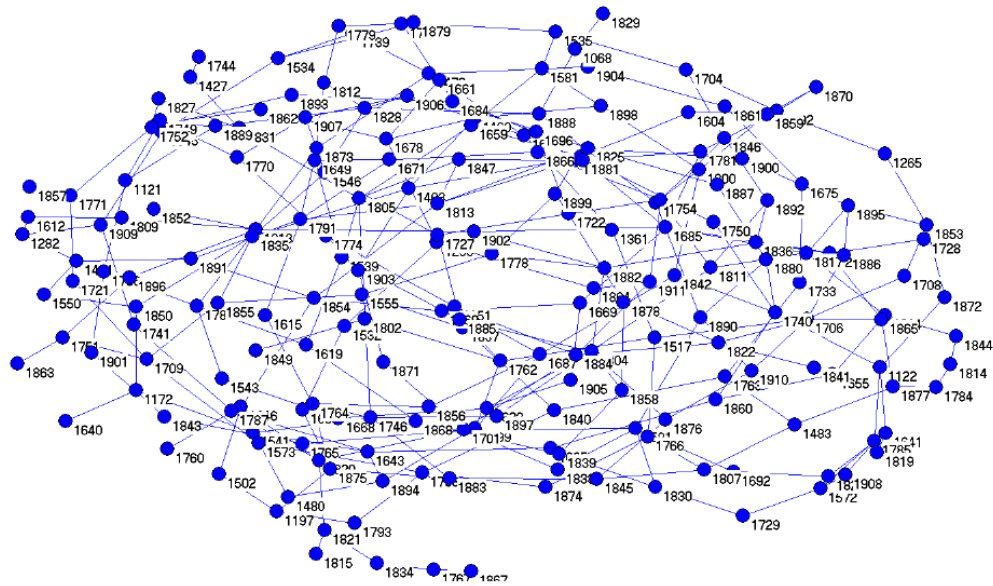


Figure 41: The evolving model’s network topology after 9500 rounds. The player’s attributes are an initial resource of 110 and a target of 200.

model.

2. The MTTA for players in the evolving model is higher than in the contracting model.

It must be noted that most of the achieving players in the evolving model are offspring. Hence, those achieving players possess a lower initial resource than those in the contracting model. As a result they have a shorter distance to bankruptcy but a greater distance to achievement.

As well as this, the exit degree is higher with degree dependent attachment rules than with the random equivalent. Figures 44 provides numerical evidence of this

Cases	Initial network size N	Neighbours k	Offspring per Achiever	Offspring k
Case 1	50	2	3	3
Case 2	50	10	3	3
Case 3	100	2	3	3
Case 4	100	10	3	3
Case 5	150	2	3	3
Case 6	150	10	3	3
Case 7	200	2	3	3
Case 8	200	10	3	3

Table 7: Details of cases investigated by varying the initial size of network N and neighbours k .

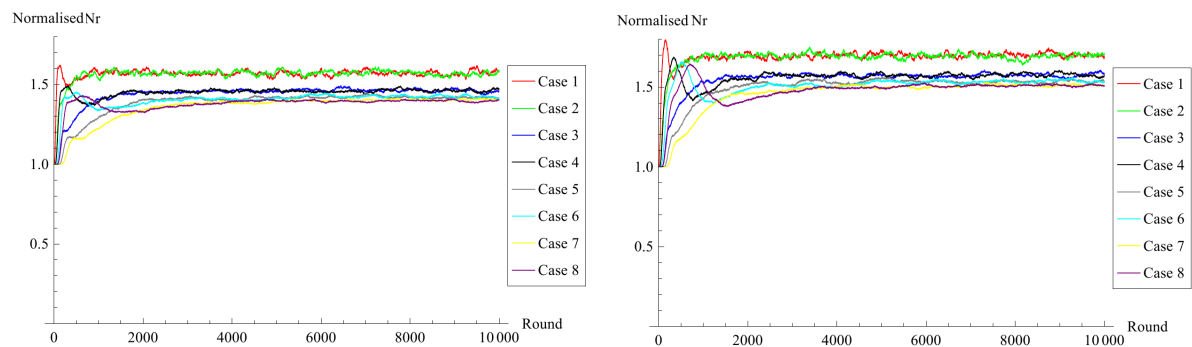


Figure 42: The influence of the random attachment rule (left diagram) and degree dependent attachment rule (right diagram), number of neighbours and initial network size N on the normalised population (size of network) Nr through time. The Nr value of 1.0 equates to the initial population size. A full description of the cases is shown in Table 7. The initial resource is the numerical initial network size plus 10. The target is double the numerical initial network size. Results averaged over 50 histories.

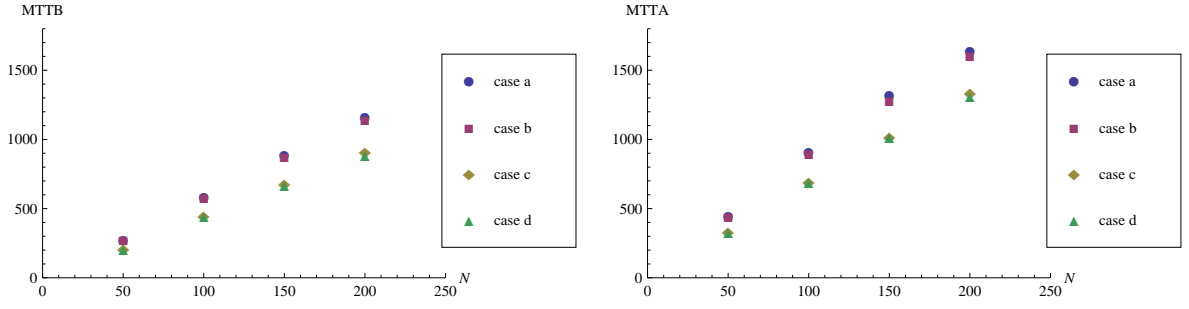


Figure 43: The influence of attachment rule, number of neighbours and initial size of network N on the MTTB (left diagram) and MTTA (right diagram). For cases see Table 6. The initial resource is the initial network size plus 10. The target is double the initial size. Results averaged over 50 histories.

statement where the figures show the achieving and bankrupt players' exit degrees respectively. Cases "a" and "b" have random attachment rules while cases "c" and "d" are degree dependent (see Table 6). It is worth mentioning both results show insensitivity to the initial size of the network. Indeed on this point, the evolving model is consistent with the contracting model (Figure 26). Conversely,

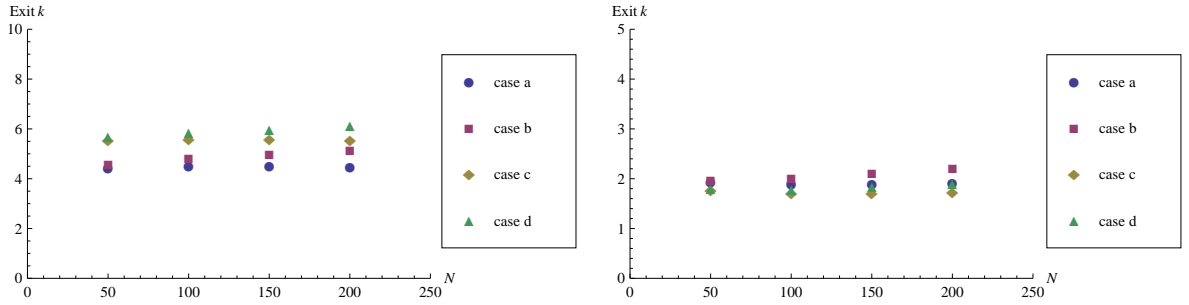


Figure 44: The influence of attachment rule, number of neighbours and initial size of network N on the achiever's (left diagram) and bankrupt player's (right diagram) exit degree $Exit k$. For cases see Table 6. The initial resource is the initial network size plus 10. The target is double the initial size. Results averaged over 50 histories.

the evolving model's exiting degree results contrast with the contracting model's as the latter is more a reflection of the initial network structure while the former represents the evolving network topology.

A global network parameter discussed for the contracting model was the average strength of the players in the network. As previously stated in section 3.2.2, Figures 27 and 31 showed that for the contracting model the average strength tended to approximately 0.5. In contrast, for this evolving model Figure 45 demonstrates in all cases an average strength that tends to 1. Figure 45 (left and right diagram) shows little difference between random and degree dependent attachment rules. Another global network parameter discussed for the contracting model was

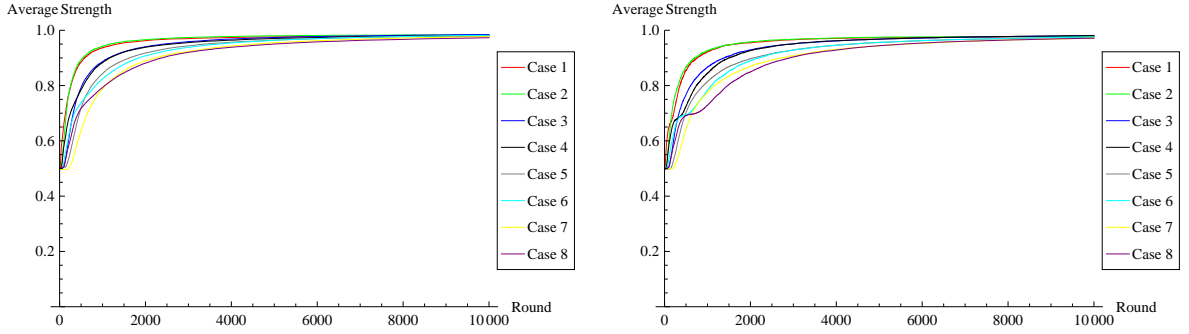


Figure 45: The influence of the random attachment rule (left diagram) and degree dependent attachment rule (right diagram), number of neighbours and initial network size on the average strength. A full description of the cases is shown in Table 7. The initial resource is the numerical initial network size plus 10. The target is double the numerical initial network size. Results averaged over 50 histories.

the gain loss performance indicator. As previously stated in section 3.2.2, Figures 28 and 32 showed that for the contracting model in all cases the gain loss parameter is approximately neutral. However, for the evolving model, Figure 46 (especially the random attachment rule) show that in most cases the gain loss parameter has a value which is negative. These results will be discussed in sec-

tion 5.1.1. The final global network parameter discussed for the contracting model

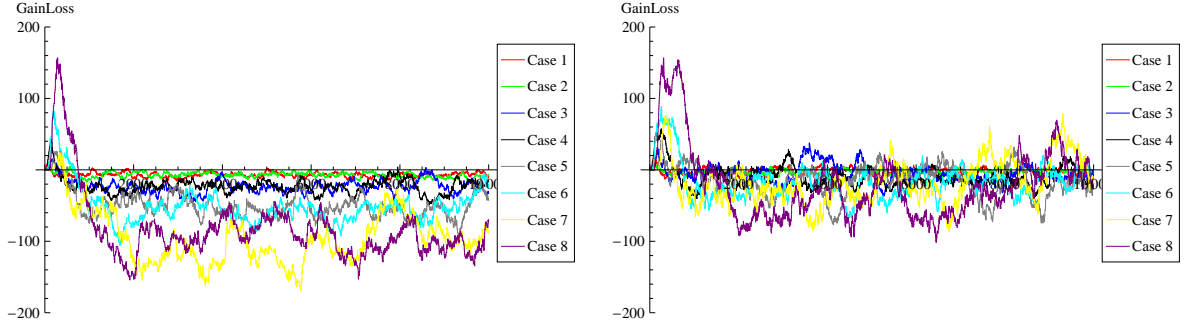


Figure 46: The influence of the random attachment rule (left diagram) and degree dependent attachment rule (right diagram), number of neighbours and initial network size on the gain loss parameter $GainLoss$. A full description of the cases is shown in Table 7. The initial resource is the numerical initial network size plus 10. The target is double the numerical initial network size. Results averaged over 50 histories.

was the player per resource. The evolving model's results, in comparison to the contracting model's, is consistently below the normalised value of 1. Figure 47 demonstrates the numerical evidence of this statement in comparison to Figures 29 and 33. This is a consequence of the evolving model introducing more players (offspring) who are competing for the same quantity of resources. Table 8 compares some key statistics between the evolving and contracting models. By way of example, the simulation scenario illustrated is a lattice network with initially 100 players. In agreement with the previous arguments, the evolving model exhibits less parity between the number of achievers and bankrupts, a higher mean time to achievement and a lower mean time to bankruptcy than its contracting alternative. As a consequence, the evolving model presented a gain loss parameter value that was mostly negative (Figure 46).

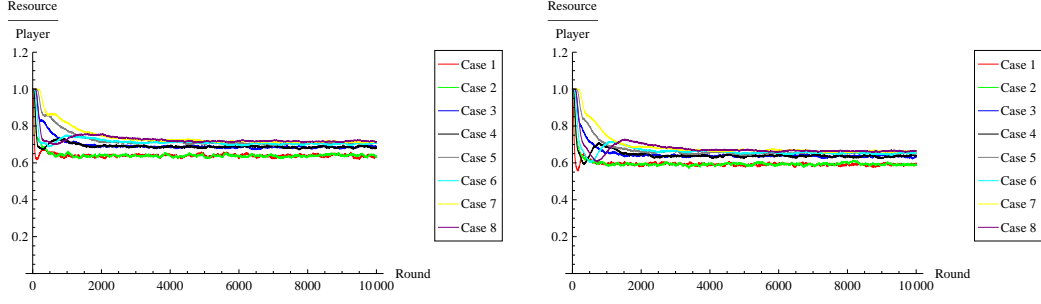


Figure 47: The influence of the random attachment rule (left diagram) and degree dependent attachment rule (right diagram) on the normalised resource per player parameter throughout the game. The normalised resource per player is calculated from its respected value for a round, divided by the initial figure for round 1. A full description of the cases is shown in Table 7. The initial resource is the numerical initial network size plus 10. The target is double the numerical initial network size. Results averaged over 50 histories.

Model	Offspring	Initial Resource	Target	Achievers	Bankrupts	MTTA	MTTB
Contracting	0	110	200	53.88	44.56	592.50	761.16
Evolving	3	66 to 110	200	656.70	1267.52	911.16	585.12

Table 8: Comparing the contracting and evolving model key statistics. Initial network topology lattice with 10,000 rounds. Results averaged over 50 histories.

In conclusion, this chapter reiterated the limitations of the contracting model version of the Extended GR problem, as outlined in section 3.2.1. The model penalized failure but did not reward success. To explore this further, the Fish-Plankton model, which is a variation of the classical predator-prey model, was considered played over a three-dimensional lattice. Here, the evolutionary rule penalized failure (the fish died) and rewarded success (the fish produced offspring). Incorporating this, another version of the Extended GR problem played over net-

works was produced: the evolving model. In comparison to the non-offspring contracting version, this evolving model will not always evolve to the classical GR problem.

5 Bespoke Preferential Attachment Rules

In this chapter we will discuss and develop a bespoke preferential attachment rule for the Extended GR problem. Although the more established degree dependent preferential attachment rules are better understood, [Borgs et al (2007)] argue that, when compared to real networks, determining the popularity of nodes only by their degree is not realistic and other factors should be taken into consideration. [Leskovec and Faloutsos (2007)] developed a bespoke preferential attachment rule with the objective of networks evolving into a desired topology. However, their rule does not take account of the player's state. On the other hand, [Dorogovtsev et al (2000)], [Fan and Chen (2004)] and [Gong and van Leeuwen (2003)] developed bespoke preferential attachment rules to investigate how players' properties can influence the way the network topology evolves.

This thesis considers a bespoke preferential attachment rule that we term 'kudos' which is influenced by the individual player's state. The first step is to explore the general objectives of a bespoke preferential attachment rule. Following this, the chapter documents the motivation and influences for using the kudos preferential attachment rule. We shall then investigate how the kudos preferential attachment rule influences the Extended GR problem and look for any new dynamical behaviour that arises.

5.1 Examples of Bespoke Preferential Attachment Rules

As we already discussed in section 1.1.3, [Berger et al (2004)] questioned whether the Barabási-Albert model's linear preferential attachment rule is the single underlying mechanism that leads to a scale free network. Moreover, [Fan and Chen (2004)], [Gong and van Leeuwen (2003)] and [Yan et al (2004)] concentrated on other variations of the Barabási-Albert model's linear preferential attachment rule to see if

they led to scale free networks. In these cases, the authors developed bespoke preferential attachment rules where the network evolves into a desired topology: a scale free network with a high clustering coefficient. [Boccaletti et al (2006)] also summarize a number of preferential attachment techniques which generate scale free networks with a high clustering coefficient. These are more representative of real world networks. However, in this thesis the objective is not to replicate a real world network.

Instead, we consider how players' properties interact and influence the evolving network topology. For example, [Krapivsky et al (2000)] developed a preferential attachment rule based on the age of the player. Using this variation of linear preferential attachment, Krapivsky argued that an evolving scale free network could be generated with any power law value λ greater than 2. Similarly, [Lehmann et al (2005)] considered how scientific papers are cited over the years and represented it as an evolving network. They argued that preferential attachment must be supplemented by appropriate additional ingredients. For example, whether a new paper attaches to an existing one depends not only on the number of citations it has, but also on other associated unique factors. For instance, all papers are considered in Lehmann et al's model as live or dead. At each time step the probability of a live paper dying is inversely proportional to the number of citations that it has received. In addition to this, a new paper does not attach to an existing one which is regarded as dead. In short, bespoke preferential attachment rules consider attractiveness rather than the player's degree.

5.1.1 Preferential Attachment Based on Attractiveness

There are a number of examples of bespoke preferential attachment rules based on attractiveness. For example, [Jensen (2008)] developed an evolving network model inspired by biological reproduction dynamics. At each time step a player has one

offspring while another is removed from the network. Jensen defines attractiveness as being connected to one's parent and their friends. For example, offspring associate with their parents' friends more than a complete stranger. The offspring in Jensen's paper attach to the players who are already connected to their parents. Jensen also explores the alternative approach of giving preference to those who are not attached to one's parent. The initial size of the network is N , and the evolutionary rules are as follows. At each time step:

1. A player is chosen at random and removed. All associated edges are removed.
2. Another player is chosen at random from the remaining $N - 1$ nodes and has one offspring.
3. The offspring is connecting to its parent with probability p_p .
4. Each player connected to the parent is connected to the offspring with probability p_e .
5. Each player that is not connected to the parent is connected to the offspring with probability p_n .

Jensen's approach differs from the evolving model for the Extended GR problem. Firstly, Jensen's network size remains fixed; at each time step one player dies and one offspring is introduced. Secondly, in Jensen's model, the network topology changes at each time step. Thirdly, in Jensen's model, the parent remains in the network and has only one offspring. In contrast, it was decided that for our evolving model the successful player would leave the network and might produce many offspring. This is because we wanted to mimic the competitive behaviour of a successful family business where the owners retire and the business is divided between the owner's offspring. Finally, in Jensen's model which players succeed or fail is chosen at random, it is not based on their performance. In summary,

Jensen's model utilizes the network structure for its attachment rule as opposed to a unique state of the player. Moreover, it illustrates that at a low value of p_n the network tends to fragment. As we saw in section 4.2, the evolving model can also illustrate networks that fragment.

[Britton and Lindholm (2009)] developed another evolving network with its own bespoke attachment rule, also inspired by biological reproduction dynamics. Here, Britton et al consider a network that evolves through continuous time where offspring are born and old players die. Furthermore, each player is assigned a different social index number which is randomly selected. The offspring in Britton's model attach proportionally to those players with the highest social index. If S_j is the social index number of player j then the probability of an offspring connecting to player j is:

$$\frac{S_j}{\sum_{k=1}^{N(t)} S_k}. \quad (5.1.1)$$

where $N(t)$ is the size of the network at time t . We note that the preferential attachment rule is based on the player's social index number not their degree. However, Britton's model differs from Jensen's as the network size does not remain fixed. For instance, if Britton's model assumes an average birth rate of λ and a death rate of μ then the network size may decay to zero or grow at an exponential rate:

$$N(t) \propto e^{t(\lambda-\mu)}. \quad (5.1.2)$$

Furthermore, Britton's approach differs from Lehmann's as Britton's preferential attachment rule is independent of the player's degree. However for Britton's model, the network topology does not influence the player's social index number and the offspring are not associated with their parents. Nonetheless, Britton's approach only considers a player's state when it influences the network topology; it does

not consider an evolving network topology that influences the player's state as in Lehmann's model.

In contrast, [Ren et al (2008)] and [Gómez-Gardeñes et al (2008)] both developed models that consider the interplay between the player's state and the evolving network topology. In both cases, these models played the iterative prisoner's dilemma over networks. In the two models the attachment rule is influenced by the player's payoff. Ren's uses the following preferential attachment probability:

$$\frac{M_i + W}{\sum_j (M_j + W)}. \quad (5.1.3)$$

where M_i is the total payoff of player i and W is a tunable parameter. As W tends to infinity the less influence the player's total payoff has on their attractiveness. Gómez-Gardeñes, alternatively, employs the following expression for preferential attachment probability:

$$\frac{1 - \varepsilon + \varepsilon f_i(t)}{\sum_{j=1}^{N(t)} 1 - \varepsilon + \varepsilon f_j(t)}. \quad (5.1.4)$$

where $f_i(t)$ is the total payoff for player i and ε is a tunable parameter ranging from 0 to 1. As ε tends to zero the less influence the player's total payoff has on their attractiveness.

[Poncela and Vespignani (2009)] also considered an iterative prisoner's dilemma played over evolving networks similar to that of Gómez-Gardeñes. However in this case, Poncela et al employed the preferential attachment probability:

$$\frac{e^{\varepsilon f_i(t)}}{\sum_{j=1}^N e^{\varepsilon f_j(t)}}. \quad (5.1.5)$$

Poncela demonstrated that the choice of ε has an influence on how the network topology evolves which in turn affects the payoff of each player. Figure 48 shows the results of the numerical simulation in Poncela et al's paper.

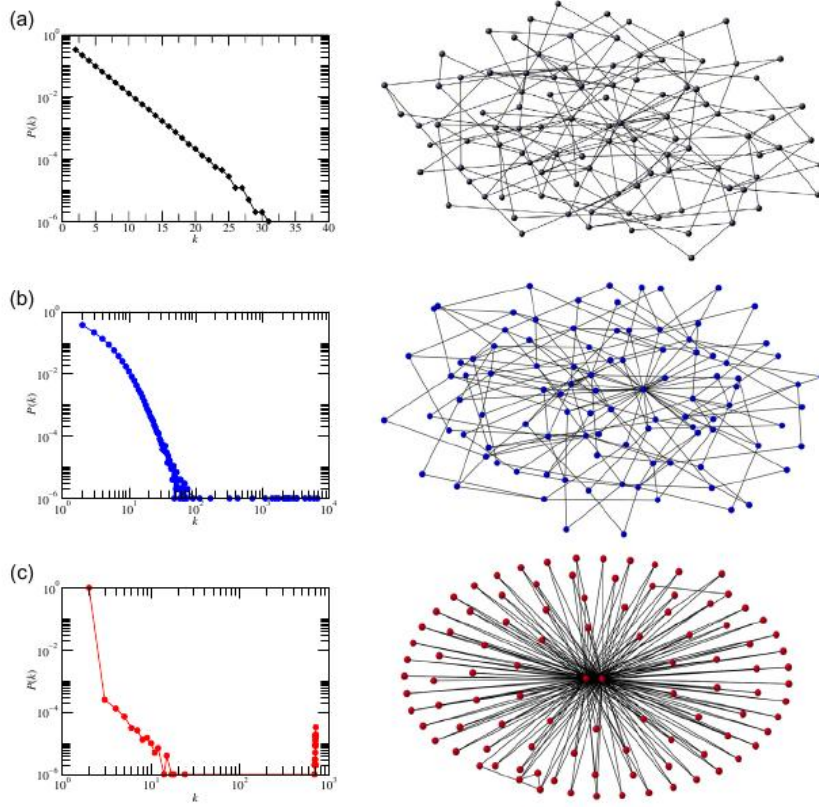


Figure 48: Evolving network topology in Poncela et al's model with (a) $\varepsilon = 0$ (b) $\varepsilon = 0.1$ (c) $\varepsilon = 1.0$; figures on the left show the degree distribution for a network of size 1000; figures on the right show a snapshot of a network of size 100 [Poncela and Vespignani (2009)].

As can be seen from Figure 48, Poncela et al show that as ε tends to 1, the network topology evolves towards a giant component. This is similar to the giant component discussed by [Erdős and Rényi (1959)] in their random network model in section 1.1.1. This is an important theme in this thesis and is discussed further in section 5.3.2.

5.2 Preferential Attachment Rule for the Extended Gambler's Ruin Problem

In Poncela et al's model, the player with the highest payoff possesses the greatest kudos in the network. In this case, kudos is defined as the player's honour, reputation, glory, acclaim and prestige. However for the evolving model, the player's kudos is not easily represented by its current properties: degree, target, strength and initial and current resources. The player's strength, for instance, becomes homogeneous throughout the network as its topology evolves (see Figure 45). Hence it does not provide a notable advantage. Moreover, the player's current resource, whether high or low, may suggest that their departure from the network is imminent; therefore no benefit is offered to the offspring attaching to it. However, to represent kudos it is necessary to include an additional player's property. This will be further explained in the next section.

5.3 The Kudos Preferential Attachment Rule

In this section we will introduce, define and explore the properties of the kudos preferential attachment rule by comparing and contrasting it with the more established methodologies: random and degree dependent. As well as this, an examination of how the kudos preferential attachment rule influences this version of the Extended GR problem.

The kudos preferential attachment rule is defined as follows:

- At the beginning of the game, a player is chosen at random and is given a **golden unit**. This player is regarded as the current **title holder**.
- At each round, the "title holder" gives the "golden unit" to its highest scoring neighbour, provided that neighbour scores higher than the "title holder". In

these circumstances, the highest scoring neighbour has now become the new “title holder”.

- Otherwise in a round, the “title holder” keeps the “golden unit” and remains the “title holder”.
- Under the circumstances that the “title holder” achieves and leaves the network, the new “title holder” will be the network’s highest scoring player for that round.

The “title holder” can never become bankrupt as they must have beaten at least one other player to gain or to keep hold of the “golden unit”. However, a “title holder” can become isolated if all their opponents leave the network in the same round. We will define a **kudos player** as a player that is still in the game and has held or is holding the “golden unit”. As well as this, we will define the **kudos population** as the total number of kudos players.

An offspring or an isolated player (including the “title holder”) preferentially attaches to an opponent with probability:

$$\frac{K_j}{\sum_{n=1}^{N(t)} K_n}. \quad (5.3.1)$$

where K_j is the number of rounds player j has held the “golden unit”, whereas $N(t)$ is the size of the network at time t . The denominator of the above expression can never be equal to zero as there is always at least one kudos player in every round. It must be noted that the probability of attachment to a certain player varies throughout the duration of the game due to:

1. The rate at which a player obtains kudos in comparison to the rest of the network.
2. The growth or decay of the kudos population through time.

Before we investigate the influence of kudos on the network topology, we will consider its influence on the player's state itself. To illustrate this further, some snapshot results from the evolving model for three individual players (player 101, player 102 and player 103) can be taken into consideration. For this example the initial resource is 100, the target is 200, initial network size 100, initial network topology is a lattice with periodic boundary conditions. Players 101, 102 and 103 are the first offspring to enter the game and all have the same parent. Therefore Player 101's initial resource is 67, while the other offspring is 66. In Figure 49, the effect on degree and resources before and after each player has obtained kudos is considered. Each player enters the game at approximately the 80th round. Furthermore, player 102 obtains kudos by winning the "golden unit" at approximately the 350th round. This is illustrated in the upper diagram of Figure 49. With this in mind, before the 350th round, each player's degree remains less than 5 and their resource steadily declines from its initial value. Subsequently after the 350th round, the degree and resources of player 102 increase rapidly, achieving the target at the 420th round. In addition to this, the same behaviour for player 101 and 103 is observed, obtaining kudos at the 450th and 500th rounds respectively as well as achieving the target at the 500th and 520th rounds respectively. Hence from Figure 49, it is observed that when a player obtains kudos, there is an increase in the degree as well as the resources which facilitate the objectives of achieving the target.

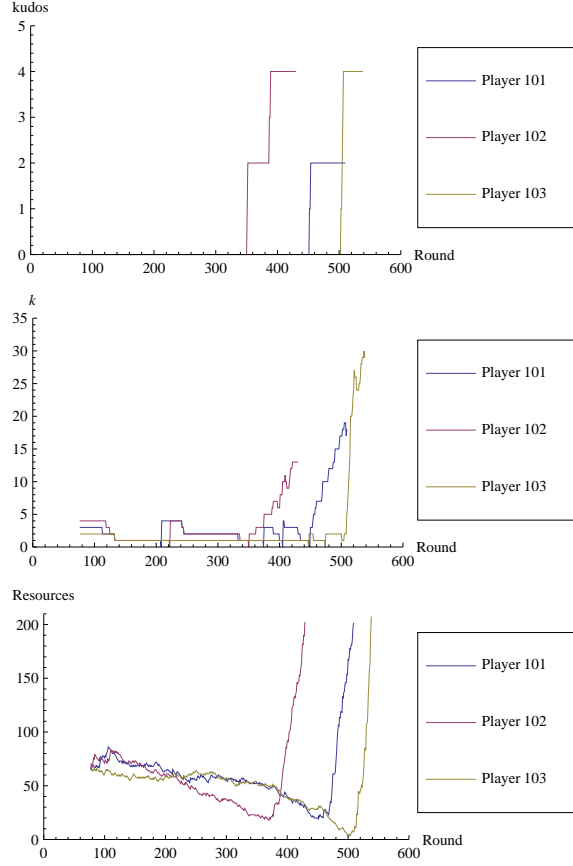


Figure 49: The kudos value (upper diagram), degree (middle diagram) and resource (lower diagram) of individual players throughout the duration of the game. Snapshots result from the evolving model. Initial resource: 100, target: 200, initial network size: 100, initial network topology: lattice with periodic boundary conditions.

In Figure 50 we show a comparison between the kudos, random and degree dependent preferential attachment rules. Here the exiting degree, MTTA and MTTB are considered. With reference to Figure 50 upper diagram, the kudos preferential attachment rule presents a larger achiever's exiting degree than its random and degree dependent counterparts. Furthermore, with reference to Figure 50 lower diagram, the kudos preferential attachment rule generates a MTTA value which

is less than the MTTB; this is not true for the more established attachment rules. In addition to this specific case, the kudos preferential attachment rule's MTTA exhibits a value which is at least seven times smaller than its random and degree dependent counterparts while MTTB it is at least twice as small. As a result, the players achieve quicker in the evolving model when kudos is the preferential attachment rule than players become bankrupt. This is a surprising result as the other attachment rules do not show this property.

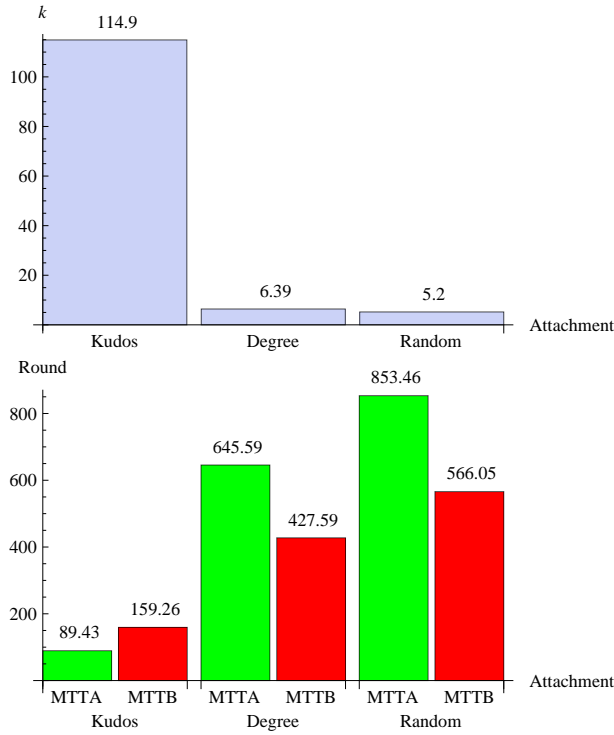


Figure 50: Comparison of preferential attachment rule's influence on achiever's exiting degree k (upper diagram), MTTA and MTTB (lower diagram). Initial periodic boundary condition lattice network, 10 by 10, 10,000 rounds, initial resource of 100 and a target of 200. Results averaged over 50 histories.

5.3.1 Comparison with the Other Preferential Attachment Rules

For this section we will discuss each attachment rule's influence on general network topology and players' performance parameters. Firstly this section will document the influence of the preferential attachment rule on the final population; this is illustrated in Figure 51. Table 9 is a list of cases that were addressed. The benchmark experiments undertaken by [Rocha and Stern (2004)] and discussed in section 4.2 are repeated.

Case	Attachment	Neighbours k	Offspring per Achiever	Offspring k
case a	random	2	3	3
case b	random	10	3	3
case c	degree dependent	2	3	3
case d	degree dependent	10	3	3
case e	kudos	2	3	3
case f	kudos	10	3	3

Table 9: Details of cases to be investigated by varying the attachment rules and neighbours k . Similar to Table 6 but with the kudos preferential attachment rule added.

In section 4.2 we investigated the influence of random and degree dependent attachment rules on normalised population, gain loss, average strength and resource per player when we varied the initial size of the network and number of neighbours of each player. Repeating the exercise this time for our kudos preferential attachment rule we found that in contrast to the established approaches, the kudos preferential attachment rule (*case e* and *case f*) produces a larger population size in the network after 10,000 rounds which steadily increases with initial population size. However in agreement with section 4.2, the number of neighbours does not greatly influence the size of the population. This is illustrated in Figure 52 where

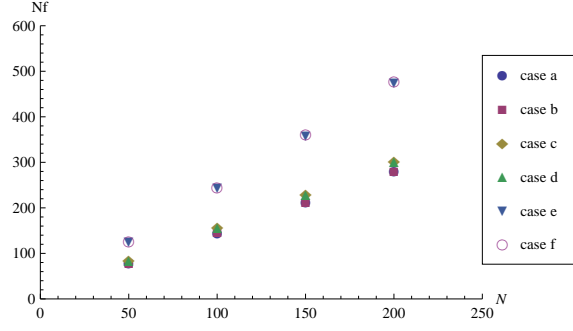


Figure 51: The final population size Nf in each of the cases of Table 9 after 10,000 rounds. Results averaged over 50 histories.

there is little variation between the cases. In comparison to Figure 42 left and

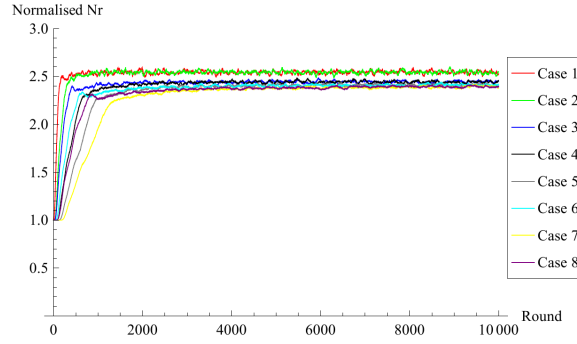


Figure 52: The influence of the kudos preferential attachment rule, number of neighbours and initial network size N on the normalised population (size of network) Nf through time. The Nf value of 1.0 equates to the initial population size. A full description of cases is shown in Table 7. The initial resource is the numerical initial network size plus 10. The target is double the numerical initial network size. Results averaged over 50 histories.

right diagram, which are random attachment and degree dependent rules respectively, the kudos preferential attachment rule converges to a higher normalised population in all cases. It is also noted that, for this approach, there is less in vari-

ation between the cases than for the established attachment rules. With this in mind, the experiments illustrated in Figure 43 left and right diagrams, the MTTB and MTTA respectively, are also repeated and are shown in Figure 53. The case scenarios described in Table 9 are used. It is noted that the kudos preferential attachment rule significantly decreases the value of both MTTA and MTTB in comparison to the established approaches. The effect of the kudos preferential

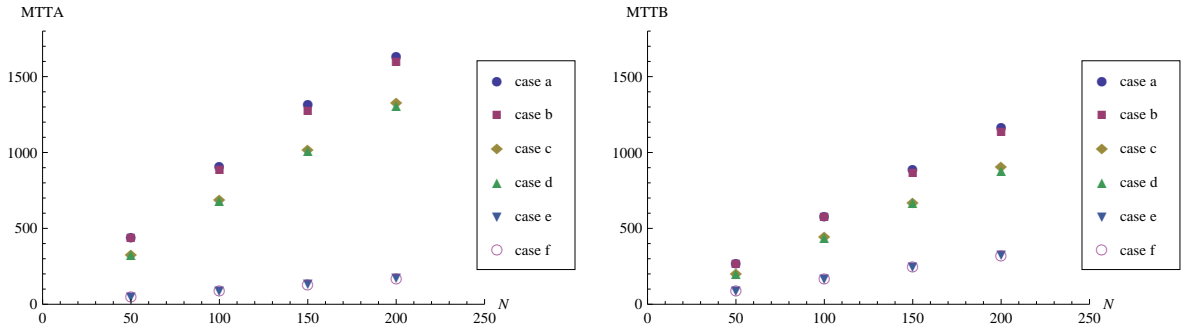


Figure 53: The influence of the preferential attachment rule, number of neighbours and initial network size N on MTTA (left diagram) and MTTB (right diagram). The initial resource is 10 more than the numerical initial network size and the target is double the numerical initial network size. A full case description is shown in Table 9. Results averaged over 50 histories.

attachment rule methodology upon the achiever and bankrupt exit degree shown in Figure 54. For kudos preferential attachment, the achiever exit degree is clearly heavily influenced by the initial size of the network much more so than in the case of the established attachment rules. We discuss this further in section 5.3.2. In contrast, the bankrupt exit degree exhibits no significant differences between the three preferential attachment rules. This result is surprising as it suggest that kudos influences players who achieve but not those who become bankrupt. Repeating the benchmark simulations illustrated in Figure 45, the influence of the kudos preferential attachment rule on the average player's strength is analysed (see Table 7

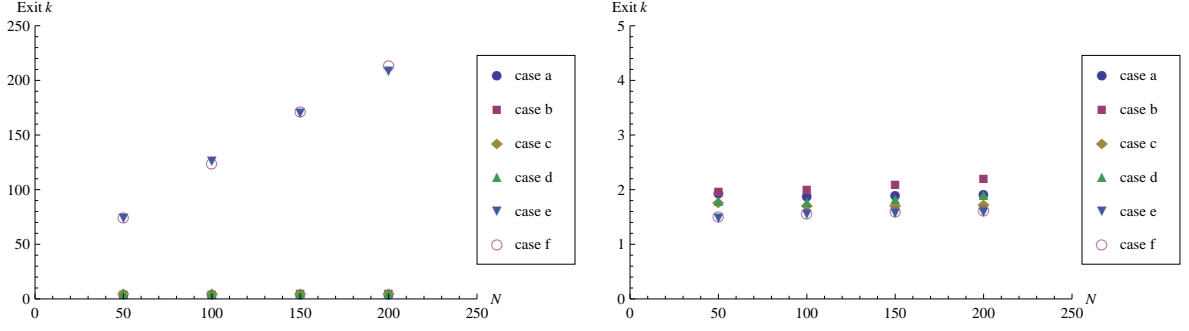


Figure 54: The influence of the preferential attachment rules, number of neighbours and initial network size N on the achiever's (left diagram) and bankrupt's (right diagram) exit degree $Exit\ k$. The initial resource is 10 more than the numerical initial network size and the target is double the numerical initial network size. A full case description is shown in Table 9. Results averaged over 50 histories.

for case description). Comparing Figure 55 and those previously mentioned, there is little difference between all three preferential attachment rules. This is to be expected as, over the duration of the game, we would expect the descendants of the strongest players to remain in the network. In section 4.2 for the gain loss parameter, the evolving model performance was inferior to the contracting network version (Figures 33 and 46). In other words, the evolving network model's offspring that become bankrupt had an adverse effect on the gain loss parameter. However, as illustrated in Figure 56, the kudos preferential attachment rule transposes this result. This is again surprising, as it shows kudos changing some but not all aspects of the evolving network topology. It suggests that with kudos more players with some distance to the target are achieving than with any other established attachment rules. Finally, repeating the benchmark simulation experiments illustrated in Figure 47, the normalised resource per player ratio is considered. From the results illustrated in Figure 57 there is some difference between kudos and the other preferential attachment rules. For kudos, the normalised resource

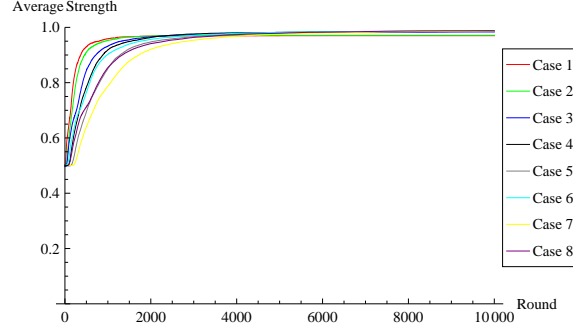


Figure 55: The influence of the kudos preferential attachment rule, number of neighbours and initial network size on the average strength. A full description of cases is shown in Table 7. The initial resource is the numerical initial network size plus 10. The target is double the numerical initial network size. Results averaged over 50 histories.

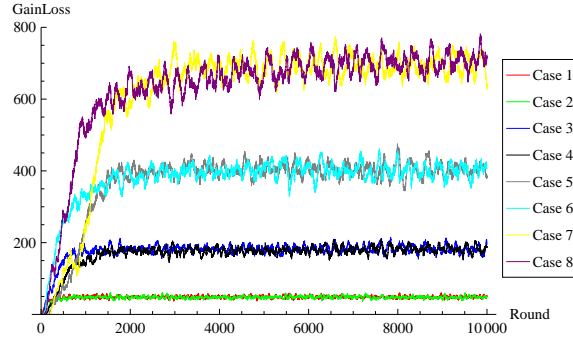


Figure 56: The influence of the kudos preferential attachment rule, number of neighbours and initial network size on the gain loss performance indicator *GainLoss*. A full description of cases is shown in Table 7. The initial resource is the numerical initial network size plus 10. The target is double the numerical initial network size. Results averaged over 50 histories.

per player ratio is approximately a third lower than that for random and degree dependent preferential attachment. This is not surprising because, as shown in Figure 52, for kudos there are more players in the game.

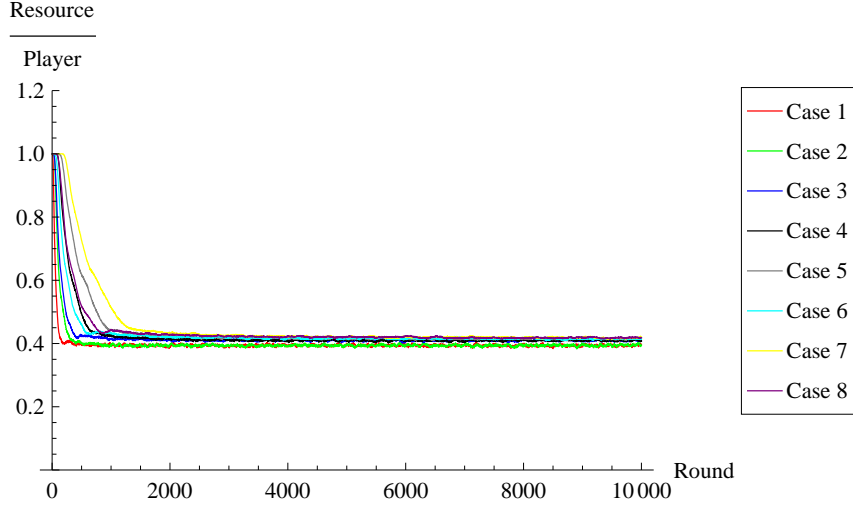


Figure 57: The influence of the kudos preferential attachment rule, number of neighbours and initial network size on the normalised resource per player parameter of the network throughout the duration of the game. A full description of cases is shown in Table 7. The initial resource is the numerical initial network size plus 10. The target is double the numerical initial network size. Results averaged over 50 histories. The normalised player per resource is calculated from its respective value for a round, divided by the initial figure for round 1.

5.3.2 Varying the Target with a Fixed Initial Resource

We have investigated how our Extended GR problem has departed from that of [Rocha and Stern (2004)]. So far, the player’s target and initial resource were linked to the initial number of players, twice the value and an addition of ten respectively. However, in this section we shall explore further properties of our Extended GR problem by varying the player’s target while fixing the initial resource. To demonstrate, Figures 58 illustrates the effect of preferential attachment rules on the final population, MTTA and MTTB respectively, when varying the target while keeping the initial resource fixed. Figures 58 show some interesting

results. For instance, the established preferential attachment rules produce similar graphs as the target is varied. However, for the bespoke preferential attachment rule kudos, there appears to be two phases. The final population declines steadily as the target increases; however, there is a point at which there is a sudden reduction. The MTTA and MTTB initially remain constant as the target increases until it reaches a certain point, after this it suddenly rises. Figure 58's results robustness is considered further in appendix A (Figures 85 and 86).

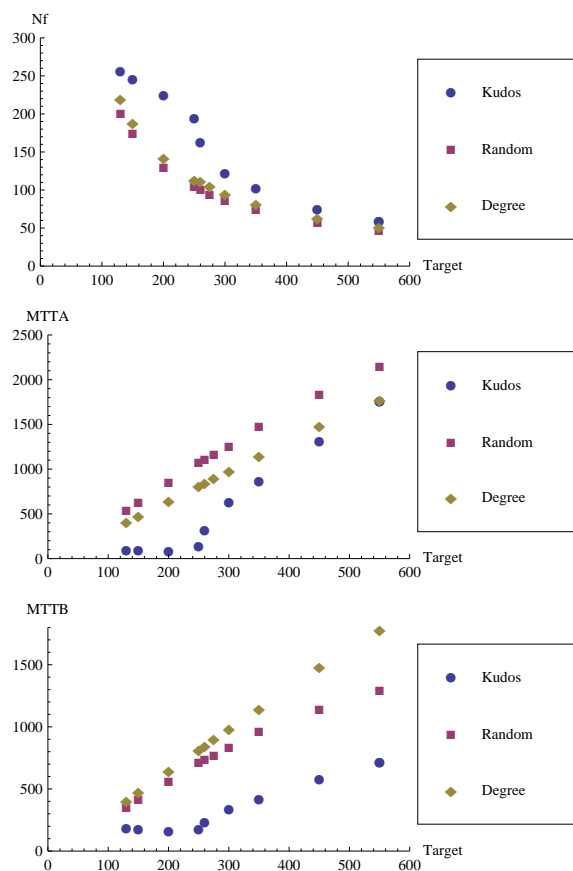


Figure 58: The influence of the target and attachment rule on final population N_f (upper diagram), MTTA (middle diagram) and MTTB (lower diagram). The initial resource is fixed at 100 units; the initial network size is 100 players; 10,000 rounds. Results averaged over 50 histories.

It appears that the kudos preferential attachment rule introduces a phase transition into the numerical simulation results of the Extended GR problem. In section 5.3.3, we shall discuss the possible scaling laws of this phase transition. However, we now continue to explore the properties of the evolving model by varying the player's target while fixing the initial resource.

As was seen in Figure 50 (lower diagram), a fundamental difference between kudos and the other attachment rules was that the MTTA is less than the MTTB. This property may give an indication why the result produced by the kudos preferential attachment rule is different. As a consequence, we shall investigate the ratio between the MTTA and MTTB further. Figure 59 illustrates the influence of the target and attachment rule on the ratio $\frac{MTTA}{MTTB}$ and exit degree k . From Figure 59 it is observed that there is more numerical evidence of a phase transition. Indeed, the established preferential attachment rules produce results that are fairly constant as the target increases. However in Figure 59 (upper diagram), for the kudos preferential attachment rule, $\frac{MTTA}{MTTB}$ remains constant before a distinctive rise as the target increases. In Figure 59 (lower diagram) k exhibits a linear decline for the first phase, followed by a constant steady value. So far this we have only considered one particular initial network size of 100 players. To understand our results further we shall now vary not only the target but also the initial network sizes, as well as the number of offspring. Figure 60 illustrates the influence these factors have on the ratio of the MTTA and MTTB and on the player's exiting degree. Also the factors' influence on the final population is shown in Figure 61. Figures 60 and 61 show more numerical evidence of a phase transition; however, the "critical" point no longer remains in the same position but is influenced by the target, initial network size and number of offspring. It must be noted that from Figure 60 lower diagram, the player's exit degree increases rapidly as the target decreases from the critical point.

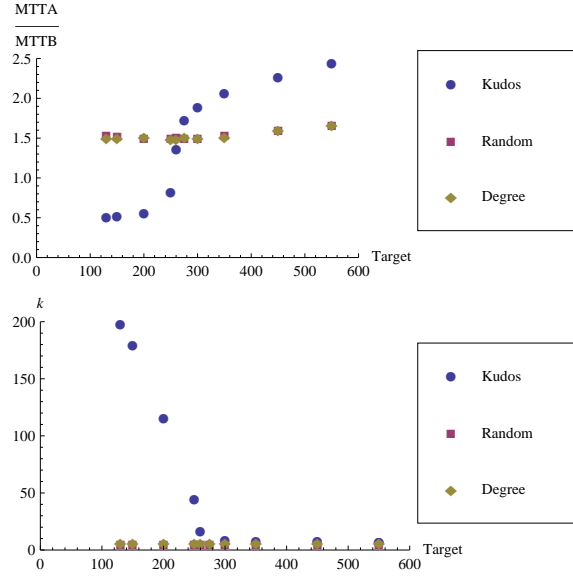


Figure 59: The influence of the target and attachment rule on the ratio $\frac{MTTA}{MTTB}$ (upper diagram) and exit degree k (lower diagram). The initial resource is fixed at 100 units; the initial network size is 100 players; 10,000 rounds. Results averaged over 50 histories.

We shall now attempt to give an explanation for the occurrence of the phase transition in the kudos preferential attachment rule. From Figure 59 it is observed that the phase transition occurs when the target is in between 250 and 260. As well as this, the ratio $\frac{MTTA}{MTTB}$ for the target 250 is less than 1 while for 260 it is greater than 1 (Figure 60). Therefore, the ratio $\frac{MTTA}{MTTB}$ may indicate how the network topology has evolved. Comparing Figure 60 lower and upper diagram, a high exiting degree corresponds to where the $\frac{MTTA}{MTTB} < 1$. Hence, we shall define subcritical and supercritical regions. The **subcritical** region is where the target is less than the critical target and is characterised by $\frac{MTTA}{MTTB} < 1$ in this region. The **supercritical** region is where the target is greater than the critical target and is characterised by $\frac{MTTA}{MTTB} > 1$. As an example, results obtained from the evolving model for both subcritical and supercritical regions (a target of 150 and

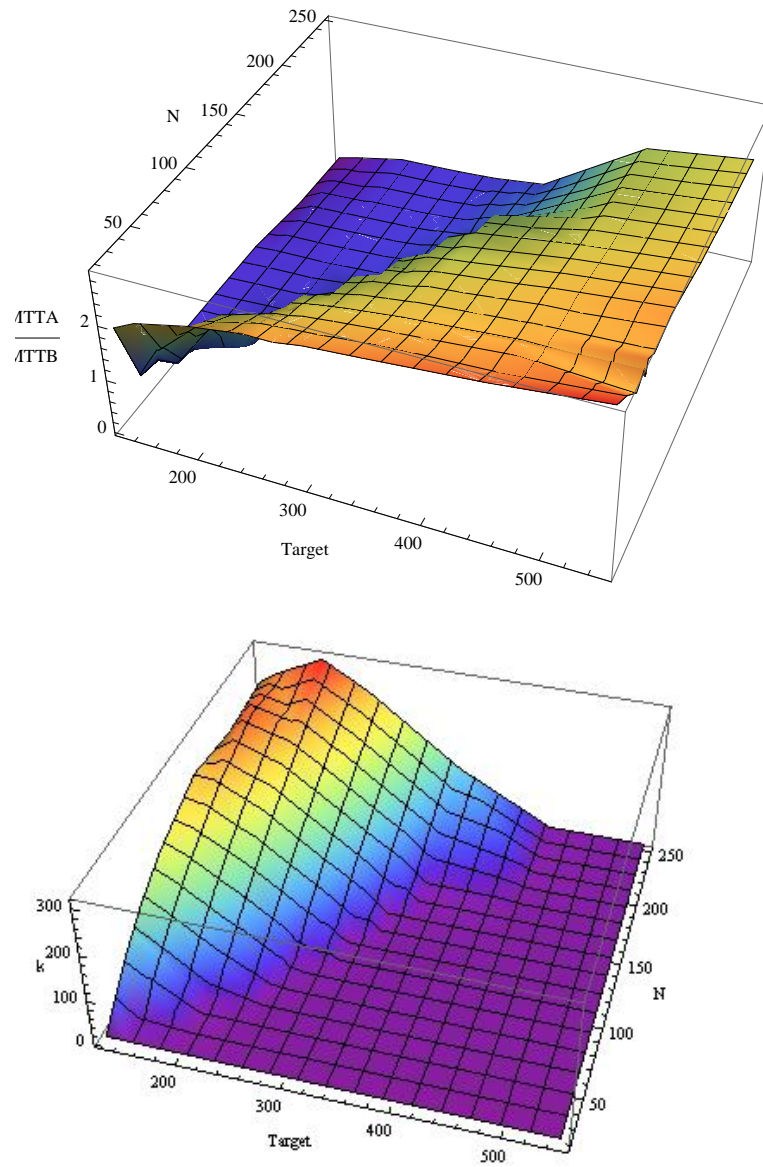


Figure 60: Varying the target and initial network size N : effect on ratio $\frac{MTTA}{MTTB}$ (upper diagram) and exit degree k (lower diagram). The initial resource is fixed to 100 units; the initial network size is 100 players; 10,000 rounds. Results averaged over 50 histories.

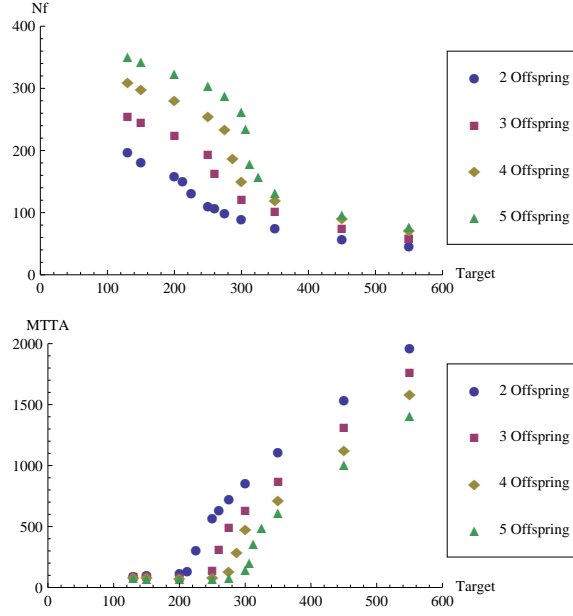


Figure 61: Varying the target and offspring: effect on final population Nf (lower diagram) and $MTTA$ (upper diagram). The initial resource is fixed to 100 units; the initial network size is 100 players; 10,000 rounds. Results averaged over 50 histories.

550 represents these regions respectively) are analysed. With this in mind the following variables are considered: the probability distribution of the exiting degree, the game's frequency of achievement, the probability distribution of the kudos population size and the probability a player will hold kudos for a given length of time before achieving. We see from Figure 62, the probability distribution of the exiting degree in the subcritical region, that a player can expect to be connected to over 150 opponents when they achieve. However in the supercritical region, a player can expect to be connected to fewer than 20 opponents. Before defining the frequency of achievement, we will define the event \mathbf{R} to be the number of rounds before the next player achieves once a player has achieved. For example, when $R = 10$, this means that when one player achieved the next player achieved 10

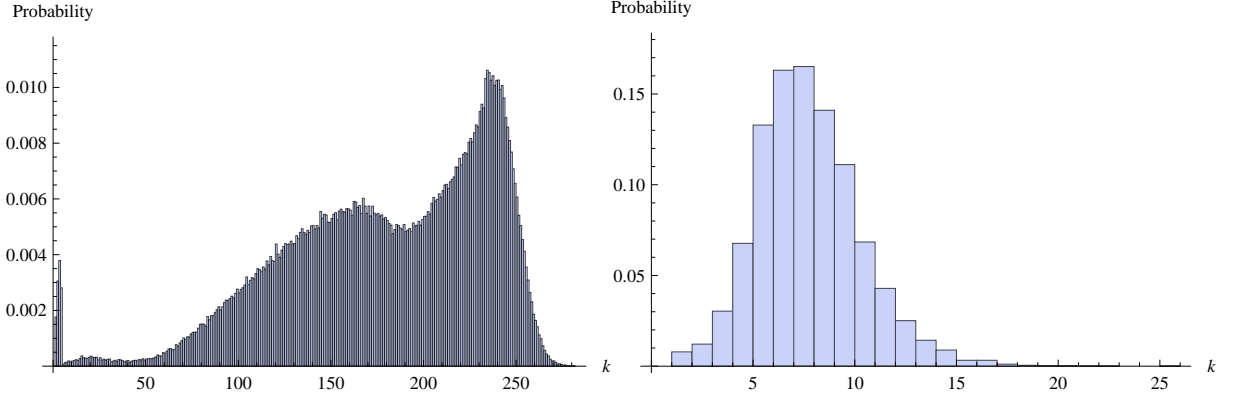


Figure 62: Probability distribution of the exiting degree k in the subcritical region (target of 150 - left diagram) and supercritical region (target of 550 - right diagram). The initial resource is fixed at 100 units; the initial network size is 100 players; 10,000 rounds. Results averaged over 50 histories.

rounds later. For each simulation we calculate the **frequency of achievement** as follows: For each $R = 1, 2, 3, \dots$ the number of times the event R occurs is calculated and then the frequency is obtained by dividing by the total number of times a player achieves their target. This gives a frequency distribution so that different scenarios (i.e. targets) can be compared.

Figure 63, representing the subcritical region (target of 150), shows the interesting result that there is approximately a 40 percent chance a player will achieve in every two or three rounds during a 10,000 round game. Moreover, in the subcritical region, achievement occurs less than once in every seven rounds. However in the supercritical region (target of 550), achievement of players can occur once in every 100 rounds, in other words, achievement occurs very infrequently. The first peak in the supercritical region's results represents those group of players that achieved at approximately the same time early in the simulation. Figure 64 shows the probability that the kudos population will be of a given size when a player achieves. The probability distributions illustrated in Figure 64 are impor-

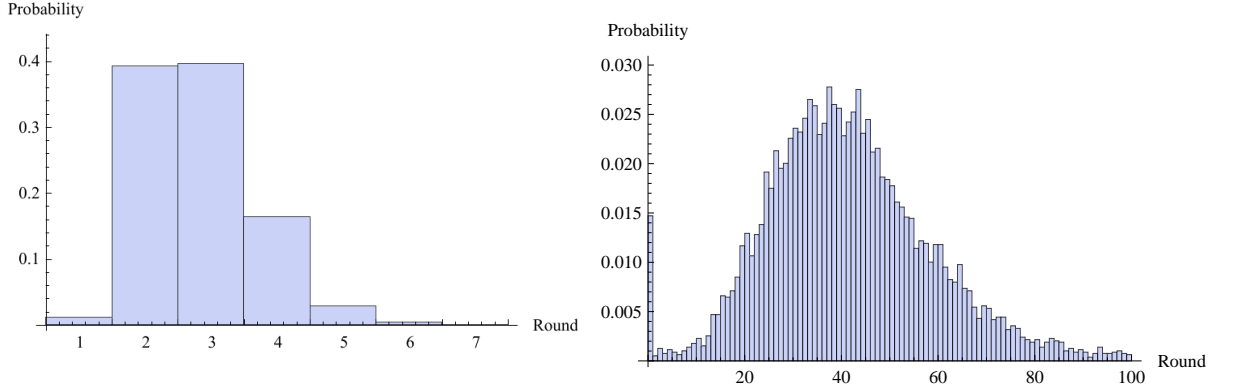


Figure 63: Frequency of achievement in the subcritical region (target of 150 - left diagram) and supercritical region (target of 550 - right diagram). This is shown as a probability distribution. The initial resource is fixed at 100 units; the initial network size is 100 players; 10,000 rounds. Results averaged over 50 histories.

tant because, for the kudos attachment rule, the offspring of the achieving player can only attach to those in the network who have kudos. In the subcritical region (target of 150), the offspring of an achieving player can only choose to attach to at most seven players during a 10,000 round simulation. For the supercritical region (target of 550), an offspring of an achieving player can choose from over 60 players who have held kudos. Figure 65 shows the probability a player will have kudos for a given length of time before achieving. In the event that a player receives the “golden unit”, the number of rounds it takes to achieve is important as shown in Figure 49. In the subcritical region (target of 150), Figure 65 shows a player can achieve within six rounds from the time they received kudos. However, for the supercritical region (target of 550), a player may take two hundred rounds to achieve from the time that they first received kudos. In all cases the contrast between the sub and supercritical regions is clear.

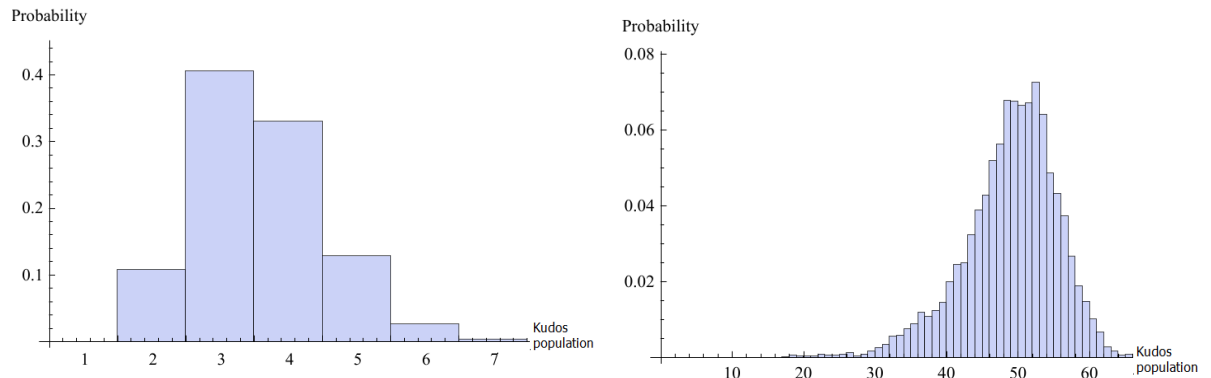


Figure 64: Probability distribution of the kudos population when a player achieves in the subcritical region (target of 150 - left diagram) and supercritical region (target of 550 - right diagram). The initial resource is fixed at 100 units; the initial network size is 100 players; 10,000 rounds. Results averaged over 50 histories.

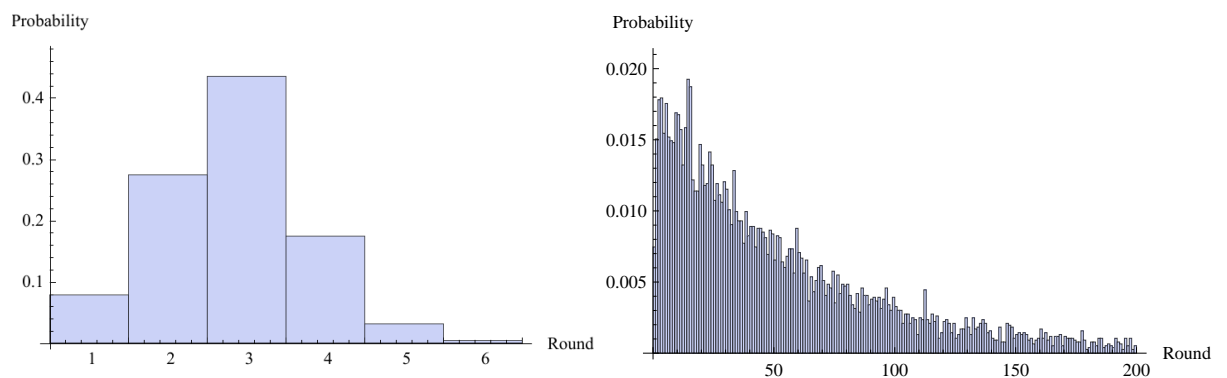
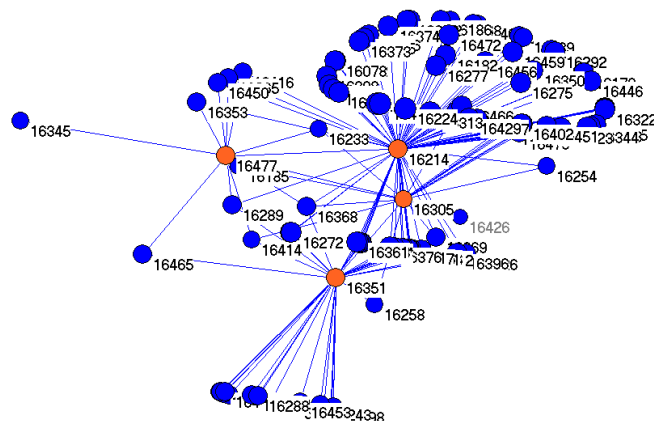


Figure 65: Probability distribution of the number of rounds it takes a player to achieve in the subcritical region (target of 150 - left diagram) and supercritical region (target of 550 - right diagram) when they have kudos. The initial resource is fixed at 100 units; the initial network size is 100 players; 10,000 rounds. Results averaged over 50 histories.

In the subcritical region, represented by a target of 150, an offspring of an achieving player is expected to arrive every two to three rounds and can only

To emphasize this point, Figures 66, 67, 68 and 69 show some network topologies for a number of successive rounds. Within these figures, the players with kudos are represented by orange nodes. Here we see that the kudos players have the largest degree.



In Figures 66, 67 and 68 we observe a repeated pattern of one round where there is large number of isolated players which is then followed by them all connecting

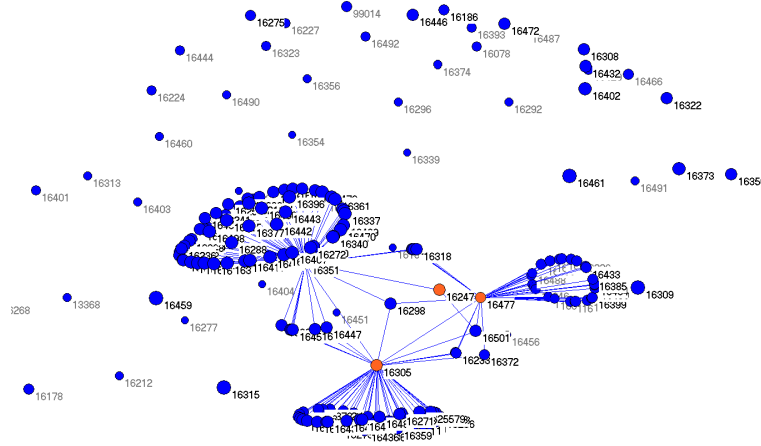
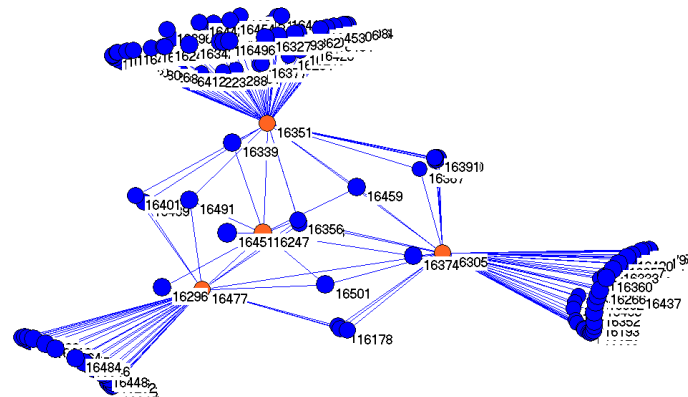


Figure 67: Second of four successive illustrative rounds (round 9982) of the evolving model. Game played in the subcritical region (target of 150). Orange nodes are players with kudos. When Player 16214 achieves it causes mass isolation.

to the few players who have kudos (the orange nodes). In the next round, at least one of the players with kudos achieves causing a large number of players to become isolated and subsequently the pattern is repeated. However, repeating the same exercise but in the supercritical region (target 550) shows a different evolution. Because the network is evolving more slowly we take a snapshot every 1000 rounds.

As can be observed from Figures 69 to 72, the networks in the supercritical region comprise more players with kudos than their subcritical counterparts. In other words, the older kudos players remain in the network longer. When a player achieves, their offspring (as well as isolated players) can thus choose to attach to a larger group of potential opponents with kudos. In summary, in the subcritical region, the few players with kudos will attain a large exiting degree because they are



the only opponents the offspring and isolated players can preferentially attach to. As an illustration, Figure 73 upper diagram illustrates the influence of varying the target on the average number of isolated players per achievement event. This also shows the number of neighbours the achiever had prior to achieving. From these figures it is observed that in the subcritical region (target less than 260), most of the achiever's neighbours become isolated when the player achieves. Furthermore, as illustrated in Figure 73 lower diagram, an achieving player can exceed their target in the subcritical region. However in the supercritical region, an achieving player will exceed their target only by a few units. To clarify this, the achieving player's exit degree influences how many units they will exceed the target by because when a player has a large degree they will beat many other players. Moreover, the exit degree increases when the target decreases in the subcritical region because there

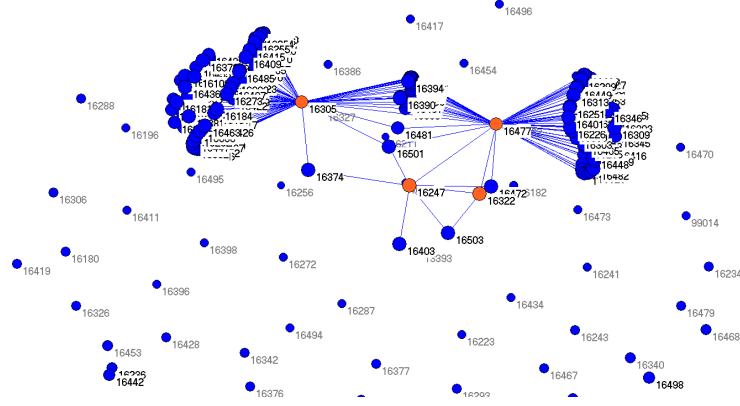


Figure 69: Fourth of four successive illustrative rounds (round 9984) of the evolving model. Game played in the subcritical region (target of 150). Orange nodes are players with kudos. When Player 16351 achieves it causes mass isolation.

is a high number of isolated players connecting to a small number of potential opponents who have kudos (Figure 64). As a consequence, the MTTA will remain approximately the same due to the large number of isolated players, the small number of potential opponents who have kudos and the large exit degree causing a gain in units in excess of the target. However in the supercritical region, the target is larger causing many of the players to become bankrupt instead. In the subcritical region a player can achieve without first bankrupting their neighbours, who then may become isolated. For a player to achieve in the supercritical region, they first may have to bankrupt their neighbours before reaching their targets, hence there will be a lower number in isolation. In short, for the supercritical region, when the target increases, the MTTA will increase also.

The **kudos population size** is defined as the number of players still playing

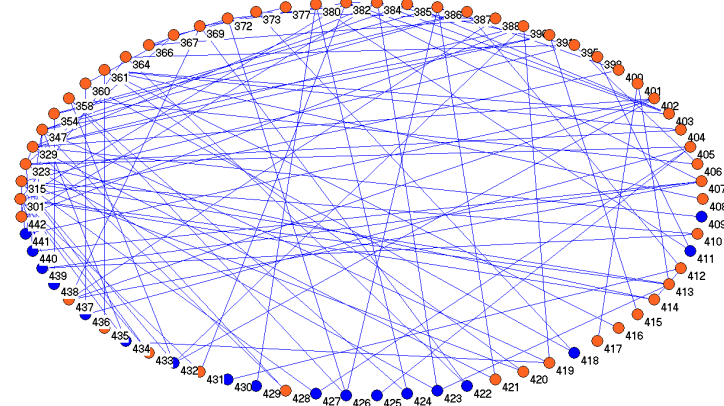


Figure 70: First of three illustrative rounds of the evolving model: round 7000. Game played in the supercritical region (target of 550). Orange nodes are players with kudos.

who have held the “golden unit”. As illustrated in Figure 64, a significant difference in this value is observed in the subcritical and supercritical regions. From a different perspective, Figure 74 illustrates the influence of different targets on the kudos population size as a proportion of the total network through time. We observe that after 10,000 rounds, the kudos population size has increased significantly from targets of 250 to 350. In this case, these targets are located either side of the critical point.

To investigate the factors that limit the growth of the kudos population as well as the phase transition we define the following;

- **Original players** are the players who were in the network at the start of the game.

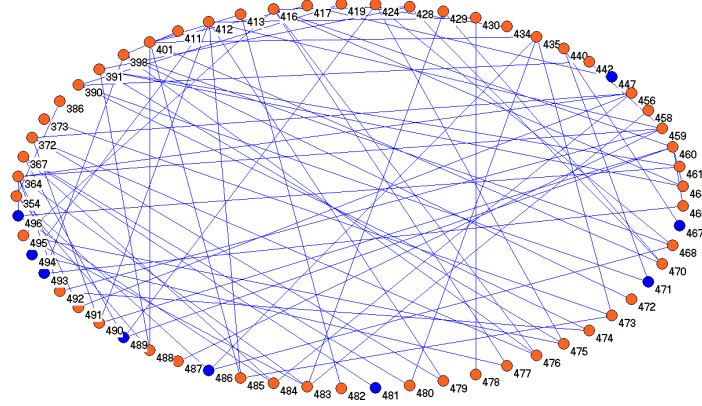


Figure 71: Second of three illustrative rounds of the evolving model: round 8000. Game played in the supercritical region (target of 550). Orange nodes are players with kudos.

- **First generation** are the offspring of the original players.

Furthermore, we shall consider whether it is the first generation that influences whether the kudos population grows or declines. The reasoning behind this is that the first generation can only preferentially attach to kudos players and hence increases the kudos player's degree. If the number of the first generation exceeds the kudos population this may result in the degree of all kudos players increasing significantly especially if the offspring connects to more than one player. As illustrated in Figure 50, the larger the player's degree the more likely they are to achieve more quickly. As a result, the kudos population will decline as the kudos players leave the network through achievement. Alternatively, if the number of the first generation does not exceed the kudos population then on average there

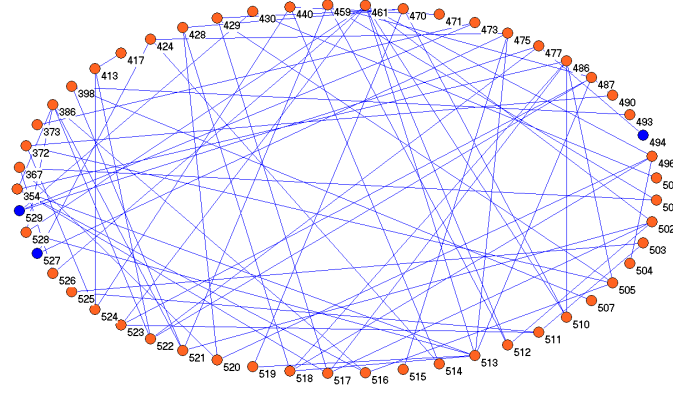


Figure 72: Third of three illustrative rounds of the evolving model: round 9000. Game played in the supercritical region (target of 550). Orange nodes are players with kudos.

is a small increase in the kudos player's degree. This may result in, as seen in Figure 65 (right diagram), the kudos player remaining in the network for a long duration and hence the kudos population grows as new players obtain the “golden unit”. We therefore make the following conjecture:

The phase transition occurs when the number of first generation multiplied by their degree is equal to the kudos population.

To explore this conjecture further, a simple analytical model was developed. The objective of the model is to approximate the sizes of the kudos population and the first generation when they attach to each other. This model may give an indication of the relationships that determines whether the kudos population will grow or decline. For this model, we will use an N player fully connected network but will make the following assumptions:

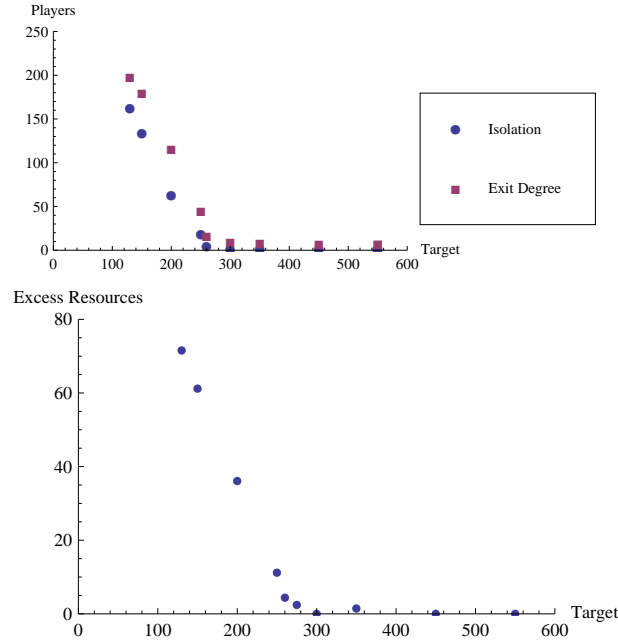


Figure 73: The influence of varying the target upon the number of neighbours of an achiever and average number of isolated players per achievement event (upper diagram). The influence upon units gained beyond the target - Excess Resources (lower diagram). The initial resource is fixed at 100 units; the initial network size is 100 players; 10,000 rounds. Results averaged over 50 histories.

1. The network consists of N players, each with an initial resource of I units and a target of T units.
2. After $T - I$ rounds a proportion A of the players in the network achieve.
3. $A = N \frac{I}{T}$. The basis for this is that it is impossible for all players to achieve without any bankruptcy. However the smaller the distance from I to T is, the greater the likelihood of achievement. Hence, we have assumed a proportional relationship to estimate the number of achievers.
4. The “golden unit” goes to a non kudos player in each round. In other words the probability of retaining or regaining the “golden unit” is small.

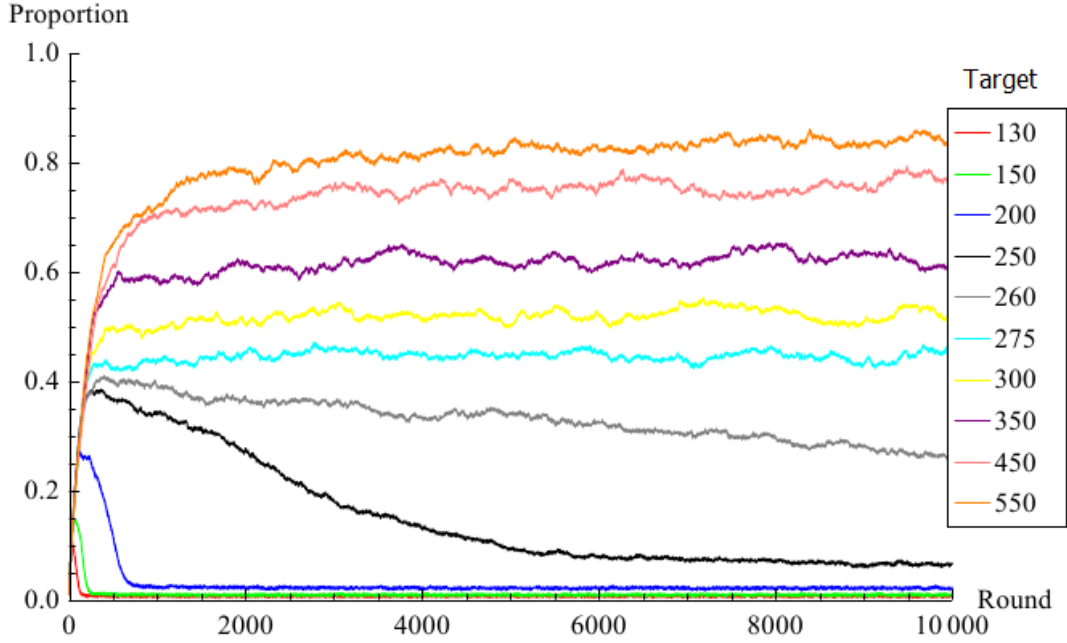


Figure 74: How the target influences the kudos population size as a proportion of the total network through time (Round). The initial resource is fixed at 100 units; the initial network size is 100 players; 10,000 rounds. Results averaged over 50 histories.

A limitation of the model is that we overestimate the kudos population, as we are assuming for each round the “golden unit” will go to a non kudos player. As well as this, we are not considering the possibility of a kudos player leaving the network through achievement or bankruptcy. In other words we are calculating the maximum size of the kudos population after a given number of rounds. Nevertheless, we will compare the analytical and numerical results in order to determine the limitations of these assumptions.

By assuming the phase transition occurs when the number of the first generation multiplied by their degree is equal to the kudos population, we obtain the

following equation:

$$N \frac{I}{T} \times (C - 1) \times k = T - I. \quad (5.3.2)$$

The variables are:

N - the initial size of the network.

I - the initial resources of each player.

T - the target for each player.

C - the number of offspring of an achiever.

k - the degree of the offspring player.

$T - I$ - the estimated size of the kudos population. There is the assumption that the “golden unit” has progressed to a different player at each round.

The left hand side of the above expression is multiplied by the initial degree (k) of the first generation player. This is important because, if the initial degree exceeds the kudos population size then all the kudos players will be attached to every offspring that arrives. Conversely, the right hand side of the expression is the estimate of the kudos population size.

Rearranging the above expression, the critical target can be approximated by:

$$T^* \approx \frac{1}{2} \times \left(I + \sqrt{I^2 + 4 \times N \times I \times (C - 1) \times k} \right). \quad (5.3.3)$$

In order to measure the accuracy of the above expression, a comparison with the numerical result is required. From the evolving model results, as shown in Figures 59 and 60, it can be seen that the phase transition (critical target) occurs where the ratio between MTTA and MTTB is equal to 1. From the results that generated the graph in Figure 60, we need to approximate the critical target for a number of network sizes N . By using the mean value theorem [Gullberg (1997)] and selected data points from either side of the critical point (shown in Table 10), the numerical critical target can be approximated for various network sizes. Figure 75 illustrates

Size N	$T_{subcritical}$	$T_{supercritical}$	$ratio_{subcritical}$	$ratio_{supercritical}$	critical target estimate
35	130	150	0.6385	1.2143	142.5572
50	150	200	0.5995	1.8033	166.6347
60	150	200	0.5622	1.3548	177.6157
65	200	250	0.8272	1.9422	207.7470
75	200	250	0.6578	1.8277	214.6259
100	250	260	0.8278	1.3631	253.2173
125	275	300	0.8343	1.6335	280.1835
150	300	325	0.8299	1.6064	305.4758
175	325	350	0.8480	1.6041	330.0271
190	325	350	0.7378	1.2079	338.9457
200	350	450	0.9510	1.9342	354.9848
250	350	450	0.6605	1.8056	379.6495

Table 10: Estimating the critical target from the simulated results selected data points (Figure 60) where $ratio = \frac{MTTA}{MTTB}$. Here $T_{supercritical}$ is the target whose respected ratio $ratio_{supercritical}$ is greater than one. Also, $T_{subcritical}$ is the target whose respected ratio $ratio_{subcritical}$ is less than one.

the comparison between the results shown in Table 10 and the simple analytical approximation of the critical target.

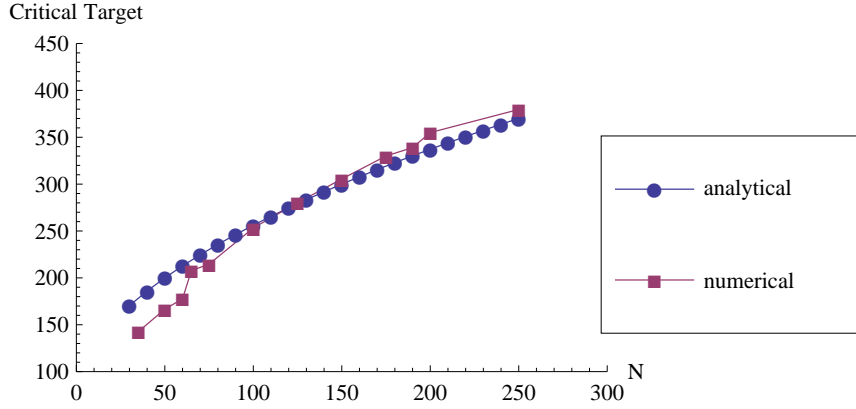


Figure 75: Critical target estimate comparison between the numerical simulation model and the analytical approximation. The initial resource is fixed at 100 units; offspring entrance degree = 2; 10,000 rounds. Result averaged over 50 histories for the numerical simulation.

Figure 75 illustrates that, for $100 < N < 200$, there is a good agreement between the numerical simulation of the evolving model and the analytical approximation. This suggests that the first generation does indeed influence whether kudos population grows or decline and the occurrence of the phase transition. Outside this range, the estimate of kudos population and the first generation do not match the numerical results as well. However, the robustness of both the numerical simulation and the analytical approximation solutions will be discussed later (section 5.3.3).

Apart from the occurrence of a phase transition, the evolving model has other properties. Firstly, as illustrated in Figure 76 (upper diagram), as the target decreases in the subcritical region there is a rapid rise in the proportion of the network connected to the node with the largest degree. Hence, the evolving model network topology can evolve into a giant component [Erdős and Rényi (1959)]. This has offered one possible explanation of how a giant component comes into being. Fi-

nally, Figure 76 (lower diagram) illustrates that the target can be regarded as a tunable parameter to generate high clustering coefficients.

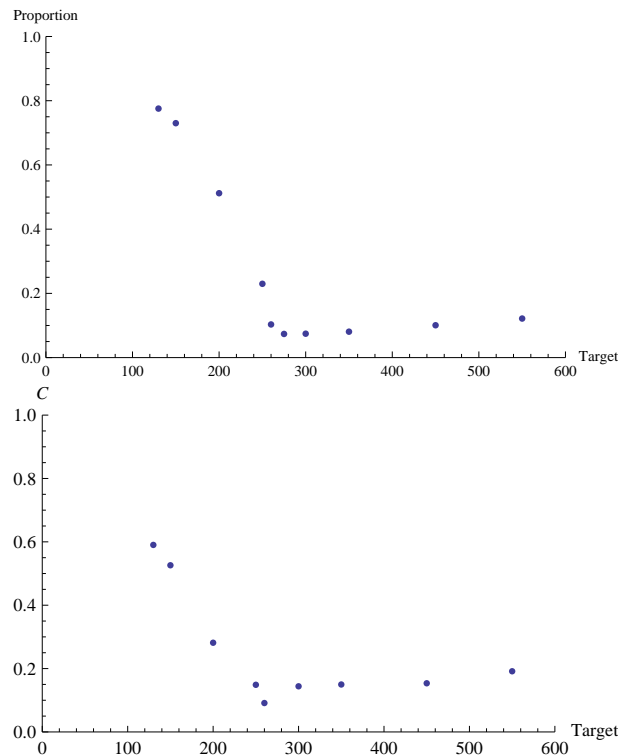


Figure 76: How the player's target influences the proportion of the network connected to the node with the largest degree (upper diagram) and network's clustering coefficient C (lower diagram). The initial resource is fixed at 100 units; the initial network size is 100 players; 10,000 rounds. Results averaged over 50 histories.

5.3.3 Critical Targets and the Scaling Laws

In this section we shall consider the scaling laws for the evolving model and how they are related to the critical target.

From the simple analytical approximation (section 5.3.2), when the initial resource and network size are doubled then the critical target is also doubled. In

Table 11 we investigate this relationship in the numerical simulation. Here, the initial network size, the initial resources and the target are increased to see if the MTTA, MTTB and the final population increase by the same factor. Taking into account the random fluctuation of the numerical simulation, it can be seen from this table that the normalised output values are indeed closely aligned to the scaling factors for the input variables. The results are indeed as expected.

Normalised Initial Network Size	Normalised Initial Resource	Normalised Target	Normalised MTTA	Normalised MTTB	Normalised Final Population
1.000	1.000	1.000	1.000	1.000	1.000
1.500	1.500	1.500	1.450	1.483	1.512
2.000	2.000	2.000	1.915	1.966	2.030

Table 11: Investigation of the scaling properties of the evolving model. The normalised inputs are the number of the initial network size = 100, initial resource = 100, target = 200. The initial network topology was a pure ring lattice; 10,000 rounds were played. Results averaged over 50 histories.

Consequently, it is hypothesized that when the critical target is increased by a scaling factor the outputs from the evolving model will also increase by the same factor. In order to investigate this further, all the parameters considered in the simple analytical approximation were varied. Table 12 shows the reference case and the other scenarios investigated. Furthermore, both analytical and numerical estimates of the critical targets were considered in order to test the robustness of each technique. It can be seen that in *Case 2*, there is not a good agreement between the analytical and numerical estimates of the critical targets. This will be discussed further at the end of this section.

Case	Initial Network Size N	Initial Resource	Off- spring	k	Analytical Critical Target	Scaling Factor	Numerical Critical Target	Scaling Factor
1	100	100	3	2	256.16	1.000	253.22	1.000
2	100	100	3	1	200.00	1.281	264.01	0.959
3	100	100	4	2	300.00	0.854	276.34	0.916
4	100	100	5	2	337.23	0.760	290.63	0.871
5	100	50	3	2	168.61	1.519	177.26	1.429
6	100	150	3	2	331.17	0.773	313.16	0.809
7	225	100	3	2	354.14	0.723	378.18	0.670

Table 12: Details of the cases investigated and parameter settings as well as critical target and scaling factors for the analytical and numerical estimating techniques.

For the remainder of this section, for each scenario the simulated results will be normalised by the reference case using either the analytical or numerical estimation of the critical targets.

Firstly, Figure 77 compares the scenario where the offspring has one degree with the reference case. It is noted that the numerical estimating techniques (right column diagrams) produced a better agreement to the reference case than its analytical estimating counterpart (left column diagrams). This is especially true for the final population Nf where there seems to be a systematic error. This will be discussed at the end of this section. Figure 78 compares the scenario where the achieving player has four or five offspring with the reference case (three offspring). It is noted with the exception of the MTTB scenario, both estimating techniques show good agreement with the reference case when they are normalised. Figure 79 compares the scenario where the initial resource of a player is plus or minus 50 units from the reference case (100 units). Certainly both estimating techniques

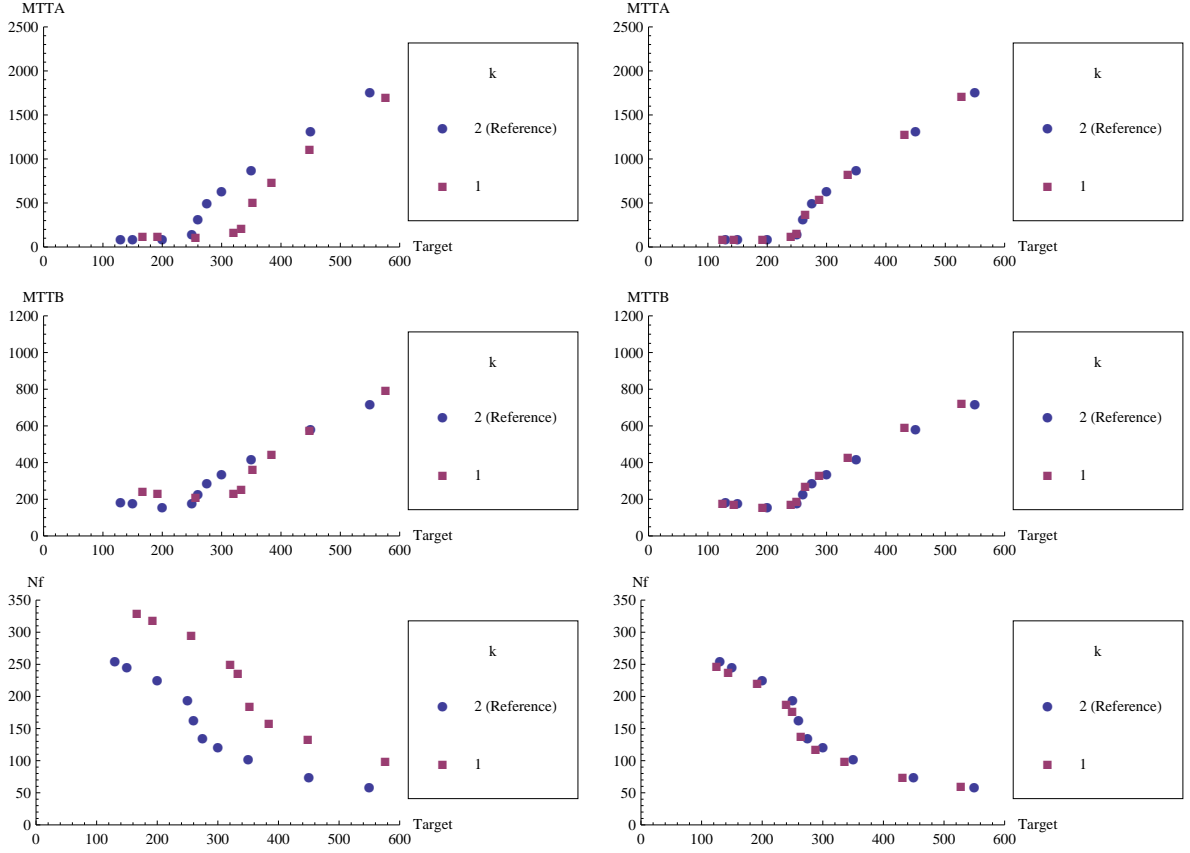


Figure 77: Normalising the MTTA (Top row), MTTB (Middle row) and final population Nf (Bottom row) to the reference case when the degree of the player's offspring k is equal to one. Left column - the analytical results, Right column - the numerical results. For the non reference scenarios, the MTTA, MTTB, final population Nf and Targets are scaled by the corresponding factor shown in Table 12 Case 2. The initial resource is fixed at 100 units; the initial network size is 100 players; 10,000 rounds. Results averaged over 50 histories.

show good agreement with the reference case when they are normalised for all scenarios. However, it must be noted that the numerical estimating technique shows the better agreement compared to its analytical counterpart. Finally, Figure 80 compares the scenario of an initial network size of 225 players with the reference

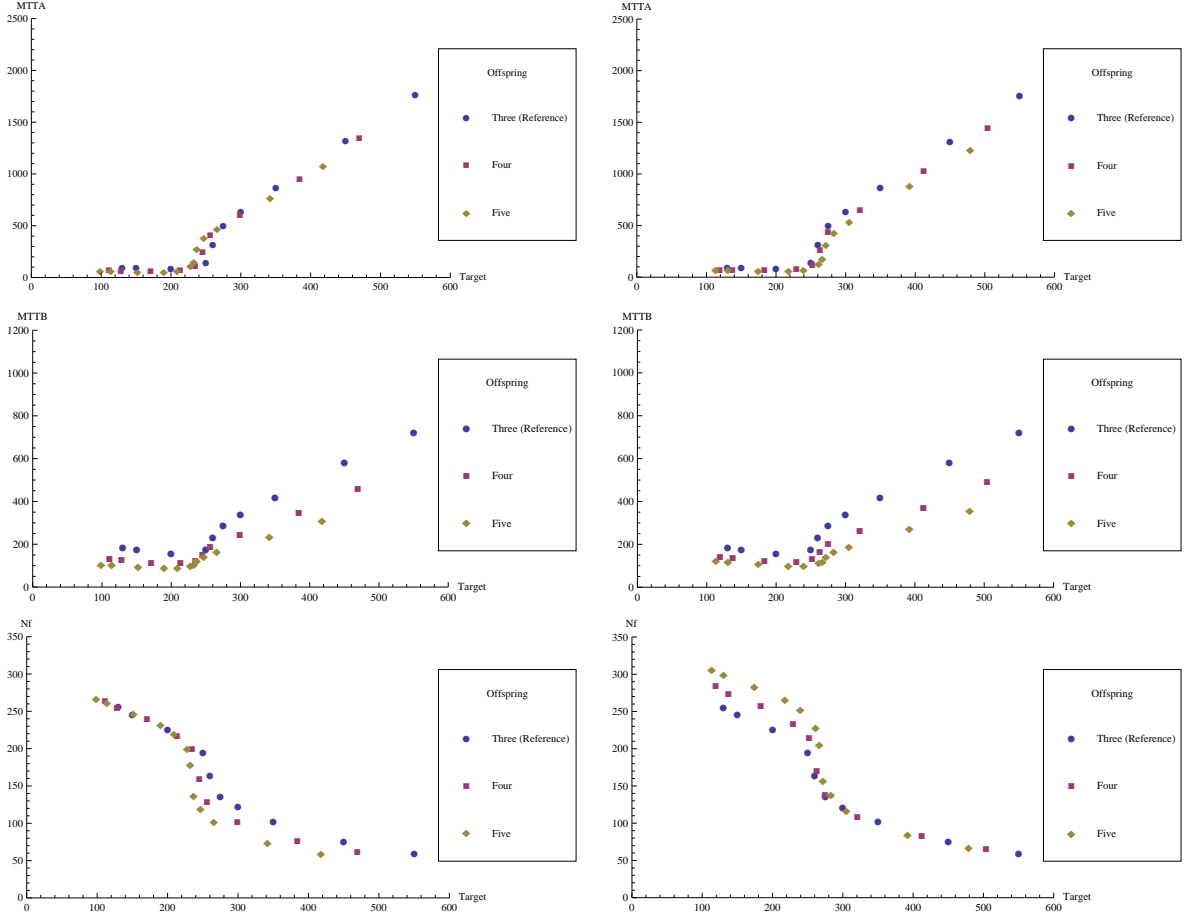


Figure 78: Normalising the MTTA (Top row), MTTB (Middle row) and final population Nf (Bottom row) to the reference case when the number of offspring is four or five. Left column - the analytical results, Right column - the numerical results. For the non reference scenarios, the MTTA, MTTB, final population Nf and Targets are scaled by the corresponding factor shown in Table 12 Cases 3 and 4. The initial resource is fixed at 100 units; the initial network size is 100 players; 10,000 rounds. Results averaged over 50 histories.

case (100 players). As with the initial resource cases, both estimating techniques show good agreement with the reference case. However yet again, it is observed that the numerical estimating technique (right column diagram) shows a better

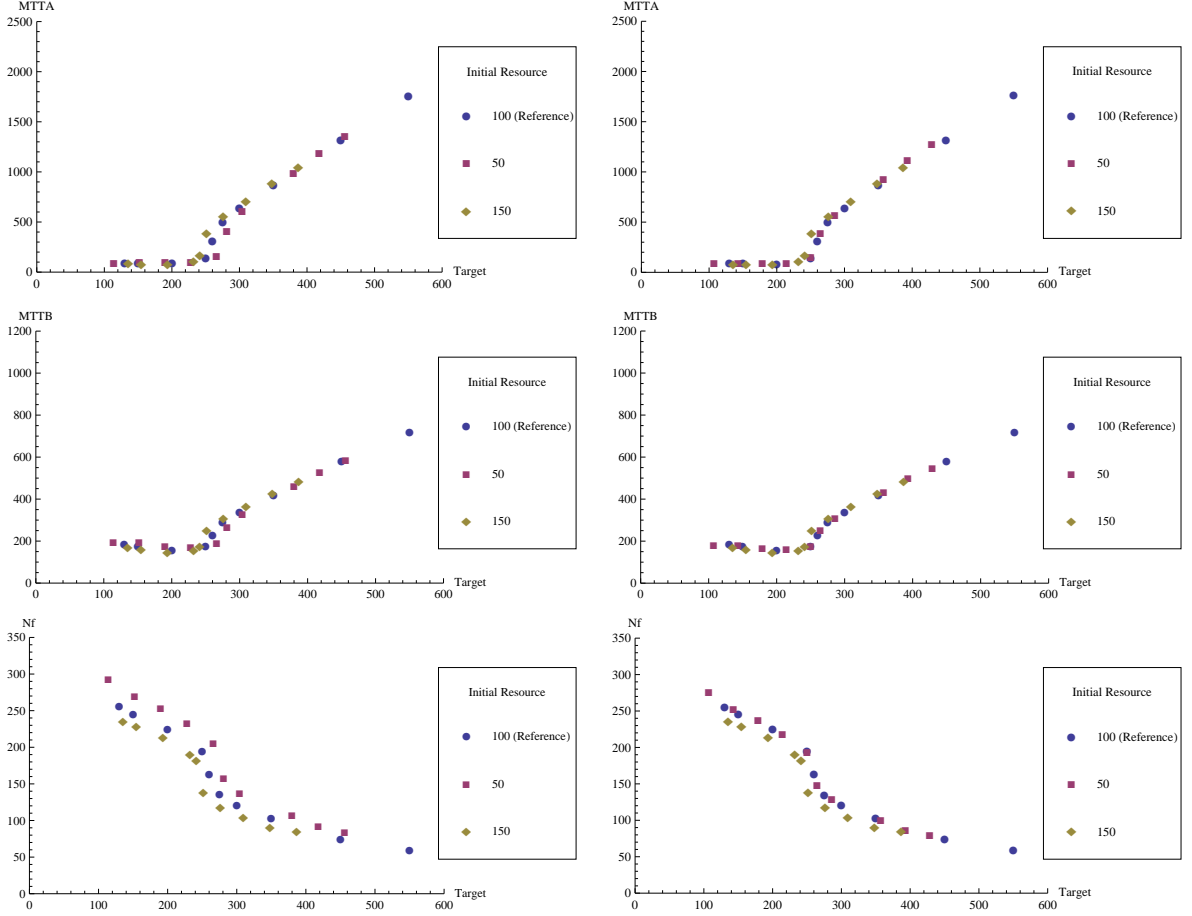


Figure 79: Normalising the MTTA (Top row), MTTB (Middle row) and final population Nf (Bottom row) to the reference case when the initial resource is 50 or 150 units. Left column - the analytical results, Right column - the numerical results. For the non reference scenarios, the MTTA, MTTB, final population Nf and Targets are scaled by the corresponding factor shown in Table 12 Cases 5 and 6. The initial resource is fixed at 100 units; the initial network size is 100 players; 10,000 rounds. Results averaged over 50 histories.

agreement than its analytical counterpart (left column diagram).

In summary, the critical target offers a good basis for determining the scaling law factor for the evolving model. Furthermore, the scaling factor shows that

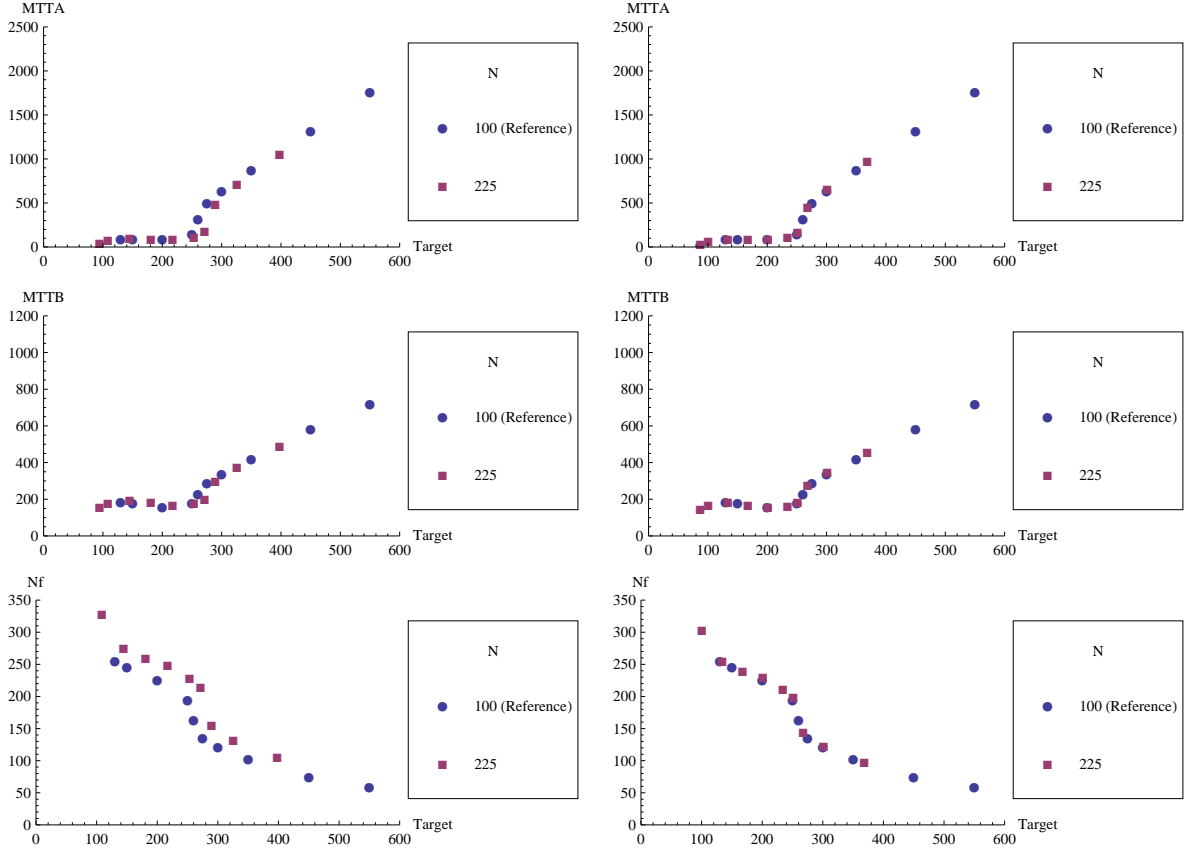


Figure 80: Normalising the MTTA (Top row), MTTB (Middle row) and final population Nf (Bottom row) to the reference case when the initial network size N is equal to 225. Left column - the analytical results, Right column - the numerical results. For the non reference scenarios, the MTTA, MTTB, final population Nf and Targets are scaled by the corresponding factor shown in Table 12 Case 7. The initial resource is fixed at 100 units; the reference initial network size is 100 players; 10,000 rounds. Results averaged over 50 histories.

the results in the previous section are not unique but are linked by their critical target values. We note that the numerical estimate of the critical target offers a better scaling law than its analytical counterpart. However, for Table 12 *Case 2* there was not a good agreement between the analytical and numerical estimates

of the critical targets. As well as this, in Figure 77, the final population Nf , there appears to be a systematic error with the analytical estimates. Both of these statements are related to the offspring degree. In equation 5.3.2 the right hand side of the expression is the estimate of the kudos population size, which is independent of the offspring's degree. However, Figure 81 illustrates that the kudos population size is not independent of the offspring's degree. Most notably for the target of 260, the kudos population size as a proportion of the total network size has increased from 9.7 to 25.3 percent (1 dp). Table 12 also shows, by increasing the offspring's degree from 1 to 2, the target of 260 is now above as opposed to below the numerical critical target. In other words, the critical target decreases when the offspring's degree increases. The reasoning behind this is that when an offspring has a larger initial degree there is more opportunity for this player to obtain the "golden unit". This increases the rate at which players are added to the kudos population. To counter this and to keep the kudos population size small (see Figure 74 and section 5.3.2 for characteristics of a subcritical region), the critical target must decrease in order to increase the rate at which kudos players are achieving. This factor is not represented in equation 5.3.2. Further work is required to improve equation 5.3.2 to take into account the degree of the offspring (see section 6.2).

5.3.4 Incorporating Regulation

In the real world of sport and business competition, if a player, team, or business is believed to have an unfair advantage then they may be subject to regulation. For instance in the United Kingdom, Ofcom regulates the communications industry to ensure a monopoly does not develop. In American Football the best teams are restricted to the quality of players they can recruit from the college draft. In 1998 the United States Government prosecuted the Microsoft Cooperation for allegedly

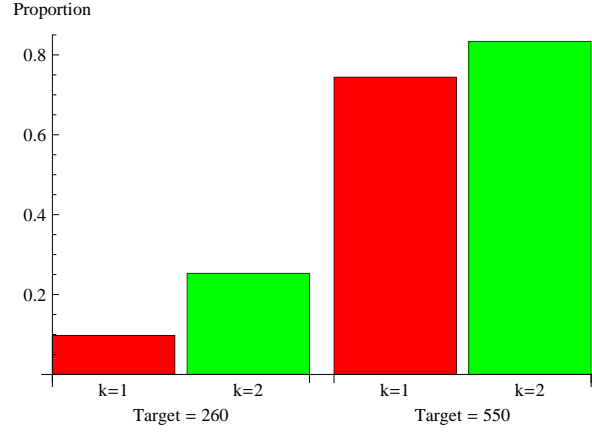


Figure 81: How the target and the degree of the player's offspring k influences the kudos population size as a proportion of the total network after 10,000 rounds. The initial resource is fixed at 100 units; the initial network size is 100 players. Results averaged over 50 histories.

restricting the market for competing web browsers. The previous section discussed that in the subcritical region only a few players obtain kudos and those that did achieved their targets quickly. As in the case of Microsoft, a regulatory body may judge such competitive rules to be unfair to the rest of the network. Furthermore, under these circumstances a regulatory body could modify the rules in order for there to be fairer competition.

In the case of the evolving model, the following was observed: when the target is in the subcritical region, an offspring will only attach to a small number of players. To incorporate competitive regulatory behaviour in the evolving model, we shall adapt the kudos attachment rule. Firstly, we choose an arbitrary weighting factor that determines whether an offspring or isolated player will attach to an opponent at random or by using kudos. Secondly, we bias this weighting factor towards the random attachment rule if an achieving player's exit degree during the simulation is regarded as being too large. We choose the weighting factor ε to have the

following form:

$$\varepsilon = 1 - e^{-\beta \sum_{j=1}^{N_r} K_j}. \quad (5.3.4)$$

where β is the influence factor, K_j is the number of rounds player j has held the “golden unit”, whereas N_r is the size of the network at round r . Within the evolving model, when ε approaches 1 the player is more likely to use kudos as their attachment rule. However, when ε approaches 0, the player is more likely to use the random attachment. For example, Figure 82 (upper diagram) compares non regulating and regulated attachment rules on the population size Nr throughout the game. There are four regulated attachment rules shown; where the objective is to keep the player’s degree < 10 , < 20 , < 50 and < 100 respectively. If a player achieves with an exit degree greater than the regulated objective then the β value is reduced by a certain percentage. In this case the β value is initially set at 10,000 and the reduction is 10 percent. For example, when the regulated objective is no more than a degree of 10, it is observed that the network follows the random attachment closely after 3000 rounds.

Figure 82 lower diagram shows the proportion of players with kudos throughout the game and the influence of regulation on this result. In this case, the weighting factor is adjusted when the achieving player’s exit degree exceeds 25. In comparison with Figure 74 it is observed that the difference in the cases in the subcritical region (targets of about 250 see Table 10) is that the proportion of players with kudos has increased where, by round 10000, at least 15 percent of the players have kudos. Under the same parameters, the influence regulation has on the final population and exit degree is illustrated in Figure 83. Due to the limitations on a player’s degree imposed by the regulating attachment rule, an achiever no longer exhibits a large exiting degree in the subcritical region. Furthermore, for the final population and exiting degree, the regulating attachment rule removes the phase

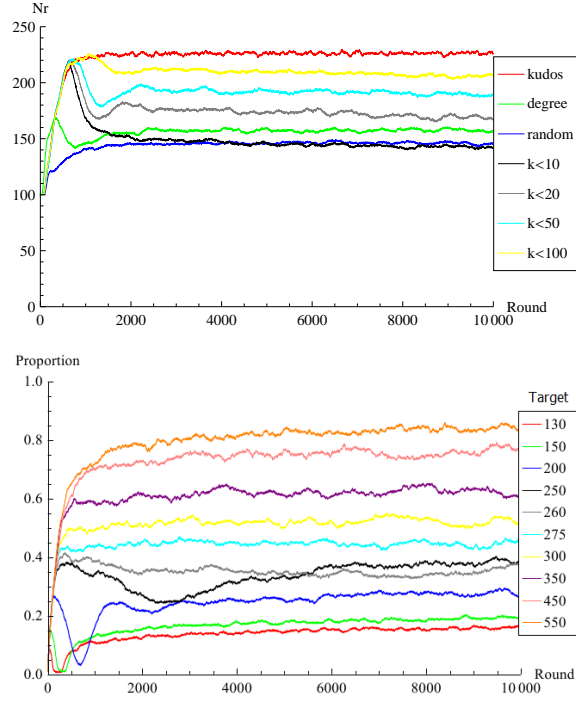


Figure 82: Upper diagram is the non regulating and regulating attachment rules' influence on the population size Nr throughout the game. The β value is initially set at 10,000 while the reduction is 10 percent. The target is 200. Lower diagram is the kudos population as a proportion of the network size with regulation for different targets; regulation activated when the exiting degree exceeds 25, β value is initially set at 10,000 and the influence factor β is reduced by 10 percent. The initial resource is fixed at 100 units; the initial network size is 100 players; 10,000 rounds. Results averaged over 50 histories.

transition observed in the previous section and hence the network imitates the random attachment behaviour, as discussed in Chapter 4.

In conclusion, this chapter has discussed the development of a bespoke preferential attachment rule for the Extended GR problem. From other bespoke preferential attachment rules it was noted that there had to be some benefit for a new

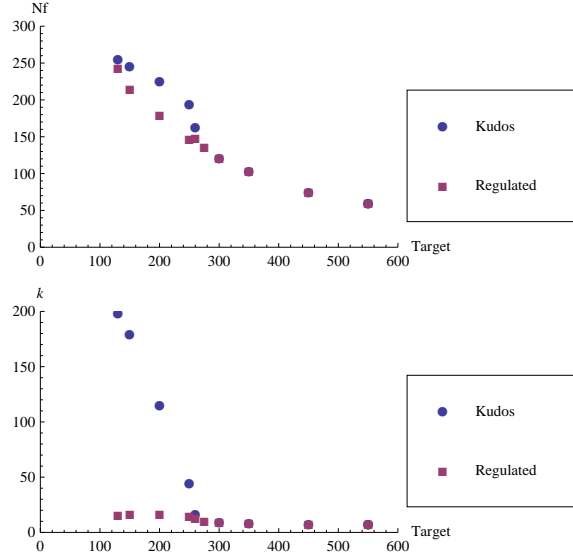


Figure 83: Influence of kudos and regulating attachment rule on the final population Nf (upper diagram) and the achiever's exiting degree k (lower diagram). Regulation activated when exiting degree exceeds 25 and the influence factor β is reduced by 10 percent. The initial resource is fixed at 100 units; the initial network size is 100 players; 10,000 rounds. Results averaged over 50 histories.

player to attach to an existing player. The kudos preferential attachment rule gives preference to the player who has held on to a “golden unit” the longest. It was found that adopting this attachment rule helped the player to achieve. However, it was also observed that this attachment rule resulted in a phase transition in a number of the simulated results. This in turn was influenced by a critical target. By investigating this further, a number of key parameters were found which estimated the critical targets and determined the scaling law for this version of the Extended GR problem. Finally, by incorporating regulation of competitive behaviour within the evolving model, it was observed that under highly regulated conditions the attachment rule will change from kudos to random selection and the phase transition is removed.

6 Conclusion and Future Work

In this thesis we investigated the problem of extending the GR problem in order for it to be played over networks. The motivation of this research was not to model the behaviour of a gambler per se, but the competitive behaviour of players in business and social environments. In order to model this competitive behaviour, a series of numerical simulations were executed using Python and NetworkX. Section 6.1 presents a synopsis of the thesis' contents and simulated results. Section 6.2 examines some limitations of the adopted approach and explores possible avenues for improvement and further work.

6.1 Synopsis

In [Hadjiliadis and Vecer (2006)], an extension of the classical GR problem is used to model the stock market. [Hunter et al (2008)] have adapted the classical GR problem to model a player who is playing a lottery-type game. Although these papers use the GR problem to model competitive behaviour, they only consider a two player game. However, Rocha and Stern [Rocha and Stern (2004)] consider an N -player GR problem to model a game of gambling. Here, the underlying network is fully connected as all players are competing against each other. In contrast, in the business world there are many examples where all players, such as multinationals, are not all competing against each other and thus the network is not fully connected. Moreover it is a dynamic network in which the 'players' may come and go and may link to, or disconnect from, other players as time passes. Thus we have devised an extension of the GR problem that could be played over dynamical networks which are not necessarily fully connected.

The N -player GR problem played over networks, however, produces a number of challenges, in particular the payment rule. The payment rule determines which

player wins resource from their opponents and how much. However, for the classical and the fully connected N -player GR problem this is trivial in each round (iteration). A player is randomly selected to win and gains one unit. In contrast, for the N -player GR problem played over networks, the game can generate more than one winning player per round. In our model a player is no longer selected to win but is given a randomly sampled score. It is these scores that determine whether a player has beaten their opponent. The payment rule we introduce is as follows:

- *In each round, a player gives one unit of resource to its highest scoring neighbour, provided that neighbour scores higher than the player.*
- *Otherwise the player keeps their resource.*

The consequence of adopting this payment rule approach is that the player can lose at most one unit of resource, which is independent of the amount of neighbours they are connected to.

For the classical GR problem (see section 3.1.1), the final round is when one of the players (who starts with an initial resource) becomes ruined, i.e. when the player's opponent has gained all of their resources. However, [Hadjiliadis (2004)] describes a version of the GR problem where the player has an objective value which is less than gaining all of their opponents resources. For the N -player GR problem played over networks, this objective value is defined as the player's target. In contrast to the classical GR problem and [Rocha and Stern (2004)]'s fully connected GR problem (see section 3.1.2), the game does not stop when one player becomes ruined (loses all of their resources) but continues to a specified user-defined final round. When a player becomes ruined they depart from the game. Under these circumstances, the actual structure of the network changes throughout the duration of the game. In other words, the size of the network

as well as the distribution of the number of opponents a player is connected to changes throughout the game, i.e. the network topology changes. To measure this and its effect on our version of the extended GR problem, we analyse the following outputs:

1. **Mean time to Achievement:** *This measures the average number of rounds it takes to achieve for only those players who reach their targets.*
2. **Mean time to Bankruptcy:** *This measures the average number of rounds it takes to bankruptcy for only those players who become ruined.*
3. **Population:** *This is the size of the network, in essence how many players are currently playing.*
4. **Degree of an Achiever:** *This measures the number of opponents a player is connected to when that player achieves their target.*
5. **Degree of a Bankrupt player:** *This measures the number of opponents a player is connected to when that player becomes ruined.*

[Barabási (2009)](see Chapter 2) argued that the dynamical behaviour of a complex system is strongly influenced by its underlying network topology. To investigate the influence of the network topology on the extended GR problem, three numerical simulation models were developed: contracting, fixed and evolving. In essence, each of these models describes the underlying network topology during the duration of the numerical simulation.

In the contracting model (see section 3.2.1), the player immediately leaves the game when either they achieve their target or become bankrupt. This results in the network topology contracting into the classical two player GR problem.

In our fixed model (see section 3.2.4), the player remains in the game even when they achieve their target or becomes bankrupt. In this event, the player's

resources are reset to its initial value in the next round. The network topology remains fixed throughout the game.

In our evolving model (see section 4.2), the player immediately leaves the game when either they achieve their target or become bankrupt. However unlike the contracting model, if the player achieves then they have offspring. The offspring divide their parent's resources amongst themselves, join the network and play the game against existing opponents. This also results in the network topology changing throughout the game but in a much richer way than in our contracting model.

We considered three preferential attachment rules: random (see section 4.2), degree dependent (biased towards the players with the highest number of opponents, see section 4.2) and kudos (see section 5.3). In this context, kudos means that the offspring try to acquire a benefit from attaching to a particular opponent. In the evolving model, to achieve their goal, the offspring attach to existing players in the network who have kudos. Their goal is to increase the likelihood of achieving their target (see section 5.3). With this in mind, the offspring can increase the likelihood of achieving their target if they increase the number of opponents they are playing. To reiterate, a player can lose at most one unit of resource which is independent from how many opponents they are playing (see section 3.2).

As explained in section 5.3, kudos has three phases: firstly, the player attaches to a competitor who is popular; secondly, the player competes with the other competitor neighbours to become popular; finally, if the player becomes popular, they attract and compete with new and existing opponents to achieve their goal. In section 5.3 we also defined the kudos players as individuals who have held or are holding the “golden unit”. It must be noted that players that become isolated (all of their opponents have achieved or become ruined) follow the same attachment rule. Subsequently, when varying the player's target and observing

the effect on parameters such as mean time to achievement (MTTA), mean time to bankruptcy (MTTB), final population and degree of achievement, there occurs a phase transition within the results (see section 5.3.2). This behaviour is not observed in the random or degree dependent attachment rules. In section 5.3.2 we defined the critical target to be where the MTTA is equal to the MTTB; the subcritical region, to be where the MTTA is less than the MTTB; and finally the supercritical region, to be where the MTTA is greater than the MTTB. In terms of the kudos preferential attachment rule and the subcritical region, a player achieves their target quicker when the game is played in subcritical conditions. Also from section 5.3.2, kudos is obtained by only a small proportion of the network, less than 5 percent. As a result, the offspring attaches to a limited number of players who have kudos. Subsequently, the kudos player's degree increases rapidly; this also improves their probability of achievement within a few rounds. Under these circumstances, when the kudos player achieves, a large proportion of their neighbours become isolated. They then attach to those few players who have kudos.

In section 5.3.2 we also detailed the case of the supercritical region. Here, because the target is large, a player is required to ruin a greater number of their opponents in comparison to the subcritical region. As a result, players obtain their target slower in this region. Consequentially, kudos is gained by a larger proportion of the network and new offspring can attach to a greater number of kudos players. Nevertheless, the kudos player's degree increases but at a slower rate in comparison to those in the subcritical region and fewer opponents become isolated every time there is an achievement. In section 5.3.2 we described both an analytical and numerical estimate of the critical target. As well as this, the scaling laws for the simulated results were discussed. It was noted that the analytical estimate works well when varying the initial size of the network and resources. However, the ana-

lytical estimate fares less well when varying the number of offspring produced per achievement and the degree of the offspring. Section 5.3.2 also detailed that in the subcritical region any arbitrary network topology evolves into a giant component. This is similar to the giant component discussed by [Erdős and Rényi (1959)] in their random network model. Finally, as discussed in section 5.3.4, we described and incorporated regulation of competitive behaviour within the evolving model. Furthermore, it was observed that under highly regulated conditions the attachment rule will change from kudos to random selection which resulted in the phase transition being removed.

6.2 Future Work

In the future, it may be possible that the numerical simulation and analysis we have given in this thesis could be extended in various directions. Firstly, in section 5.3.2 we described the analytical estimate of the critical target. This estimate provided good agreement when the initial size and initial resource were varied. However, this was not as good when varying the number of offspring and especially when varying the degree of offspring. Hence, future research would consider discovering a better analytical estimate for the critical target. Another key point also discussed in section 5.3.2 is the numerical estimate of the critical target. It was stated that the numerical estimate of the critical target occurred when the MTTA and the MTTB were equal. In this thesis, however, we have offered no explanation as to why this relationship occurs. With this in mind, future research could investigate further the relationship between the MTTA, MTTB and the critical target.

Secondly, in sections 3.2.1, 3.2.4 and 4.2 we explored some properties of the Extended GR problem. However, the largest network generated was approximately 350 players. A future research project could consider undertaking numerical simulations of much larger networks, a million players for example. By simulating a

much larger network, possible future work may further validate the conclusions of this thesis as well as discover possible new properties of the Extended GR problem.

Thirdly, section 3.2.1 described our payment rule of the Extended GR problem. However, future research could consider more generalized payment rules:

- In each round, a player gives 1 unit of resource to the e neighbours with the highest score, if those neighbours scores higher than the said player.
- If the player only has z resources left, where $z < e$, then the player gives only 1 unit to each of his z highest scoring neighbours, if and only if those neighbours score higher than the said player.
- Otherwise the player keeps their resource.

This payment rule would model social and business competitive behaviour more realistically than the one in this thesis. For example, if two businesses were the players and the customers were the units, then it could be argued that a business could lose more than one customer to its competitor in one round. The changes in these payment rules have the potential to create new emergent behaviour on the macroscopic scale.

Fourthly, in section 5.3 we described a player who has held or is holding the “golden unit” as the kudos player. Section 5.3.2 described how in the supercritical region, a high proportion of the network have kudos. However, future research may wish to explore kudos that decays with time. For instance, the longer a player holds kudos, the more it depreciates. This possibly has the implication of increasing the critical target. Finally, section 2.2.2 discussed evolutionary game theory, most notably the iterative prisoner’s dilemma. Here, the players were given or chose a strategy to achieve their goals. However, in the numerical simulations of the Extended GR problem, there is not a strategy given or chosen by the players. Hence in this thesis, the player’s success or failure is driven purely by random

processes. A theme of research considered but never pursued was to give the players a strategy. Future research may wish to investigate the effect a player's strategy has on the Extended GR problem. For instance, in an N -player network, we might consider a scenario in which seven individual players have different strategies. The other $N - 7$ players are driven purely by random processes. The seven strategies we could consider are:

1. **Appraisal Period:** *The player with this strategy, after a predefined set number of rounds, switches opponents (rewires) if their loss of resources is deemed as too great. The motivation behind this strategy is to find opponents that are easier to beat.*
2. **Adapt Target:** *The player with this strategy decreases their target if their opponents are deemed as being too strong. The motivation behind this strategy is to achieve with a smaller target and hope that their offspring fares better.*
3. **Suspension:** *The player with this strategy suspends playing their opponents if they are deemed as being too strong. The motivation behind this strategy is to protect their resources and hope the opponents achieve during the duration of suspension.*
4. **Search:** *The player with this strategy switches opponents (rewires) after a predefined set number of rounds if they have not obtained kudos. The motivation behind this strategy is to actively find and hopefully beat the player with the "golden unit", so that kudos is obtained.*
5. **Merger:** *The player with this strategy merges with a non-strategy player after a predefined set number of rounds and hence combines resources. The motivation behind this strategy is to achieve through competition and merger.*

6. **Weakest:** *The player with this strategy only attaches to opponents that are weaker.*
7. **Franchise:** *The player with this strategy splits into franchise agents. Each agent then connects to different parts of the network and plays the GR problem. If the sum of all the agents' resources is equal to or greater than the target, then all the franchise agents combine into one player and leave the network through achievement.*

The offspring of these players adopt the same strategy. By considering the above strategies, future research could investigate the behaviour that emerges on the macroscopic scale. This model would relate more closely to social and business competitive behaviour.

A The Robustness of the Numerical Simulations

Throughout this thesis we have used numerical simulation as a tool to assist with the research. However, some parameters have remained fixed throughout the thesis, such as the number of rounds and histories. In this appendix we will offer an explanation as to why these parameters were selected and we will test the robustness of the solutions quoted.

In terms of the number of rounds, Figure 42 show that, for a variety of network sizes, the number of players reaches a steady state in between 2,000 and 4,000 rounds. However, the results quoted in this thesis are for 10,000 rounds. In the case of any future modelling activity, we decided not to shorten the simulation duration.

Figure 84 demonstrates the robustness of the number of histories that were selected. This analysis was undertaken with the contracting, fixed and evolving models. Throughout the thesis we have decided to use 50 histories for each analysis. As can be seen in the case of the fixed and evolving model, for the MTTA and MTTB, the results become stable after about 40 histories. The results for the contracting model are less stable. Nevertheless, the main results of Chapter 5 are obtained from the evolving model. Table 13 illustrates that, for each target stated, there is not much difference between results obtained from 50 or 100 histories.

Figure 85 illustrates the uncertainty of the results. Here for the evolving model, the uncertainty is shown for the MTTA as the target is increased. The error bars represent plus and minus one standard deviation from the mean. In concurrence with Figure 58, a phase transition is still observed at each end of the error bars.

In section 3.2 we stated that the standard deviation was fixed so that the strongest player (strength of 1) has a $\frac{5}{6}$ chance of beating the weakest opponent. The choice of standard deviation value was chosen to calibrate with earlier methodology undertaken in the research. Originally for the numerical simulation, the

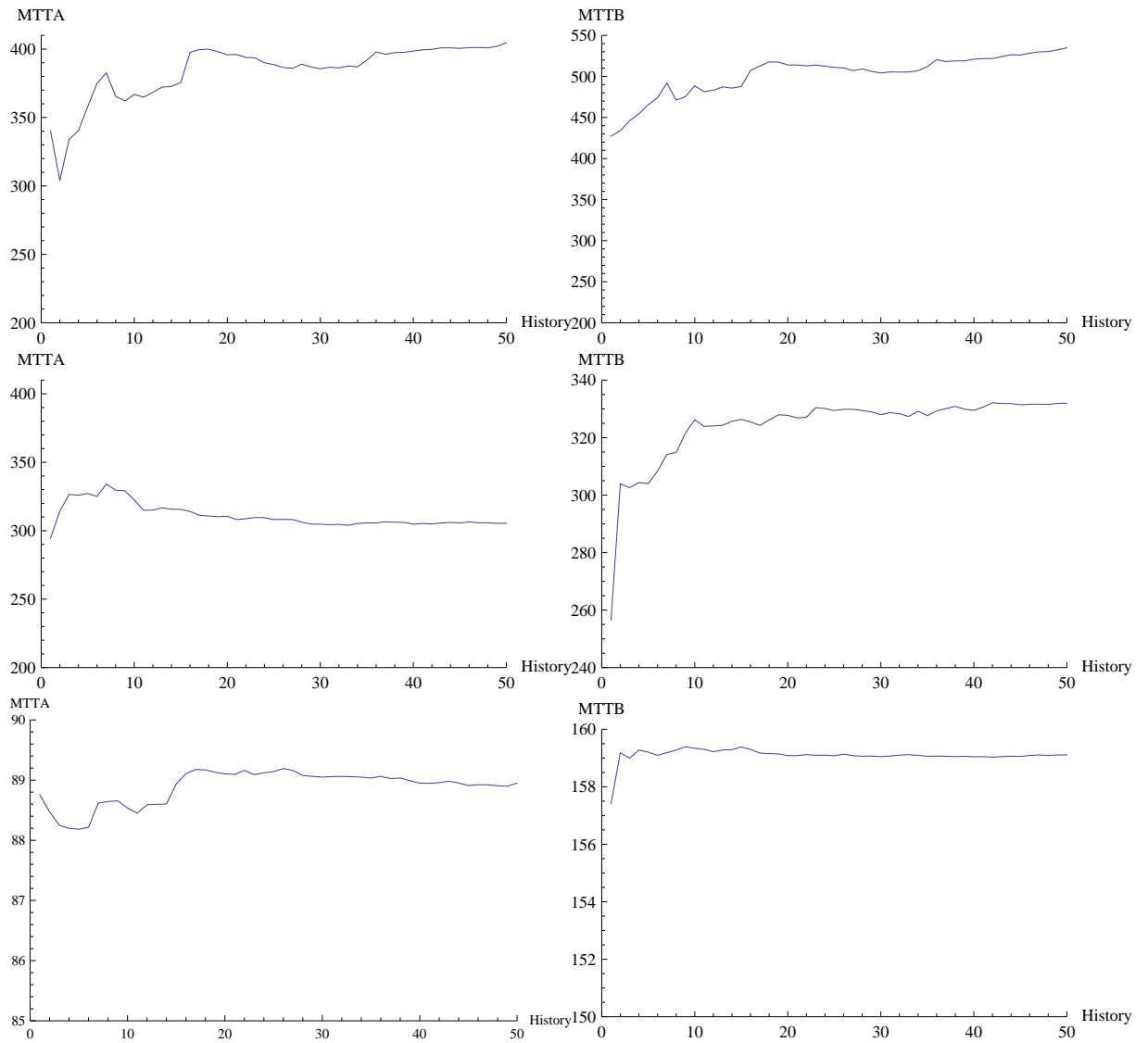


Figure 84: Variation of the MTTA - Left column and MTTB - Right column over the number of histories simulated. Contracting model - Top row, Fixed model - Middle row and Evolving model (kudos attachment rule) - Bottom row. Network topology is a pure ring with 100 players, initial resources of 100 and a target of 200.

Target	MTTA	MTTA	MTTB	MTTB	Nf	Nf
	50	100	50	100	50	100
	Histories	Histories	Histories	Histories	Histories	Histories
130	95.18	95.15	184.91	185.01	255.92	256.57
150	92.38	92.32	177.85	177.68	245.98	245.62
200	89.10	89.08	159.29	159.17	225.48	225.41
250	146.64	144.94	177.16	176.63	194.86	194.54
260	304.93	304.07	231.03	227.24	163.60	163.16
275	500.12	497.03	289.87	289.02	135.58	135.86
300	638.17	640.04	337.98	338.72	121.86	121.81
350	872.50	873.77	421.23	421.84	102.92	101.75
450	1317.72	1320.34	580.74	576.90	75.18	76.26
550	1764.10	1752.20	720.87	720.40	59.50	60.21

Table 13: Variation of the MTTA, MTTB and Nf over 50 and 100 histories. Initial resource is fixed at 100 units, initial network size is 100 players and there are 10,000 rounds. Results averaged over 50 or 100 histories. Results rounded to 2 decimal places.

player would have sampled from not a normal distribution but from a triangular distribution. However, it was argued that it was the triangular distribution, most particularly the discontinuous first derivative, that contributed to the phase transition (see Figure 58). In order to investigate this, a normal distribution with an appropriate standard deviation was chosen. This ensured that the same probability for a player with strength 1 beating an opponent with strength 0 was used. Repeating the numerical simulations, with the discontinuous first derivative now removed, the results still showed a phase transition. Therefore, this effect was independent of the probability distribution chosen.

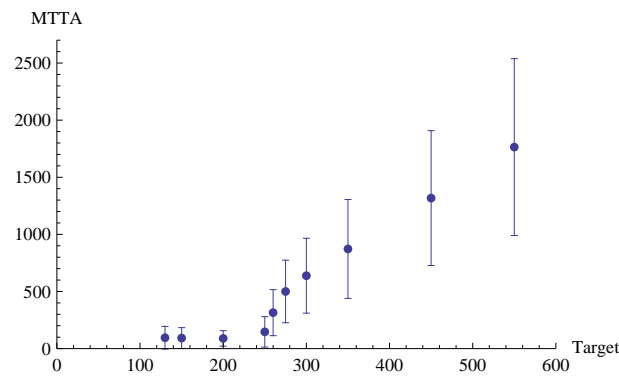


Figure 85: The influence of target on the MTTA. The error bars represent plus and minus one standard deviation from the mean. Initial resource is fixed at 100 units, initial network size is 100 players, 10,000 rounds. Results averaged over 50 histories.

Furthermore, Figure 86 demonstrates by varying this probability between $\frac{1}{2}$ and 1 that the resulting MTTA remains within one standard deviation of the reference case ($\frac{5}{6}$). Nevertheless, the critical target in all three cases remains in approximately the same position.

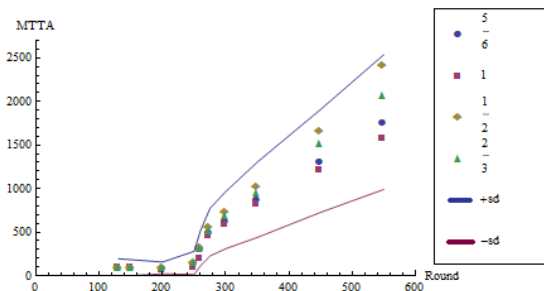


Figure 86: The influence of target and of the probability of the strongest player beating the weakest opponent on the MTTA. Initial resource are fixed at 100 units, initial network size is 100 players, 10,000 rounds. Results averaged over 50 histories.

In summary, the numerical simulation is robust for 10000 rounds, 50 histories and a choice of $\frac{5}{6}$ for the probability of the strongest player beating the weakest.

B References

References

- [Albert and Barabási (2002)] Albert R and Barabási A (2002), *Statistical mechanics of complex networks*. Reviews of Modern Physics, 74:47–97, 4.
- [Bailey (1975)] Bailey N (1975), *The Mathematical Theory of Infectious Diseases*. Mathematical Biology, Springer-Verlag.
- [Barabási (2009)] Barabási A (2009), *Scale-Free Networks: A Decade and Beyond*. Science Vol 325, 412-413.
- [Barabási and Albert (1999)] Barabási A and Albert R (1999), *Emergence of scaling in random networks*. Science 286: 509–512.
- [Barabási et al (2000)] Barabási A, Albert R and Jeong H (2000), *Scale-free characteristics of random networks: the topology of the world-wide web*. Physica A 272: 173-187.
- [Barrat and Weigt (2000)] Barrat A and Weigt M (2000), *On the properties of small-world network models*. Eur Phys J B 12, 547-560.
- [Barrat et al (2008)] Barrat A, Barthélemy M, and Vespignam A (2008), *Dynamical processes on complex networks*. Cambridge University Press.
- [Barthélemy and Amaral (1999)] Barthélemy and Amaral (1999), *Small-world networks: Evidence for a crossover picture*. Phys. Rev. Lett. 82, 5180.
- [Benenson et al (2009)] Benenson I, Hatna, E, and Or, E (2009), *From Schelling to spatially explicit modelling of urban ethnic and economic residential dynamics*. Sociological Methods and Research, 37(4), 463–497.

- [Benito et al (2009)] Benito C, Branas-Garza P, Hernadez J and Sanchis J (2009), *Strategic Schelling Dynamics*. Mimeo.
- [Berger et al (2004)] Berger N, Borgs C, Chayes J, D’Souza R and Kleinberg R (2004), *Competition-Induced Preferential Attachment*. Automata, Languages and Programming Lecture Notes in Computer Science, 2004, Volume 3142/2004, 208-221.
- [Bianconi and Barabási (2001)] Bianconi G and Barabási A (2001), *Competition and multiscaling in evolving networks*. Europhys. Lett., 54 (4), 436.
- [Biggs et al (1976)] Biggs N, Lloyd K and Wilson R (1976), *Graph Theory 1736-1936*. Oxford, England: Oxford University Press.
- [Boccaletti et al (2006)] Boccaletti S, Latora V, Moreno Y, Chavez M and Hwang D (2006), *Complex networks: Structure and dynamics*. Physics Reports Volume 424, Pages 175-308.
- [Bollobás and Riordan (2004)] Bollobás B and Riordan O (2002), *The diameter of a Scale-free Random Graph*. Combinatorica 24 (1), 5-34.
- [Borgs et al (2007)] Borgs C, Chayes J, Daskalakis C and Roch S (2007), *First to market is not everything: an analysis of preferential attachment with fitness*. Proceedings of the 39rd annual ACM Symposium on the Theory of Computing (STOC), 135-144.
- [Britton and Lindholm (2009)] Britton T and Lindholm M (2009), *Dynamic random networks in dynamic populations*. Journal of Statistical Physics Volume 139, Number 3, 518-535.
- [Chang (1995)] Chang D (1995), *A game with four players*. Statist. Probab. Lett. 23 111-115.

- [Dorogovtsev et al (2000)] Dorogovtsev S, Mendes J and Samukhin A (2000), *Structure of Growing Networks with Preferential Linking*. Phys Review Letter Volume 85 Number 21.
- [Edwards (1983)] Edwards A (1983), *Pascal's Problem: The Gambler's Ruin*. International Statistical Review 51, 73-79.
- [Eguiluz and Zimmerman (2005)] Eguiluz V and Zimmerman M (2005), *Cooperation; social networks and the emergence of leadership in a prisoner's dilemma with adaptive local interactions*. Phys. Rev. E 72, 056118.
- [Erdős and Rényi (1959)] Erdős P and Rényi A (1959), *On random graph*. Publ. Math. 6, 290-297.
- [Fagiolo et al (2009)] Fagiolo G, Valente M and Vriend N (2009), *Dynamic Models of Segregation in Small-World Networks*. Networks, Topology And Dynamics:Theory And Applications To Economics And Social Systems Volume: 613 Pages: 111-126.
- [Fan and Chen (2004)] Fan Z and Chen G (2004), *Evolving Networks driven by Node Dynamics*. International Journal of Modern Physics B, vol 18, nos 17-19.
- [Gómez-Gardeñes et al (2008)] Gómez-Gardeñes J, Floría L, Sánchez A, Moreno Y (2008), *Complex Cooperative Networks from Evolutionary Preferential Attachment*. PLoS ONE 3(6): e2449.
- [Gong and van Leeuwen (2003)] Gong P and van Leeuwen C (2003), *Emergence of scale-free network with chaotic units*. Physica A 321, 679.
- [Gullberg (1997)] Gullberg J (1997), *Mathematics From the Birth of Numbers*. W W Norton and Company.

- [Hadjiliadis (2004)] Hadjiliadis O (2004), *Change-point detection of two-sided alternatives in Brownian motion model and its connection to the gambler's ruin problem with relative wealth perception*. PhD Thesis, Columbia University.
- [Hadjiliadis and Vecer (2006)] Hadjiliadis O and Vecer J (2006), *Drawdowns preceding rallies in a Brownian motion model*. J Quant Financ 5(5):403–409.
- [Hayward (1999)] Hayward J (1999), *Mathematical Modeling of Church Growth*. Journal of Mathematical Sociology 23(4).
- [Holme and Kim (2002)] Holme P and Kim B, *Growing scale-free networks with tunable clustering*. Phys Rev E 65.
- [Huang et al (2004)] Huang C, Sun C, Hsieh J and Lin H, (2004), *Simulating SARS: Small-World Epidemiological Modeling and Public Health Policy Assessments*. Journal of Artificial Societies and Social Simulation vol. 7, no. 4.
- [Hunter et al (2008)] Hunter B, Krinik A and Nguyen C (2008), *Gambler's Ruin with Catastrophes and Windfalls*. Journal of Statistical Theory and Practice, Volume 2, No. 2.
- [Jensen (2008)] Jensen H (2008), *Emergence of network structure in models of collective evolution and evolutionary dynamics*. Proc. R. Soc. A 2008 464, 2207-2217.
- [Kalnins and Lafontaine (1960)] Kalnins A and Lafontaine F (1996), *The Characteristics of Multi-Unit Ownership in Franchising: Evidence from Fast-Food Restaurants in Texas*. NBER Working Paper No. 5859.
- [Klopfer (2008)] Klopfer E. (2008), *Augmented Learning: Research and Design of Mobile Educational Games*. MIT Press. Cambridge, MA.

- [Kot (2001)] Kot M, (2001), *Elements of Mathematical Ecology*. Cambridge University Press.
- [Krapivsky et al (2000)] Krapivsky P, Redner S and Leyvraz F (2000), *Connectivity of Growing Random Networks*. Phys Review Letter Volume 85 Number 21.
- [Laurie and Jaggi (2003)] Laurie A and Jaggi N (2003), *Role of 'Vision' in Neighbourhood Racial Segregation: A Variant of the Schelling Segregation Model*. Urban Studies 40(13), 2687–2704.
- [Lehmann et al (2005)] Lehmann S, Jackson A and Lautrup B, (2005), *Life, death and preferential attachment*. EPL (Europhysics Letters), Volume 69, Number 2.
- [Leskovec and Faloutsos (2007)] Leskovec J and Faloutsos C (2007), *Scalable Modeling of Real Graphs using Kronecker Multiplication*. Proceedings of the 24th International Conference on Machine Learning, Corvallis, OR.
- [Newman and Watts (1999)] Newman M and Watts D (1999), *Scaling and percolation in the small world network*. Phys. Rev. E 60, 7332-7342.
- [Newman et al (2001)] Newman N, Stogatz S and Watts D (2001), *Random graphs with arbitrary degree distributions and their applications*. Phys. Rev. E 64, 026118.
- [Newman et al (2006)] Newman N, Barabási A and Watts D (2006), *The structure and dynamics of networks*. Princeton University Press.
- [Nowak and May (1992)] Nowak M and May R (1992), *Evolutionary games and spatial chaos*. Nature 359, 826-829.

- [Ore (1953)] Ore O (1953), *Cardano, The Gambling Scholar*. Princeton University Press.
- [Pastor-Satorras et al (2001)] Pastor-Satorras R and Vespignani A (2001), *Epidemic spreading in scale-free networks*. Phys. Rev. Lett. 86. 3200-3203.
- [Poncela and Vespignani (2009)] Poncela J, Gómez-Gardeñes J, Traulsen A and Moreno Y (2009), *Evolutionary game dynamics in a growing structured population*. New Journal of Physics 11 083031.
- [Ren et al (2008)] Ren J, Wu X, Wang W, Chen G, Wang B (2008), *Interplay between evolutionary game and network structure: the coevolution of social net; cooperation and wealth distribution*. arXiv:physics/0605250v2.
- [Rocha and Stern (1999)] Rocha A and Stern F (1999), *The gambler's ruin problem with N player and asymmetric play*. Stat. Probabil. Lett. 4487-95.
- [Rocha and Stern (2004)] Rocha A and Stern F (2004), *The asymmetric N -player gambler's ruin problem with equal initial fortunes*. Advances in Applied Mathematics 33.
- [Sandell (1989)] Sandell D (1989), *A game with three players*. Stat. Probabil. Lett 7 61-63.
- [Schelling (1971)] Schelling T (1971), *Dynamic model of segregation*. Journal of Mathematical Sociology 1: 143-186.
- [Shoesmith (1986)] Shoesmith E (1986), *Huygens' solution to the gambler's ruin problem*. Historia Math. 13 (2) , 157-164.
- [Solomonoff and Rapoport (1951)] Solomonoff R and Rapoport A (1951), *Connectivity of Random Nets*. Bulletin of Mathematical Biophysics, Volume 13. 107-117.

- [Southwell and Cannings (2010)] Southwell R and Cannings C (2010), *Some Models of Reproducing Graphs. III Game Based Reproduction*. Applied Mathematics 1, 334–342.
- [Stern (1975)] Stern F (1975), *Conditional expectation of the duration in the classical ruin problem*. Math Mag 48 286-288.
- [Szabo and Fath (2007)] Szabo G and Fath G (2007), *Evolutionary games on graphs*. Physics Reports 446 (4-6), 97-216.
- [Watts (2003)] Watts D (2003), *Six Degrees: The Science of a Connected Age*. W. W. Norton and Company.
- [Watts and Strogatz (1998)] Watts D and Strogatz S (1998), *Collective dynamics of small world networks*. Nature 393, 440-442.
- [Weaver (1948)] Weaver W (1948), *Science and Complexity*. E:CO Vol. 6 No. 3, 65-74.
- [Wolfram (2002)] Wolfram S (2002), *A new kind of science*. Wolfram media inc.
- [Yan et al (2004)] Yan G, Zhou T, Jin Y, Fu Z, (2004), *Self-Organization Induced Scale-Free Networks*. <http://arxiv.org/abs/cond-mat/0408631>.